2012-07-31

Role of Perivascular and Visceral Adipose Tissues in Murine Models of Obesity and Atherosclerosis: A Dissertation

Timothy P. Fitzgibbons
University of Massachusetts Medical School

ROLE OF PERIVASCULAR AND VISCERAL ADIPOSE TISSUES IN MURINE MODELS OF OBESITY AND ATHEROSCLEROSIS

A Dissertation Presented

By

TIMOTHY P. FITZGIBBONS M.D.

Submitted to the Faculty of the

University of Massachusetts Graduate School of Biomedical Sciences, Worcester

in partial fulfillment of the requirements for the degree of

DOCTOR OF PHILOSOPHY

JULY 31, 2012

MILLENNIUM MD/PHD PROGRAM

ROLE OF PERIVASCULAR AND VISCERAL ADIPOSE TISSUES IN MURINE MODELS OF OBESITY AND ATHEROSCLEROSIS

A Dissertation Presented By

Timothy P. Fitzgibbons, M.D.

The signatures of the Dissertation Defense Committee signifies completion and approval as to the style and content of the Dissertation

_____

Michael Czech, Ph.D., Thesis Advisor

_____

Marcus Cooper, M.D., Member of Committee

_____

John Keaney, M.D., Member of Committee

_____

Jason Kim, Ph.D., Member of Committee

_____

Jorge Plutzky, M.D., Member of Committee

The signature of the Chair of the Committee signifies that the written dissertation meets the requirements of the Dissertation Committee

_____

Stuart Levitz, M.D., Chair of Committee

The signature of the Dean of the Graduate School of Biomedical Sciences signifies that the student has met all graduation requirements of the school.

_____

Anthony Carruthers, Ph.D.
Dean of the Graduate School of Biomedical Sciences

Millennium MD/PhD Program
July 31, 2012

Acknowledgements

First, I would like to express my sincere gratitude and thanks to my thesis advisor Dr. Michael P. Czech for his generosity, enthusiasm, patience, and support. I'm extremely grateful to Mike for his personal interest in my development as a person and a scientist. My favorite memories of this training program will be the time I spent in Mike's office discussing science. As with all great teachers, he is a devotee of Socrates, choosing to answer questions with questions.

I would like to especially thank Dr. John Keaney for believing in me, encouraging my interest in research, mentorship, not to mention tangibles such as salary support and letters of recommendation. I would also like to thank him for the many improvements he has made in the clinical, research, and educational enterprise of the Division of Cardiovascular Medicine since his arrival in 2005.

I would like to thank the other members of my dissertation committee including the Chair, Dr. Stuart Levitz, Dr. Marcus Cooper, and Dr. Jason Kim for their feedback and expertise during TRAC Meetings and my thesis defense. I would also like to thank Dr. Jorge Plutzky for agreeing to serve as the outside reviewer for my thesis defense and his thoughtful contributions on that day.

I would like to thank Dr. Hardy Kornfeld for convincing me to apply to the Millennium MD/PhD program and his mentorship during the past three years.

I would like to thank all of my other past and present scientific and clinical mentors from whom I continue to learn, including; Dr. Charlie Hoffman, Dr. Robert Smith, Dr. Yilei Mao, Dr. Gerard Aurigemma, and Dr. Dennis Tighe.

I would like to thank all members of the Czech lab family, past and present, for their collegiality, kindness, and inspiration. In particular, I would like to thank Myriam Aouadi, Greg Tesz, Dr. Joseph Virbasius and Sara Nicoloro. Joe, thank you for your all encompassing scientific advice, assistance with grant

submissions, sense of humor, and friendship. Sara, thank you for unwavering insistence on excellence, sharing your technical and scientific expertise, enthusiasm, friendship, and thoughtfulness.

I would like to thank my parents, Mark and Ilona Fitzgibbons for providing everything I needed to succeed. Your love has given me the courage to persevere. I would also like to thank my siblings John, Patrick and Kathleen for their love, support, and laughter.

I would like to thank my son Matthew for his hugs, kisses, and sense of perspective. Finally, and most importantly, I would like to thank my wife Dr. Christine Fitzgibbons. Without your friendship, love, hard work and devotion none of this would have been possible.

Abstract

Expansion of visceral adipose tissue correlates with the metabolic syndrome and increased cardiovascular risk. Hypertrophied visceral fat becomes inflamed, causing increased lipolysis, decreased triglyceride storage, and lipotoxicity in skeletal muscle and liver resulting in insulin resistance. Perivascular adipose tissue is a normal component of the adventitia of arteries in humans and animals. Whether or not perivascular adipose also becomes inflamed in obesity is an important question, as this may be an additional, direct mechanism by which obesity causes vascular inflammation and disease.

Thus, for the first part of my thesis, we asked the question: does perivascular adipose in mice become inflamed with high fat feeding? In contrast to visceral adipose, macrophage gene expression was not increased in perivascular adipose in response to high fat diet, and this correlated with reduced F480 antigen positive cells as seen by immunohistochemistry and flow cytometry. Interestingly, perivascular adipose surrounding the thoracic aorta was similar to brown adipose tissue, a highly thermogenic fat depot, as shown by histology and DNA microarrays. Moreover, inter-scapular brown adipose was also resistant to diet induced inflammation in comparison to visceral adipose. These findings suggest that brown adipose in the perivascular niche may serve to protect the vasculature from diet induced inflammation, or from cold exposure, or both; whether or not brown perivascular adipose tissue exists in humans has yet to be determined.

In the second part of my thesis, we evaluated the role of perivascular adipose tissue in the apolipoprotein E knockout mouse, which exhibits severe hyperlipidemia and atherosclerosis, but is resistant to diet induced obesity and glucose intolerance. We tested the hypothesis that in this model of severe atherosclerosis, inflammation of perivascular adipose does occur. However, we were surprised to find that macrophage specific gene expression, as determined by either microarray analysis or quantitative polymerase chain reaction, was not increased in either the perivascular or the visceral adipose of high fat diet fed apolipoprotein E knockout mice. While the visceral adipose of wild type mice had extensive alterations in gene expression in response to high fat diet, in particular, enrichment of inflammatory gene expression and broad down regulation of peroxisome proliferator activated receptor gamma target genes, apolipoprotein E knockout visceral adipose did not. Importantly, the apolipoprotein E knockout visceral adipose instead showed increased expression of genes encoding enzymes in fatty acid oxidation pathways. High fat diet fed apolipoprotein E knockout visceral adipose was also characterized by smaller adipocyte size.

We conclude that, 1) inflammation in thoracic perivascular adipose does not occur in conjunction with diet induced obesity in normal animals nor with atherosclerosis in apolipoprotein E knockout mice, 2) thoracic perivascular adipose tissue is essentially identical to brown adipose tissue in mice, thus potentially protecting the vasculature from the cold, and 3) apolipoprotein E knockout mice remain lean on a high fat diet, despite hyperlipidemia and

atherosclerosis, and the decreased adiposity correlates with decreased adipocyte size and adipose inflammation but increased oxidation of fatty acids. Consistent with previous work showing apolipoprotein E controls adipocyte uptake and deposition of triglyceride, its absence prevents adipocyte hypertrophy and resultant inflammation of visceral adipose tissue. Thus limiting adipocyte acquisition of fatty acids may be advantageous, provided that compensatory mechanisms to prevent sustained hyperlipidemia and peripheral organ lipotoxicity can be activated.

Table of Contents

Approval Page…….. ii

Acknowledgements……. iii

Abstract……. v

List of Tables……. xi

List of Figures…… xii

List of Frequently Used Abbreviations…….. xiv

Copyright Information…….. xviii

CHAPTER I: Introduction…… 1

Obesity, Metabolic Syndrome, and Cardiovascular Disease..... 2

Role of inflammation in human adipose tissue……. 9

Inflammation in mouse models of diet induced obesity… 11

Factors which contribute to immune cell recruitment….. 14

Adipocyte cell death…….. 14

Lipolysis……. 17

Chemokines…….. 21

Pathophysiology of Atherosclerosis…….. 24

The “Response to Retention Hypothesis”……. 24

Perivascular Fat and the “Yudkin Hypothesis”…. 28

Evidence for a Role of Perivascular and Epicardial Fat in Cardiovascular Disease…….. 31

Human Studies……. 31

Animal Studies……. 35

Specific Aims…… 41

CHAPTER II: Similarity of Mouse Perivascular and Brown Adipose and Their Resistance to Diet-Induced Inflammation…… 42

Abstract…… 43

Introduction…… 44

Experimental Procedures…… 46

Results…… 52

Cidea and *Ucp-1* are Highly Expressed in BAT and PVAT Independent of Obesity…… 52

Mouse Thoracic PVAT is Morphologically Similar to BAT…… 56

Microarray Analysis Confirms PVAT has a Characteristic Brown Adipose Gene Expression Signature…… 60

Thoracic PVAT and Inter scapular BAT are Relatively Resistant to Macrophage Infiltration under HFD Conditions…… 68

FACS Analysis Confirms Prolonged HFD in Mice Results in Little Macrophage Infiltration of BAT Compared with VAT…… … 71

Discussion…… 73

Limitations …… 79

CHAPTER III: Protection against diet induced obesity and insulin resistance in the apoE knockout mouse is accompanied by an attenuated transcriptional response in visceral fat…… 81

Abstract…… 82

Introduction…… 83

Experimental Procedures…… 86

Results……. 91

Atherosclerosis is not associated with increased expression of F480, Cd68, or Mcp-1 in thoracic PVAT…… 91

EKO mice are resistant to DIO after 24 and 38 weeks HFD..……. 93

Metabolic cage studies reveal no differences in energy expenditure, food intake, or physical activity…… 97

EKO mice have increased post-prandial, but not total, VO2 and EE…….. 97

EKO mice are protected against hepatic steatosis induced by 24 weeks of HFD…… 102

Comparative insensitivity of EKO VAT gene expression in response to HFD……. 104

Reduced cell size and macrophage F480 staining in EKO HFD VAT…… 109

Discussion…..... 111

Limitations……... 118

CHAPTER IV: Summary and Future Directions…… 120

Influence of adipocyte specific Mcp-1 knockout on abdominal aortic aneurysm formation in HFD fed mice…….. 121

Comparison of inflammatory gene expression in epicardial fat in patients with and without coronary disease…… 126

Conclusions…….. 129

References…… 130

List of Tables

TABLE 1.1 Clinical criteria for the diagnosis of the metabolic syndrome… 4

TABLE 1.2 Differences between adipose tissue inflammation in diet induced obese mice and fasting/caloric restriction…… 20

TABLE 1.3 Vasocrine mediators released from PVAT…… 40

TABLE 2.1 Depot-specific expression of select gene categories in normal diet conditions……..... 64

TABLE 2.2 Comparative expression of immune cell enriched genes in VAT, SAT, PVAT and BAT in normal and high fat diet conditions…… 67

TABLE 3.1 Metabolic parameters of WT and EKO mice fed ND and HFD for 24 weeks..……. 96

TABLE 3.2 ANCOVA reveals that VO2 (m/hr) and EE (kcal/hr) are associated with HFD but not genotype…….. 100

TABLE 3.3 BIOCARTA Pathway Analysis of Differentially Expressed Genes Sets……. 107

TABLE 3.4 Differential regulation of metabolic gene sets in response to HFD in WT vs. EKO mice…….. 108

List of Figures

FIGURE 1.1 Selective insulin resistance in the liver contributes to the hyperglycemia and hypertriglyceridemia of Type II diabetes mellitus…… 8

FIGURE 1.2 Time course of inflammation in VAT in the DIO model……..13

FIGURE 1.3 Macrophage infiltration of visceral fat with HFD and the β3 agonist CL316,243……16

FIGURE 1.4 The “Response to Retention” Model of Atherosclerosis…… 27

FIGURE 1.5 Proposed role of PVAT in vascular health and disease…… 30

FIGURE 2.1 Thirteen weeks of high HFD results in obesity, glucose intolerance and hyperinsulinemia in C57BL6/J Mice…..…… …… 54

FIGURE 2.2. *Cidea* and *Ucp-1* are highly expressed in BAT and PVAT independently of obesity…… 55

FIGURE 2.3. Perivascular adipose tissue appears morphologically similar to brown adipose tissue…….58

FIGURE 2.4. Transmission electron microscopy reveals many similarities between perivascular and brown adipose tissues……..59

FIGURE 2.5. Microarray analysis reveals that PVAT is more similar to BAT than SAT or VAT…….....63

FIGURE 2.6. Perivascular and BAT are resistant to inflammation after 13 weeks HFD……..69

FIGURE 2.7. Perivascular and brown adipose tissue are resistant to inflammation after 20 weeks high fat diet ……...70

FIGURE 2.8. Brown adipose tissue is resistant to inflammation after 11and 20 weeks of HFD…… 72

FIGURE 3.1. Expression of macrophage markers *F480* and *Cd68* is increased in the VAT of HFD mice but not the PVAT or VAT of EKO mice.. 92

FIGURE 3.2. EKO mice are resistant to diet induced obesity and impaired glucose tolerance after 24 and 38 weeks of HFD…… 95

FIGURE 3.3. High fat feeding increases VO2 irrespective of genotype……99

FIGURE 3.4. Post-prandial VO2 is increased in HFD
EKO mice compared to wild type ND and HFD mice…….....101

FIGURE 3.5. EKO mice are protected against hepatic steatosis induced
by 24 weeks of HFD……103

FIGURE 3.6. mRNA expression of genes encoding key transcription
factors and metabolic enzymes which regulate fatty acid metabolism
are up-regulated in WT but not EKO HFD adipose tissue…….. 105

FIGURE 3.7 WT HFD VAT has larger adipocytes and greater
F480+ Macrophage staining……110

FIGURE 4.1. A working model for the contribution of PVAT
to abdominal aortic aneurysm formation in obesity……. 123

FIGURE 4.2. Increased *Mcp-1* and *F480* mRNA in abdominal PVAT
correlates with macrophage infiltration…… 124

FIGURE 4.3. Experimental design of the REACD (Role of Epicardial
Adipose in Coronary Disease) Study…….....128

List of Frequently Used Abbreviations

Abbreviation	Term
AAA	Abdominal aortic aneurysm
ADPN	Adiponectin
Adrp	Adipophilin
AMPK	AMP-activated protein kinase
ANCOVA	Analysis of Covariance
apoE	apolipoprotein E
ATII	Angiotensin 2
Atgl	Adipose triglyceride lipase/desnutrin
BAT	Brown adipose tissue
CAD	Coronary artery disease
Ccl18	Chemokine (C-C motif) ligand 18
Ccr2	Chemokine (C-C motif) receptor 2
Cd36	CD36 antigen
Cd11b/Itgam	Cd11 like antigen family member B/Integrin alpha M
Cd11c/Itgax	Cd11 like antigen family member C/Integrin alpha X
Cd68	Cd68 antigen
CIDEA	Cell death-inducing DFFA-like effector A
CLS	Crown-like structure
CPT1B	Carnitine palmitoyltransferase 1B
CR	Caloric restriction
CRP	C-reactive protein
CSF-3	Colony stimulating factor 3

Csfr1	Colony stimulating factor receptor 1
CXCL10	Chemokine (C-X-C) motif ligand 10
CVD	Cardiovascular disease
DIO	Diet induced obesity
EAT	Epicardial adipose tissue
EE	Energy expenditure
EKO	apolipoprotein E knockout mouse
F480	F480 antigen
FA	Fatty acid
FoxO1	Forkhead box protein O1
GO	Gene ontology
GTT	Glucose tolerance test
HDL	High density lipoprotein
HFD	High fat diet
HOMA-IR	Homeostasis model of assessment-insulin resistance
Hsl	Hormone sensitive lipase
IDL	Intermediate density lipoprotein
IL6	Interleukin 6
IL1β	Interleukin 1 beta
IL8	Interleukin 8
IL10	Interleukin 10
IR	Insulin resistance
LDL	Low density lipoprotein
LDLr	Low density lipoprotein receptor

LOX-1	Lectin type oxidized LDL receptor 1
LPL	Lipoprotein lipase
LRP1	Low density lipoprotein related protein 1
MACE	Microarray computational environment
MARCO	Macrophage receptor with collagenous structure
M-CSF	Macrophage-colony stimulating factor
Mcp-1/Ccl2	Macrophage chemoattractant protein 1
Mip1α/Ccl3	Macrophage inhibitory protein 1 alpha
Mip1β/Ccl4	Macrophage inhibitory protein 1 beta
MGC	Multi-nucleate giant cell
MS	Metabolic syndrome
ND	Normal diet
NEFA	Non-esterfied fatty acid(s)
NLRP3	NLR family, pyrin domain containing 3
PAME	Palmitic acid methyl ester
PDGF	Platelet derived growth factor
PI3K	Phosphoinositide 3 kinase
PKB/Akt	Protein kinase B
PLAUR	Plasminogen activator, urokinase receptor
Plin1	Perilipin 1
PPARγ	Peroxisome proliferator activated receptor
PRDM16	PR domain containing 16
Psgl-1	P-Selectin glycoprotein ligand-1
PVAT	Perivascular adipose tissue

RMA	Robust multi-array average
RANTES/CCL5	Regulated upon Activation, Normal T-cell Expressed and Secreted
SAT	Subcutaneous adipose tissue
SELE	E-selectin
SRA	Macrophage scavenger receptor 1
SR-B1	Scavenger receptor class B, member 1
Srebp-1c	Sterol regulatory element binding protein 1c
SVC	Stromal vascular cell
TG	Triglyceride
TGRL	Triglyceride rich lipoprotein
TLR	Toll like receptor
TNFα	Tumor necrosis factor alpha
UCP-1	Uncoupling protein 1
VAT	Visceral adipose tissue
VCAM-1	vascular cell adhesion molecule 1
VLDL	Very low density lipoprotein
VO2	Oxygen consumption

Copyright Information

CHAPTER I: Introduction

It is estimated that 86.3% of adults in the United States will be obese or overweight in the year 2030[1]. At this rate, healthcare costs attributed to obesity/overweight will double every decade, to approximately 900 billion dollars in 2030; accounting for 15-20% of total US healthcare costs[1]. This expenditure is related to the cost of treatment of important co-morbidities such as diabetes mellitus, coronary artery disease, heart failure, and cancer. The metabolic syndrome, which is mediated by insulin resistance, is thought to be the final common pathway by which obesity causes these disorders.

It is within this context that there has been a massive effort in the scientific community to understand the role of adipose tissue in normal and obese conditions. There is no doubt that normal adipose tissue is extremely important to human physiology; the fact that patients with lipodystrophy suffer from the same risk of diabetes and cardiovascular disease as obese patients, highlights this physiologic importance. Much of the basic science in the metabolism field has focused on ways in which adipocytes become dysfunctional in obese conditions. This is with the recognition that making fat function better, by storing excess calories, may actually be beneficial. The nuclear hormone receptor peroxisome proliferator activated receptor gamma (PPARγ) is the master regulator of adipocyte differentiation and function [2]. In clinical practice, efforts to promote normal function of adipose tissue using certain PPARγ agonists has recently been hampered by an increased risk of myocardial infarction [3]. This is

contrasted by a second school of thought which aims to promote the formation of brown adipose tissue (BAT), or fat that burns excess calories via fatty acid oxidation. While efforts to activate brown fat with β3 adrenergic agonists have failed, efforts to promote BAT formation and activity remain a promising therapeutic strategy [4, 5]. By far the most important and effective therapy now and in the future will be the primary and secondary prevention of obesity by interventions on an individual, community, and global scale. For those with established obesity bariatric surgery will become an increasingly important and effective option [6]. In the meantime, research efforts, such as that described herein, which aim to understand the role of physiology of adipose tissue in normal and obese conditions, will inform the future science and policy regarding this global health crisis.

Obesity, Metabolic Syndrome and Cardiovascular Risk

Central obesity is associated with an increased risk of death and the development of atherosclerotic coronary artery disease, heart failure, and Type 2 diabetes mellitus [7]. Although the exact mechanism by which this occurs is unknown, insulin resistance (IR), and the metabolic syndrome (MS) are thought to contribute [8, 9]. MS is a constellation of metabolic and underlying risk factors that promote the development of atherosclerotic cardiovascular disease (CVD) (Table 1.1). Central obesity is a risk factor for developing this syndrome, as is

insulin resistance and associated conditions such as aging, physical inactivity, and hormonal imbalance [9].

TABLE 1.1. Clinical criteria for the diagnosis of Metabolic Syndrome

Measure	Categorical cut points
Elevated waist circumference	≥102 cm (≥40 inches) in men ≥88 cm (≥35 inches) in women
Elevated triglycerides	≥150 mg/dL (1.7 mmol/L) or On drug treatment for elevated triglycerides‡
Reduced HDL-C	≤40 mg/dL (1.03 mmol/L) in men ≤50 mg/dL (1.3 mmol/L) in women or On drug treatment for reduced HDL-C‡
Elevated blood pressure	≥130 mm Hg systolic blood pressure or ≥85 mm Hg diastolic blood pressure or On antihypertensive drug treatment in a patient with a history of Hypertension
Elevated fasting glucose	≥100 mg/dL or On drug treatment for elevated Glucose

*Any 3 of 5 criteria

‡Fibrates and nicotinic acid are the most commonly used drugs for elevated TG and reduced HDL-C. Patients taking one of these drugs are presumed to have high TG and low HDL

Table adapted from Grundy *et al*.[9]

Recent data has led to the recognition of two important limitations to the clinical criteria for the metabolic syndrome. First, anthropometric measures of obesity such as body mass index (BMI) and waist circumference have limited sensitivity for visceral adiposity, and there are individuals with increased intra-abdominal fat who do not meet clinical criteria for obesity; such patients should be considered as “normal weight” obese [10]. Proxy measures of visceral adiposity such as the measurement of epicardial fat thickness with 2D echocardiography might be useful in these patients [11]. Second, insulin resistance is present at the tissue level long before clinically apparent manifestations such as elevated fasting blood glucose [8]. Selective defects in the phosphoinositide 3 kinase (PI3K) arm of insulin signaling, leading to impaired glycogen synthesis in skeletal muscle, is one of the first indications of insulin resistance in humans [8]. Therefore more sensitive measures of insulin resistance and MS are needed to detect patients who are at increased risk of CVD.

The predominant mechanism by which central adiposity leads to insulin resistance is thought to be related to “lipotoxicity”, a term first coined by Unger in 1995[12]. In the setting of chronic caloric excess, visceral adipocytes hypertrophy, causing increased lipolysis and decreased storage of fatty acid as triglyceride (TG), resulting in increased plasma levels of non-esterfied fatty acids (NEFAS)[13]. Increased serum NEFAS accumulate as toxic lipid metabolites (e.g. fatty acyl CoA, diacylglycerols, ceramides) in liver and skeletal muscle,

causing insulin resistance [13]. This paradigm has come under scrutiny as of late, with evidence that lipolysis and subsequent increases in plasma NEFAs are actually reduced per unit of fat mass in obese humans [14, 15]. Additionally, mobilization of TG from post-prandial chylomicrons appears to be impaired in obese humans, owing to down regulation of mRNAs encoding lipoprotein lipase (LPL) and other genes responsible for uptake of fatty acid in adipose tissue[15]. Nonetheless, there is no doubt that increased tissue levels of fatty acid metabolites causes IR in liver and skeletal muscle, as shown in humans using magnetic resonance spectroscopy and lipid infusions, and mice by tissue specific over expression of LPL [16-18]. The resultant IR in skeletal muscle and liver is a harbinger of the clinically apparent components of MS (Table 1.1).

Impaired insulin stimulated glucose uptake in skeletal muscle contributes to hyperglycemia, leading to increased insulin secretion and hyperinsulinemia [8]. Hepatic “selective insulin resistance” in the PI3K pathway accounts for the hypertriglyceridemia which accompanies MS and Type 2 Diabetes. The failure of insulin to stimulate protein kinase B (PKB/Akt) phosphorylation results in constitutive Forkhead box protein O1 (Foxo1) activity in the nucleus, leading to increased transcription of genes responsible for hepatic gluconeogenesis (e.g.*Pepck,G6PC)* and increased hepatic glucose output [19, 20](Figure 1.1). In contrast, insulin continues to stimulate sterol regulatory element binding protein 1c (Srebp1-c), which transcribes enzymes responsible for fatty acid synthesis, leading to increased hepatic very low density lipoprotein (VLDL) output and

hypertriglyceridemia [19, 20]. In addition, hyperinsulinemia causes stimulation of mitogen activated protein kinase pathways in peripheral tissues, resulting in increased vascular smooth muscle cell proliferation, collagen formation, and excessive production of growth factors and inflammatory cytokines [8]. The adverse effects of hyperinsulinemia caused by exogenous insulin treatment are yet unknown, but apparent as an average 8.6 kg weight gain in type 2 diabetic patients starting insulin despite an improvement in HbA1c% [8].

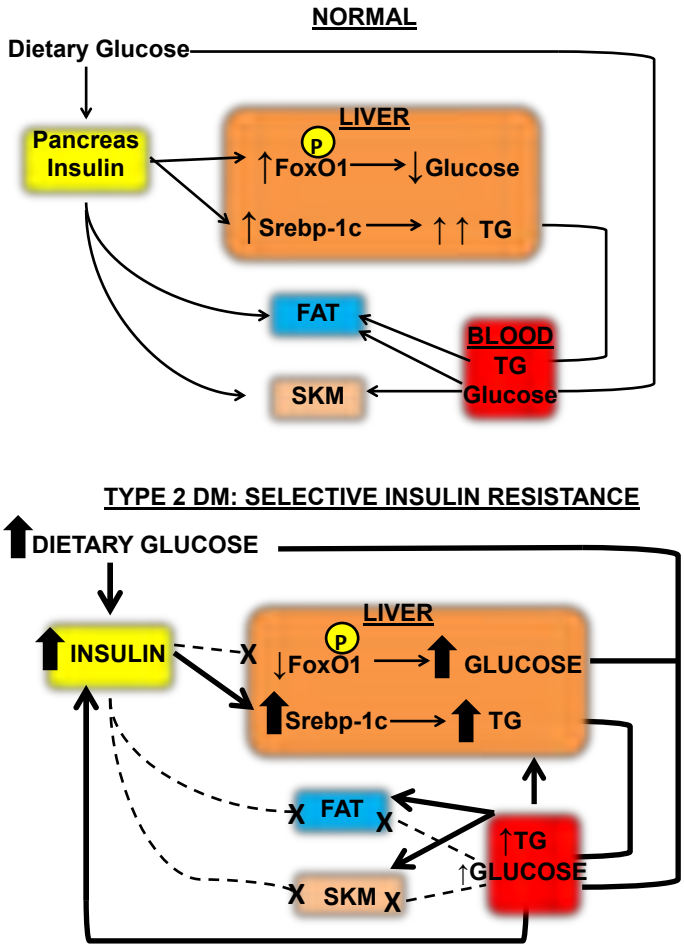

FIGURE 1.1 Selective insulin resistance in the liver contributes to the hyperglycemia and hypertriglyceridemia of Type II diabetes mellitus. In normal conditions (top), the pancreas secretes insulin in response to glucose. Insulin triggers inhibitory phosphorylation of FoxO1, which then fails to activate transcription of mRNAs encoding gluconeogenic enzymes. Srebp-1c is stimulated normally to activate transcription of fatty acid synthesis genes which synthesize TG to fuel peripheral tissues. In obese conditions (bottom), hyperglycemia stimulates hyperinsulinemia. The liver is resistant to insulin in the Akt pathway and cannot stimulate inhibitory phosphorylation of FoxO1; transcription of gluconeogenic enzymes continues and hepatic glucose output increases. "Selective insulin resistance" allows for hyperactivation of the Srebp-1c pathway, which is not insulin resistant, increasing hepatic VLDL output. Increased blood TG contributes to lipotoxicity of skeletal muscle, liver and other tissues. X=insulin resistance, SKM=skeletal muscle, TG=triglyceride. Adapted from Brown et al. 2008[19].

Role of Inflammation in Human Adipose Tissue

The production of inflammatory cytokines by human adipose tissue was first reported by Hotamisligil *et al.* in 1995, when they demonstrated greater tumor necrosis factor alpha (*TNFα)* mRNA and protein in the subcutaneous adipose tissue (SAT) of obese compared to lean pre-menopausal women [21]. Adipose tissue TNFα levels correlated with hyperinsulinemia, and it was hypothesized that TNFα contributed to IR in fat in an autocrine or paracrine fashion, as plasma levels were undetectable. Weight loss led to reductions in TNFα production by adipose tissue in some of the subjects [21]. Subsequently, Weisberg *et al*. found increased expression of macrophage specific genes in the SAT of obese humans [22]. Using immunohistochemistry for the mature macrophage marker F480 antigen (*F480)*, the authors showed that the percentage of tissue macrophages correlated positively with adipocyte cell size and BMI. In lean humans, macrophages were estimated to number 10% of the total cells in adipose tissue, whereas almost 40% of the cells in adipose tissue of obese subjects were F4/80+ [22]. The majority of these F480+ cells were present in multinucleate syntitia or “crown like structures”(CLS), which surround dead or dying adipocytes [23]. Hence, adipocyte cell death was thought to be one of the triggers for macrophage recruitment to adipose tissue, where they function to scavenge toxic free fatty acids and cellular debris [22].

Multiple subsequent studies have shown increased macrophage infiltration in SAT and visceral adipose tissue (VAT) of obese humans [23-26]. The

percentage of macrophage accumulation in VAT is greater than SAT and correlates directly with the degree of abdominal adiposity ($r=0.535$, $p<0.0001$), cell size, individual components of MS, and hepatic steatosis [26, 27]. Once present, macrophages and other immune cells secrete pro-inflammatory cytokines such as TNFα, interleukin 1 beta (IL1β), and interleukin 6 (IL6) and establish a chronic immune response. Cytokines exaggerate the dysregulated metabolism of local adipocytes, increasing lipolysis, decreasing TG esterfication, and reducing production of beneficial adipokines such as adiponectin (ADPN); these effects are mediated in part by TNFα which down regulates adipocyte PPARγ mRNA and protein [13]. Thus inflammation in human adipose tissue, which may initially serve as a protective effect, becomes exaggerated and chronic, resulting in adipocyte dysfunction, deleterious effects on the liver, and systemic inflammation manifest as increases in serum acute phase reactants such as C-reactive protein (CRP), orosomucoid, and serum amyloid A [13, 28]. Weight loss induced by gastric bypass has been shown to decrease the number of macrophages in SAT, decrease the expression of inflammatory chemokines, and alter the activation state of remaining macrophages, as shown by increased expression of the anti-inflammatory cytokine interleukin 10 (IL10) [28]. Although this unrestrained and chronic inflammatory response in human VAT is deleterious to whole body metabolism, these studies underestimate the complexity of adipose physiology.

Inflammation in mouse models of diet induced obesity

Studies in mouse models of diet induced obesity (DIO) have been crucial in defining this complex relationship between innate immunity and metabolism. Two reports in 2003 highlighted the establishment of a chronic inflammatory condition in the VAT of dietary and genetic mouse models of obesity [22, 29]. In the context of human data, three primary questions remain: 1) is inflammation in VAT a direct cause of whole body insulin resistance? 2) why is visceral fat disproportionately affected by inflammation? and 3) what is primary stimulus for inflammation?

In regards to the first question, Strissel *et al*. showed that within 6-8 weeks of starting a high fat diet (HFD), there is a threefold increase in the stromal vascular cell number in adipose tissue [30]. mRNAs for *F480*, Cd11 antigen like family member C (*Cd11c/Itgax)*, Cd68 antigen (*Cd68)*, and *Tnfα* become significantly increased when compared to normal diet control mice at this time point [30](Figure 1.2). This is coincident with increased adipocyte cell size and the onset of adipocyte cell death (16% of adipocytes). Importantly, fasting plasma glucose, homeostasis model of assessment-insulin resistance (HOMA-IR), and the area under the curve for the insulin tolerance test all were significantly elevated at this time, suggesting that inflammation in VAT contributes to whole body IR [30, 31]. With the large increase in adipocyte death in VAT, and an apparent reduction in differentiation of new cells, there is a 40% net loss in VAT mass [30]. By 16 weeks of HFD there is increased fibrosis and collagen

formation in adipose tissue, decreases in *Tnfα* and *Cd11c* mRNA, and increases in *Il10*. Interestingly, by 20 weeks of HFD, insulin resistance is actually improved compared to 16 weeks, albeit not to baseline levels [30]. This signifies a switch back to an "alternatively activated" M2 phenotype, which is reminiscent of adipose tissue macrophages from lean mice not exposed to HFD [32].

In contrast to VAT, there is a sustained 10 fold increase in the mass of SAT during HFD [30]. This is due to both increased adipocyte size and a doubling of adipocyte number. However, the mean size of subcutaneous adipocytes remains less than half of that seen in VAT and the rate of cell death in SAT never exceeds 3%, whereas in VAT it reaches 80% after 16 weeks of HFD [30].

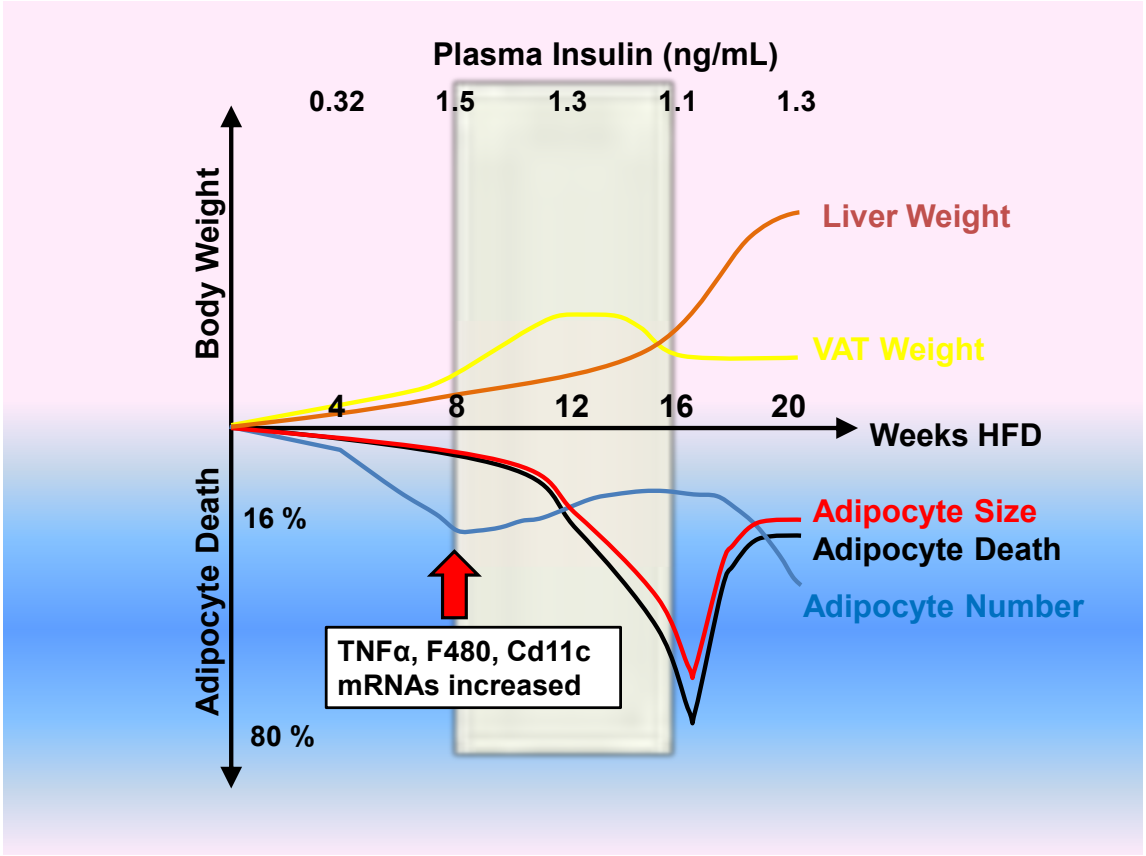

FIGURE 1.2 Time course of pathophysiologic change in VAT and metabolism in the DIO model. The number of inflammatory cells in the visceral fat gradually increases during high fat feeding. After 6-8 weeks of HFD mRNAs encoding *F480*, *Cd11c*, and *Tnfα* become significantly enriched in VAT. This is coincident with increasing adipocyte size and increases in adipocyte cell death. That inflammation in VAT causes whole body IR is suggested by the onset of IR (white background) at 8 weeks, when the inflammatory cell number and representative mRNAs become enriched. The peak of adipocyte cell death (80%) at 16 weeks, signals a transition of macrophages to M2 polarization, with decreased *Tnfα* mRNA and increased *Il10* mRNA. At 20 weeks, measures of insulin resistance are actually improved compared to 16 weeks, but not back to baseline. Note that the net loss of visceral fat mass is accommodated by high rates of cell death, and a greater number of smaller adipocytes at 20 weeks. Data from Strissel *et al*.[30]

In summary these studies have been crucial to our understanding of inflammation in adipose tissue by confirming that macrophage infiltration correlates with increased cell size, cell size and rates of cell death are significantly greater in VAT, and these events correlate with the onset of insulin resistance. An important question that remains is: what is the initial stimulus for macrophage infiltration in obesity? We will focus on three specific possibilities: adipocyte death, free fatty acids, and chemokines.

Factors Which Contribute to Immune Cell Recruitment

Adipocyte Death

Macrophage infiltration in humans is directly and positively correlated with BMI and adipocyte cell size [22, 23, 25]. Two papers have shown definitively that bone marrow derived monocytes home to adipose tissue where they are attracted to dying adipocytes [23, 30]. Dying adipocytes are surrounded by a ring of activated macrophages which form a “crown like structure” containing multinucleated giant cells (MGC)(Figure 1.3). MGCs are a feature of chronic inflammation due to persistent mycobacterial infections, non-infectious granulomatous diseases (e.g. sarcoidosis, rheumatoid arthritis) or the presence of non-phagocytosable foreign bodies [33]. Transmission electron microscopy showed that hypertrophied adipocytes develop features of necrotic cell death, including ruptured plasma membranes, dilated endoplasmic reticuli, and cellular debris in the extracellular space [23]. Furthermore, expression of lipid droplet proteins such as adipophilin (*Adrp*) and perilipin (*Plin1*) is reduced. That

macrophages engulf the released free fatty acids and cholesterol is suggested by the fact that they develop lipid droplets and induce expression of the same lipid droplet proteins (e.g. *Adrp, Plin1*) [23]. The authors then showed that adipocyte hypertrophy was crucial to the development of cell death, using hormone sensitive lipase (*Hsl*) null mice. Mice with deletion of *Hsl* cannot hydrolyze stored triglyceride in response to metabolic cues, and therefore develop large adipocytes; the cell size of *Hsl*$^{-/-}$ adipocytes was three fold greater than wild type on normal diet. After 12 weeks, there was a 15 fold increase in CLS formation in *Hsl*$^{-/-}$ compared to controls (29 CLS per 100 adipocytes vs. 2 CLS per 100 adipocytes)[23]. Hence, it appears that adipocyte hypertrophy is a source of cellular stress which triggers necrotic death. Potential sources of cellular stress in larger sized adipocytes include ER stress, hypoxia, increased TNFα expression, altered cholesterol concentrations, reactive oxygen species, or increased local free fatty acids [34]. In light of recent evidence, free fatty acids are a particularly attractive candidate as entities which may promote the initial inflammatory response.

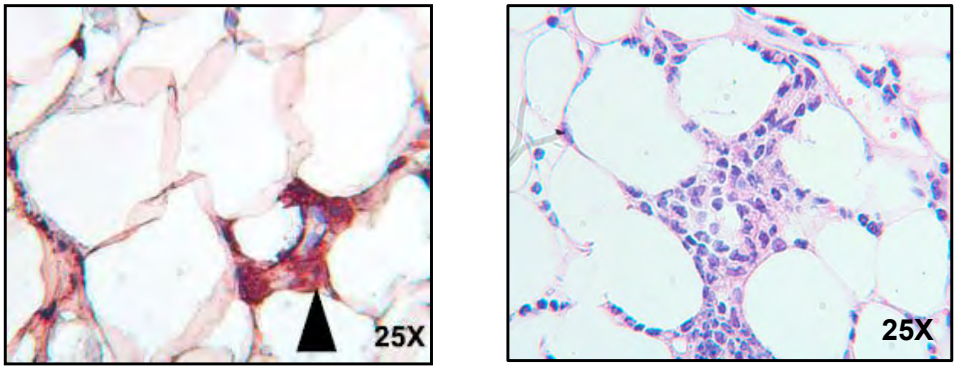

FIGURE 1.3. Macrophage infiltration of VAT with HFD and the β3 agonist CL316,243. Shown at left are F480+ macrophages after 13 weeks of HFD in the visceral fat of mice. On the right, hematoxylin & eosin staining of visceral fat 16 hours after treatment with the β3 agonist CL316,243. At left, a multinucleate giant cell can be seen (arrow) within a crown like structure. Macrophages in this case are likely attracted to visceral fat to phagocytose the remnants of dying adipocytes (surrounded by macrophages). On the right, although a macrophage specific stain was not used, note the multiple single nuclei cells between adipocytes, without crown like structure formation. (Tim Fitzgibbons, unpublished data)

Lipolysis

Adipocytes store fatty acids in the form of triglyceride, which can be hydrolyzed to provide oxidative fuels to peripheral tissues at times of energy deprivation such as fasting or exercise. Adipocytes have two modes of lipolysis, a basal continual low level, and a hormone stimulated or "demand" lipolysis [34]. The rate of basal lipolysis is directly proportional to cell surface area ($4\pi r^2$), and therefore increases dramatically in larger adipocytes. Given this, and the fact that macrophage accumulation positively correlates with cell size and BMI, Kosteli *et al*. asked the question "is adipocyte lipolysis responsible for macrophage recruitment to adipose tissue?"[34]. Lipolysis should be greatest in large adipocytes (high basal lipolysis) which are subject to demand lipolysis (fasting or weight loss). To test this hypothesis, they performed a series of elegant experiments using both caloric restriction (CR) and fasting of obese mice. After 3 days of CR (70% *ad libitum* fed), or 24 hours of fasting, there was a dramatic increase over baseline in the percentage of macrophages in VAT (26.3% vs. 38.6% of total cells for CR, 22.9% vs. 37.9% for fasting) and in expression of the macrophage specific genes *F480* and colony stimulating factor receptor 1 (*Csfr1*) [34](Table 1.2). This was accompanied by increased serum free fatty acid (FFA) levels, and increased lipolysis in explants of adipose tissue from the same mice. Stimulation of lipolysis with a β3 adrenergic agonist (CL316,243) also induced potent macrophage accumulation within 24 hours. To confirm that macrophages were responding to increased lipolysis of adipocytes,

the authors then performed fasting in mice deficient for the major TG lipase, desnutrin or (*Atgl*). *Atgl*$^{-/-}$ knockout mice have very low levels of basal lipolysis and are unable to stimulate demand lipolysis in response to fasting. When compared to control mice, *ad libitum* fed *Atgl*$^{-/-}$ knockout mice had decreased numbers of macrophages in adipose tissue, and there was no increase seen after 24 hours of fasting [34].

Despite the dramatic increases in macrophage accumulation after 3 days of CR, 24 hours of fasting, and injection of the β3 agonist, there was no increase in expression of inflammatory genes such as *Cd11c* or *Tnfα*, and mice remained insulin sensitive in all conditions [34]. This is in stark contrast to the increased expression of inflammatory genes (e.g. *Tnfα*, *IL6, IL1b*) which accompanies macrophage infiltration in obese conditions [22, 29, 30]. The authors proposed that short term alterations in lipid flux, due to fasting or CR, result in a transient increase in macrophage infiltration, which gradually resolves without promoting inflammation and peripheral insulin resistance. In the setting of chronic high fat feeding, accumulated macrophages become inflammatory, expressing *Cd11c* and cytokines, and causing peripheral insulin resistance. This situation is somewhat analogous to foam cell formation seen in atherosclerotic plaques. Once established, if the primary insult (e.g. hyperlipidemia) is resolved, by treatment with statins for example, macrophages may exit and plaque may regress. However, with continued chronic exposure to high cholesterol or other

risk factors, macrophages themselves are activated, unable to egress, secrete inflammatory cytokines and even undergo apoptosis [35].

In summary, FFAs released from adipocytes may serve as the initial stimulus for macrophage accumulation. FFAs may stimulate Toll-like receptor 4 (Tlr4) on adipocytes, or endothelium, to up regulate adhesion molecules and chemokines which attract monocytes from the bloodstream [36]. However, there are several key distinctions to be made between the inflammation in adipose tissue seen in obesity and fasting (Table 1.2). Macrophages in diet induced obesity form CLS, express macrophage markers such as *F480*, CD11 like antigen family member B (*Cd11b/Itgam)* and *Cd11c/Itgax*, and transcribe genes encoding inflammatory cytokines (*Tnfα, Mcp-1, Il6*). In mice, this inflammation associated with a reduction in adipocyte cell number and an increase in peripheral IR. In fasting conditions, although there are increased macrophages in adipose tissue, they tend not to form CLS, they express only *F480* and *Cd11b*, and inflammatory cytokine production is not increased (Table 1.2). Finally, although there is a reduction in cell size, there is not a reduction in cell number nor is there an increase in peripheral insulin resistance during fasting or CR.

TABLE 1.2. Differences between adipose inflammation in mice in HFD induced obesity and fasting/CR

	Obesity	Fasting/CR
Macrophage number and morphology	-Up to 50% of adipose tissue cells -CLS and MNGC	-Up to 38% of adipose tissue cells vs. 26% in obese control mice -non CLS macrophage accumulation
Macrophage markers	*F4/80, Cd11b, Cd11c*	*F4/80, Cd11b*
Inflammatory gene expression	↑↑*Tnfα, Il6, iNOS, Mcp-1*	Not increased compared to control mice
Adipocyte cell death	Present	Absent
Adipocyte cell size	Increased	Decreased
Metabolism	Insulin resistant	Insulin sensitive
Serum FFA	Increased 0.6 vs. 0.4 mmol/L in chow fed	Increased 0.8 vs. 0.6 mmol/L in obese, fed
CLS=crown like structures, MNGC=Multinucleate giant cells Data from references [22, 30, 34]		

Chemokines

There are likely multiple redundant mechanisms which promote greater macrophage infiltration into VAT than SAT, including cell death, hypoxia, lipolysis, and chemotactic regulation [37]. The latter mechanism appears particularly important. Studies in mice have shown that diet induced obesity (DIO) stimulates a robust increase in transcription of chemokine genes such as macrophage chemoattractant protein 1 (*Mcp-1)*, Regulated upon Activation Normal T-cell Expressed and Secreted (*RANTES/Ccl5)*, and macrophage inhibitory protein 1 alpha (*Mip1α/Ccl3)* in VAT [22, 29]. In obese humans, expression of chemokine genes such as *MCP-1*, plasminogen activator, urokinase receptor (*PLAUR)*, and colony stimulating factor 3 (*CSF-3)* is increased and associated with macrophage infiltration and CLS formation in SAT [28]. 3 months after gastric bypass surgery, during which time an average of 20 kg fat mass was lost, there was a dramatic reduction in macrophage number and virtual disappearance of CLS formation [28]. This was associated with decreased transcription of *MCP-1* and *CSF-3* mRNAs (25 and 10 fold respectively). Macrophages, rather than adipocytes, were mostly responsible for expression of these factors [28].

A second human study matched gastric bypass patients for BMI, dichotomized them into IS (HOMA2-IR < 2.3) and IR (HOMA2-IR ≥ 2.3) groups, and then performed microarray analyses on omental fat [25]. Interestingly, the only two Gene Ontology (GO) terms significantly different between groups were

"chemokine activity" and "chemokine receptor binding". Among the 37 genes differentially expressed were the chemokines *MCP-1/CCL2, MIP1α/CCL3,* macrophage inhibitory protein 1 beta *(MIP1β/CCL4),* chemokine (C-C motif) ligand 18 *(CCL18)*, and interleukin 8 (*IL8/CXCL8)* [25]. *MCP-1* is perhaps the most well studied of these genes in mouse models [38-40].

Kanda *et al*. published a paper that strongly suggested the adipocyte was a major source of *Mcp-1* [39]. *Mcp-1* mRNA expression was induced in 3T3LI adipocytes cells following glucose deprivation, and greatly increased in both the stromal vascular fraction and adipocyte fraction of HFD fed mice [39]. Adipocyte specific over-expression of *Mcp-1* and whole body *Mcp-1* knockout, resulted in increased and decreased macrophage infiltration into VAT respectively. Chemokine (C-C motif) receptor 2 (*Ccr2)* knockout mice also have reduced macrophage infiltration into VAT, supporting the notion that adipocyte secreted *Mcp-1* is a ligand for *Ccr2* on macrophages [40]. However, there is some controversy in the literature regarding Mcp-1, as two subsequent studies in whole body *Mcp-1*$^{-/-}$ mice demonstrated no differences between WT or KO mice in macrophage infiltration of VAT or whole body insulin sensitivity after HFD[38, 41]. It is possible that the macrophage Mcp-1 receptor (*Ccr2*) recognizes multiple chemokines, hence there is some redundancy in these molecules and whole body deficiency of Mcp-1 may not have an effect in some circumstances.

Adipose tissue is a dynamic organ which contains many cell types, including adipocytes, pre-adipocytes, endothelial cells, stems cells and immune cells [42].

In fact, it is estimated that over 90% of adipokine release, except for that of adiponectin and leptin, is due to non-fat cells, either the matrix or the stromal vascular cell (SVC) fraction [42]. An important question which has yet to be answered definitively is which is the exact cell in adipose tissue that secretes Mcp-1 in response to high fat feeding?

A recent study by Ohman *et al*. was very informative in this regard [43]. The authors have previously shown that transplantation of VAT to apolipoprotein E knockout (*Apoe*$^{-/-}$) mice increases inflammation and atherosclerosis in these mice in comparison to non transplanted controls or those transplanted with SAT[43]. Using this model, the authors attempted to determine what cell type is the relevant source of Mcp-1. When VAT was transplanted to *Apoe*$^{-/-}$ mice there was increased atherosclerosis and plasma Mcp-1 compared to non transplanted controls (78.7 vs. 31.4 pg/mL). In contrast, when VAT was transplanted into *Apoe*$^{-/-}$ *Mcp-1*$^{-/-}$ double knock-out mice, there was no increase in atherosclerosis and plasma Mcp-1 was barely detectable. Therefore, the source of circulating Mcp-1 is not the donor adipocytes [43]. Using bone marrow transplantation, the authors went on to show that the endothelium is the predominant source of circulating Mcp-1 in acute and chronic inflammation, although leukocytes do provide some local Mcp-1 in VAT [43].

In summary, it appears Mcp-1 is an important factor which stimulates the infiltration of macrophages into VAT. It is likely that increased FFA release, reactive oxygen species, or ER stress of visceral adipocytes cause activation of

the resident endothelium or tissue macrophages, leading to increased *Mcp-1* expression and macrophage infiltration. Preliminary data from our laboratory suggests that the endothelium regulates monocyte infiltration into visceral fat, by altering expression of adhesion molecules in response to metabolic cues (Rachel Roth, unpublished data).

Pathophysiology of Atherosclerosis

The "Response to Retention" Hypothesis

The past two decades have led to an exponential increase in our understanding of the pathophysiology of atherosclerosis, much of which became possible with two simultaneous reports of the creation of the first transgenic mouse model of atherosclerosis, the *Apoe*$^{-/-}$ mouse [44, 45]. Mice are inherently resistant to atherosclerosis, partially because they have low serum cholesterol on a chow diet (60-80 mg/dL), mostly in the form of high density lipoprotein (HDL) [46]. The *Apoe*$^{-/-}$ mouse has extremely high plasma total cholesterol and TG due to inability to uptake chylomicron remnants and VLDL. Despite the development of severe atherosclerosis, this model is not prone to plaque rupture, which is the process which ultimately leads to the morbidity and mortality of human subjects. Nonetheless, the *Apoe*$^{-/-}$ and low density lipoprotein receptor (*LDLr*$^{-/-}$) mouse have contributed greatly to our understanding of the pathophysiology of atherosclerosis, which has gradually evolved to the current paradigm in which atherosclerosis is an inflammatory disease of medium and large arteries which is initiated by the sub-endothelial retention of LDL.

Cholesterol is transported in the blood predominantly by LDL which contains esterfied cholesterol, triglyceride, phospholipids, and apolipoprotein B100. apoB100 binds to proteoglycans in the arterial intima, leading to sub-endothelial trapping of lipoproteins, and exposing the lipids to oxidative modification by myeloperoxidase, lipoxygenase, and reactive oxygen species [47](Figure 1.4). Oxidatively modified lipids such as lysophosphatidylcholine activate endothelial cells and macrophages, resulting in increased expression of adhesion molecules E-selectin (SELE) and vascular cell adhesion molecule 1(VCAM-1), chemokines (Mcp-1/CCL2, RANTES/CCL5, chemokine (C-X-C) motif ligand 10 (CXCL10)) and growth factors (macrophage-colony stimulating factor (M-CSF))[47]. Circulating blood monocytes then adhere to the activated endothelium, diapedese, and enter the arterial intima where they differentiate into macrophages.

Macrophages are the predominant immune cell type of plaques, but T cells are also present (4:1 or even 10:1 ratio)[47]. Macrophages express scavenger receptors such as macrophage scavenger receptor 1 (*SRA),* macrophage receptor with collagenous structure *(MARCO),* CD36 antigen *(CD36),* scavenger receptor class B, member 1 (*SR-B1),* and lectin type oxidized LDL receptor 1 (*LOX-1)* which uptake modified lipids and cellular debris resulting in the development of “foam cells”. Macrophages initially serve a protective function, scavenging oxidatively modified lipid and toxic free cholesterol in the process of efferocytosis [35]. Furthermore, because this cholesterol remains intracellular

and soluble, instead of extracellular in the form of crystals, it can be exported via ABC type transporters to HDL for reverse cholesterol transport to the liver [35]. However, factors which cause increased macrophage cellular stress, such as excess cholesterol, insulin resistance, or ER stress, lead to macrophage apoptosis and the release of intracellular cholesterol [35]. This process contributes to the “necrotic core” of atherosclerotic plaques, which are prone to rupture and the development of acute coronary syndromes. In addition, continued exposure of macrophages to modified LDL results in stimulation of innate immunity, prompting cytokine release, and the recruitment of other immune cells to the lesion, which in turn, prompt the transition to adaptive immunity and chronic inflammation [48]. Two specific stimuli for macrophage innate immunity are oxidized LDL derived epitopes via Toll Like Receptors (TLR) and cholesterol crystals via the inflammasome protein receptor NLR family , pyrin domain containing 3 (NLRP3)[49-51]. Finally, continued hypercholesterolemia results in loss of protective regulatory T cells from the vessel wall, whereas cholesterol lowering preserves their number and function [48].

Therefore, just as in adipose tissue, the macrophage appears to orchestrate an immune response in the atherosclerotic plaque which may initially be protective. However, in the setting of chronic metabolic stress, the macrophage becomes dysfunctional and even apoptotic, leading to increased inflammation, matrix metalloproteinase release, and plaque rupture.

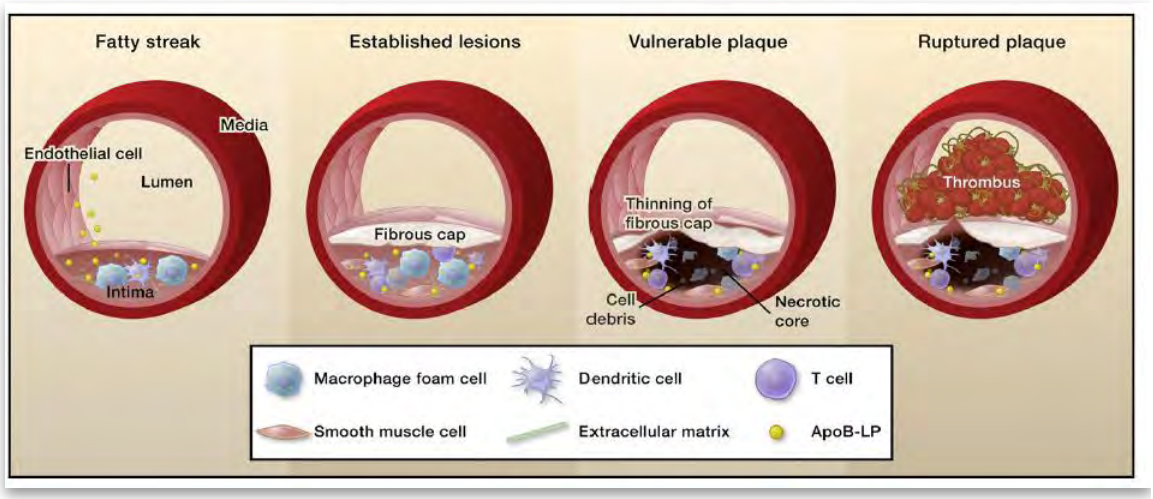

FIGURE 1.4. The "Response to Retention Model" of Atherosclerosis. The sub-endothelial retention of apoB containing lipoproteins triggers activation of adhesion molecule expression in endothelium. Monocytes are then attracted and adhere, diapedese, and differentiate into macrophages. Macrophages of established atherosclerotic plaque scavenge oxidatively modified lipid and transport cholesterol out of the vessel. Chronic cell stress (e.g. continue hyperlipidemia, ER stress, insulin resistance) cause macrophage apoptosis, leading to the necrotic core and increased risk for plaque rupture. Figure adapted from Moore *et al.*[35]

Perivascular Fat and the "Yudkin Hypothesis"

The "response to retention" hypothesis holds that atherosclerosis develops from the arterial intima to the media, or from "inside to outside"(Figure 1.4). However, recently there has been interest in an alternative hypothesis, which posits that atherosclerosis and other vascular diseases are initiated or promoted by factors within the adventitia, with disease proceeding from "outside to inside" the arterial wall (Figure 1.5)[52-54]. Although this concept has long standing experimental support, there are three principal findings which have led to the promotion and sustained investigation of this possibility [55-58].

First, recent studies have shown increased adventitial macrophages associated with expansion of the vasa vasorum in early atherosclerotic lesions *prior to* plaque neovascularization [52]. Second, following balloon angioplasty of porcine coronary arteries, there is a profound inflammation of the adventitia, which is followed by neointimal hyperplasia [57]. This also suggests that factors within the adventitia regulate intimal disease. Finally, there are local deposits of fat surrounding arterioles which supply skeletal muscle. Insulin stimulates robust capillary recruitment in skeletal muscle by stimulating nitric oxide mediated vasodilation [59]. However, in obese conditions, nitric oxide synthesis is impaired, resulting in unopposed vasoconstriction, mediated by Endothelin-1. This impairment in nitric oxide production is thought to be due to release of TNFα by local fat which acts in a vasocrine fashion to inhibit insulin signaling in the adjacent endothelium [59]. As with visceral fat, adipocytes within these

regulatory perivascular fat depots hypertrophy in obese conditions, and depending upon the anatomical context and metabolic milieu, are prone to inflammation. Inflammation in perivascular adipose tissue (PVAT) may directly impact vascular disease of the underlying artery, perhaps contributing to atherosclerosis, peripheral vascular disease, hypertension, or arteriosclerosis.

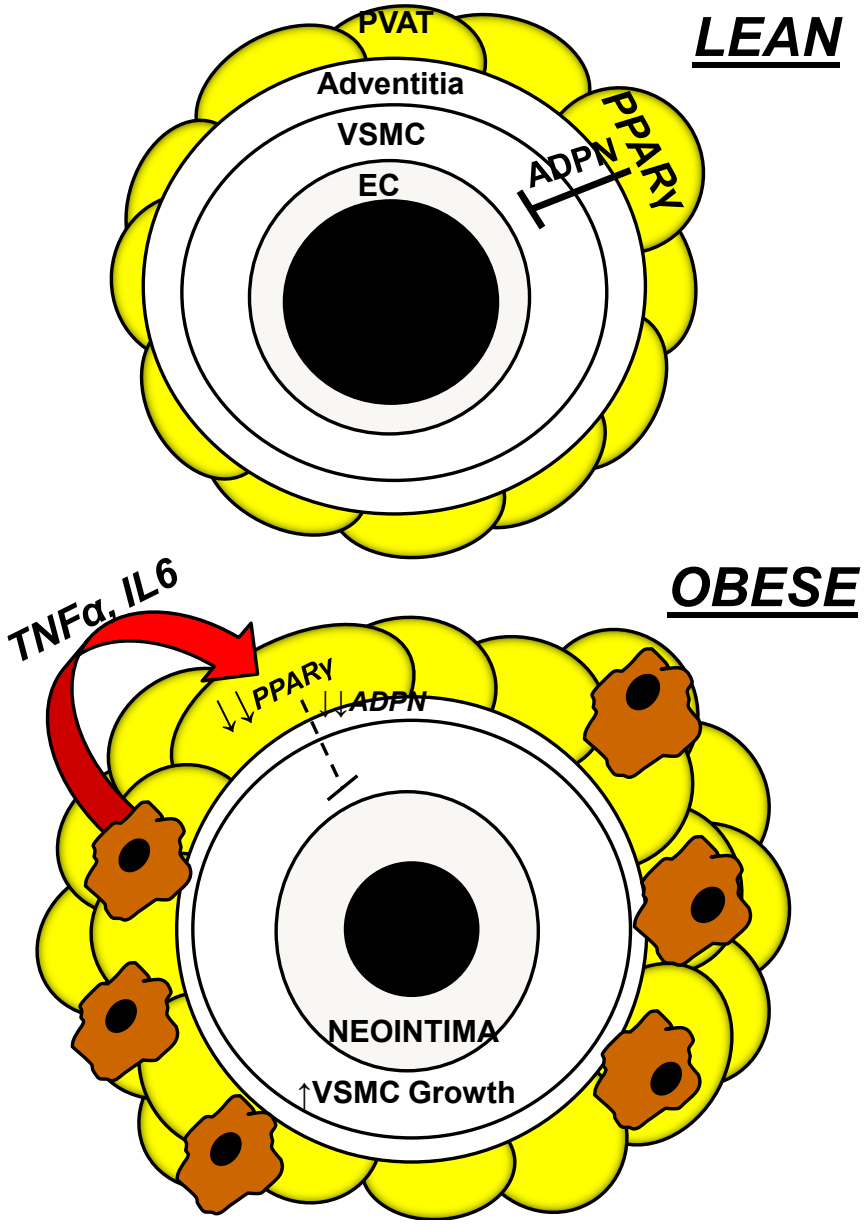

FIGURE 1.5. Proposed role of PVAT in vascular health and disease. In lean conditions (top), PVAT functions normally, signaling through PPARγ to secrete beneficial cytokines such as adiponectin (ADPN) in a paracrine manner. ADPN inhibits VSMC hyperplasia, vasodilates smooth muscle, and prevents inflammation. In obese conditions (bottom), PVAT hypertrophies, macrophages infiltrate, and inflammatory cytokines such as TNFα are secreted. TNFα down regulates PPARγ through transcriptional and post-transcriptional mechanisms, leading to decreased secretion of adiponectin and other beneficial factors by PVAT. Potential consequences of decreased adipokines are increased VSMC proliferation, vasoconstriction, and vascular inflammation.

Evidence for a Role of Perivascular Fat in Cardiovascular Disease

Human Studies

In reviewing the literature on the role of perivascular fat in vascular disease, it becomes evident that the findings depend upon several variables in particular: 1) the species and the strain of animal studied, 2) whether or not the subject is lean or obese, and 3) the anatomic context of the fat and vessel studied. It should be emphasized that PVAT is a normal component of the arterial adventitia in mammals. It surrounds the coronary arteries (epicardial fat), aorta (periaortic fat), and microvasculature of the brain, mesentery, skeletal muscle, and kidney [59]. PVAT should not be considered an ectopic fat depot *per se*, but a normal fat depot that is subject to the plasticity of other fat depots observed in lean and obese conditions.

In humans, the first evidence that PVAT was associated with vascular disease came from a report by Mazurek *et al*. in 2003 [60]. Paired samples of epicardial and subcutaneous adipose tissue were obtained from 42 patients with coronary artery disease (CAD) undergoing coronary artery bypass graft surgery. mRNA and protein expression of inflammatory genes was compared in epicardial adipose tissue (EAT) versus SAT in the same patients [60]. mRNA expression of *IL-1β*, *IL-6*, *MCP-1*, and *TNFα* was significantly increased in the EAT versus the SAT of all patients. Protein release of these same factors by EAT explants in conditioned media was also significantly increased, ranging from 7.0 fold for IL6 (3.4-70.8, $p<0.001$) to 118.6 (12.6-7416, $p<0.001$) for TNFα [60].

Immunohistochemistry showed dense infiltrates of inflammatory cells in EAT including macrophages, T cells, and mast cells, whereas there were no such infiltrates in SAT. The inflammatory features of EAT were present despite the fact that 50% of patients were taking statins and 93% were taking aspirin [60]. Furthermore, the release of cytokines by EAT did not correlate with plasma levels of cytokines, suggesting that they were in fact paracrine mediators which could not be impacted by systemic anti-inflammatory medications.

This study raised several interesting questions. Was the inflammation present before the development of CAD, was it a result of the CAD, or simply an epiphenomenon? Did the inflammation closely correlate with local atherosclerotic lesions? Was there inflammation in VAT of the same patients? Despite these questions, this study remains the most significant and interesting in the field to date.

A second paper by Henrichot *et al*. studied PVAT surrounding the aortas of humans with abdominal aortic aneurysms [61]. They found that PVAT surrounding the abdominal aorta secreted MCP-1 and IL-8, in concentrations similar to SAT from the same patients. In atherosclerotic aortas, local PVAT contained CD68+ and CD3+ cells [61]. These cells were more numerous in the PVAT directly adjacent to the aorta than in the peripheral PVAT; however, they were still greater in PVAT than in SAT or in PVAT from non-diseased arteries. Conditioned media from PVAT was chemotactic for granulocytes, monocytes, and T cells in transwell assays, although not greater than SAT [61]. The two

major findings of this study were that 1) PVAT surrounding the atherosclerotic aorta contains inflammatory cells and 2) PVAT expresses MCP-1 and IL8 which are functional in transwell assays. The authors speculated that PVAT may be particularly relevant in obesity associated vascular disease [61].

Multiple subsequent human studies have demonstrated that PVAT around coronary arteries (i.e. EAT), expresses increased mRNAs encoding inflammatory genes [60, 62-64]. More recently, others have demonstrated that PVAT might have a beneficial effect in lean humans [62, 65]. Karasterigiou *et al*. studied EAT in four groups of patients: normal weight patients with and without CAD (BMI ≤27 kg/m^2) or obese patients with or without CAD (BMI ≥ 27 kg/m^2) [62]. Even in lean patients without CAD, EAT was found to secrete 13 cytokines into conditioned media. Of these 13, CCL5/RANTES was the only cytokine significantly independently associated with the presence of CAD [62]. Interestingly, adiponectin was found to be independently associated with both BMI and the presence of CAD. That is, in comparison to controls, adiponectin release from EAT was *decreased* in obese patients and in lean patients with CAD [62]. Serum adiponectin concentrations were not decreased in the lean CAD group. That CAD is associated with a reduction in adiponectin secretion by EAT has been confirmed by other groups [66-68]. Adiponectin has anti-inflammatory properties and has been shown to reduce the adhesion of monocytes to human coronary endothelial cells *in vitro* [62].

The beneficial properties of PVAT derived adiponectin were recently extended to a role in the direct stimulation of nitric oxide production in vascular endothelium [65]. PVAT surrounding small arteries in subcutaneous fat from healthy lean controls promoted endothelium dependent vasodilation of the underlying artery. This vasodilatory effect was lost with removal of the PVAT, and also with incubation with an Adiponectin type 1 receptor antibody or a nitric oxide synthase inhibitor (L-NAME)[65]. This vasodilatory effect of PVAT was absent in obese patients, in whom the cell size of perivascular adipocytes was greater, and associated with immunohistochemical evidence of inflammation (increased *TNFR1* staining). This was the first study in humans to confirm the initial hypotheses of Yudkin, that PVAT from healthy subjects exerts a vasoprotective influence which is abrogated in obese conditions [59].

In summary, data from humans has shown that PVAT, much like VAT, has evidence of inflammation in obesity and in cardiovascular diseases such as CAD or peripheral vascular disease. It has not been established whether or not inflammation in PVAT is causative or merely with associated disease. Furthermore, it is not known whether there is inflammation in the VAT of the same patients, which would indicate whether or not EAT is an autonomous fat depot which may independently promote disease, or is merely a marker for visceral adiposity. Clinical imaging studies suggest that the latter is the case, for when the volume of EAT by echocardiography or MRI is controlled for by VAT mass, there is no additional risk of CVD [69, 70]. However, it does appear that

perivascular fat surrounding small arteries from lean patients promotes vasodilation of the underlying artery [62, 65]. This beneficial effect is mediated by the paracrine effects of adiponectin which stimulates nitric oxide synthase in the adjacent endothelium. These beneficial properties of PVAT are abrogated in obese patients, due to decreased adiponectin expression, increased expression of inflammatory cytokines, and increased reactive oxygen species. Therefore, it appears that PVAT has a physiological function akin to other types of fat; beneficial in lean conditions but pathologic in obese conditions. As we shall review in the next section, studies from mice have largely confirmed these findings.

Animal Studies

Studies of PVAT in mice are prone to several limitations: there are no models of PVAT deficient mice that have been described yet. The genetic ablation of specific fat depots in mice is a technological hurdle that has yet to be achieved. Second, the small amount of PVAT in mice somewhat limits the experimental procedures that can be performed. Nonetheless, in general, there is accumulating evidence that the function of PVAT in mice is much like that which has been described for humans; beneficial and protective in lean conditions and inflammatory and pathologic in obese conditions.

That PVAT has a vasodilatory effect was first shown by Soltis *et al*. in 1991 when they demonstrated that intact PVAT prevented constriction of aortic rings in

response to epinephrine [71]. Since then, the majority of work regarding PVAT has been done in the field of hypertension, in search of the elusive “adipocyte derived relaxation factor” (ADRF), which was thought to act in an endothelium independent mechanism by direct activation of K+ channels on vascular smooth muscle [72]. This factor was recently identified by Lee *et al*. as palmitic acid methyl ester (PAME)[72]. PAME is released from the PVAT of Sprague Dawley rats and directly vasodilates aortic rings devoid of endothelium. PAME release from the PVAT of spontaneously hypertensive rats is dramatically reduced, while Angiotensin II (ATII) release is increased. The vasoconstrictor response to PVAT of hypertensive rats is inhibited by incubation with the ATII receptor blocker losartan [72]. Therefore, an endothelium independent vasodilator, PAME, is released from the PVAT of lean rats to promote dilation of smooth muscle. Whether or not other vasodilatory factors exist in rats or mice, such as adiponectin, which are dependent upon the endothelium, is an area of active investigation.

A previously cited study by Henrichot *et al*. showed that rats fed a HFD developed increased amounts of PVAT around the abdominal but not the thoracic aorta [61]. Interestingly, the abdominal, but not the thoracic aorta, is prone to aneurysm formation. Obesity is an independent risk factor for the development of abdominal aortic aneurysm (AAA) formation [73]. Therefore, the authors concluded that growth of peri-aortic PVAT in the abdominal region of obese patients may contribute to aneurysm formation.

A recent paper by Police *et al*. extended these findings by using a mouse model of AAA to study associated changes in PVAT [74]. Mouse were fed a HFD for 1-4 months and then infused with ATII via osmotic mini-pumps for 28 days. The incidence of aortic aneurysm increased with the duration of HFD[74]. PVAT surrounding the abdominal aorta secreted greater amounts of Mcp-1 than PVAT surrounding the thoracic aorta. Similarly, conditioned media from abdominal PVAT stimulated transwell migration of monocytes to a greater extent than conditioned media from PVAT surrounding the thoracic aorta. Macrophages were seen infiltrating the abdominal PVAT, and the degree of macrophage staining correlated with AAA formation [74]. The authors concluded that increased chemokine secretion in the abdominal PVAT of obese mice may recruit macrophages which subsequently degrade the external elastic lamina of the aorta via secretion of matrix metalloproteinase, thus initiating AAA formation [74].

In the absence of models which are devoid of PVAT, there have been a series of elegant papers which use removal and transplantation of PVAT to study disease in the associated vessel [75, 76]. Perhaps the most of definitive of these studies, was performed by Takaoka *et al*., using the mouse wire injury model[76]. Wire injury of the mouse femoral artery stimulates neointimal hyperplasia, and is similar to the pathophysiology of in-stent restenosis after percutaneous intervention in humans. The authors found that mice fed a HFD had reduced expression of adiponectin, and increased expression of *Mcp-1*, *Tnfα*, *Il6*, and *Pai-*

1 in PVAT surrounding the femoral artery. This was associated with increased macrophage infiltration of femoral PVAT in HFD mice as shown by Mac-3 staining. These changes translated into a large increase in neointima formation after wire injury in the HFD fed mice [76]. Removal of PVAT from lean mice also promoted wire injury neointimal hyperplasia after wire injury; in contrast, transplantation of SAT from lean mice prevented neointimal hyperplasia. Adiponectin alone applied to the vessel in the absence of PVAT prevented robust neointimal hyperplasia. *In vitro*, adiponectin was subsequently shown to inhibit platelet derived growth factor (PDGF) stimulation of smooth muscle cell growth via AMP-activated protein kinase (AMPK). This anti-proliferative effect of adiponectin is abrogated in the PVAT from obese mice. These findings are highly clinically relevant to human disease, as obese diabetic patients have higher rates of in-stent restenosis following PCI, which may be due to reduced adiponectin secretion by epicardial fat [77].

A second study used transplantation of VAT to the carotid artery of *Apoe*$^{-/-}$ mice to determine if inflammation in the perivascular fat depot could impact atherosclerosis [75]. Transplantation of VAT to the carotid artery worsened underlying atherosclerosis in the carotid artery, compared to arteries that received transplants of SAT. In addition, endothelium dependent relaxation of the underlying carotid artery was impaired when VAT was transplanted [75]. The observed increase in atherosclerosis could be prevented by whole body deficiency of P-Selectin glycoprotein ligand-1(*Psgl-1)* or antibodies to Psgl-1.

Although this is an artificial model of inflammation, it does suggest that inflammation in the adventitia can initiate atherosclerosis via activation of underlying vascular endothelium [75].

In summary, the data from human and mouse studies suggest that PVAT serves a beneficial function in lean conditions, to directly or indirectly vasodilate the underlying smooth muscle cells, or to restrain smooth muscle cell hyperplasia, both effects being mediated by adiponectin [65, 76]. Palmitic acid methyl ester is a second paracrine mediator secreted by PVAT which has direct vasodilatory effects on vascular smooth muscle, and there are likely many others which are yet undiscovered [72](Table 1.3). However, in obese conditions, perivascular adipocytes may hypertrophy, leading to the infiltration of macrophages, decreased adiponectin expression, and increased expression of pro-inflammatory cytokines such as TNFα, IL6, and MCP-1 (Figure 1.5). This has been observed to occur in human disease and mouse models of vascular disease [60, 61, 74, 78]. Whether or not inflammation in perivascular adipose tissue directly contributes to the development of atherosclerosis, peripheral vascular disease, or neointimal hyperplasia is a very intriguing hypothesis that has yet to be demonstrated.

TABLE 1.3. Vasocrine Mediators Released From PVAT

Factor	Context	Source	Effect
Beneficial Factors			
Palmitic acid methyl ester[72]	-released from PVAT of SD rats and mouse 3T3L1 cells in culture -decreased release from PVAT of SH rats	-perivascular adipocytes	-vasodilation via direct stimulation of VSMC potassium channels
Adiponectin[65]	-released from lean human PVAT surrounding small arteries in SAT; expression reduced in obese humans	-perivascular adipocyte?	-endothelium dependent vasodilation
Adiponectin[76]	-released from PVAT surrounding femoral arteries of lean mice; expression reduced in obese mice	-perivascular adipocytes	-inhibition of vascular smooth muscle proliferation *in vivo* and *in vitro* via AMPK dependent pathway
Leptin[79]	-studied the response of SH rats to exogenous leptin	-perivascular adipocytes?	-endothelium dependent dilatation of conduit arteries
Pathologic factors			
TNFα[65]	-increased expression in PVAT surrounding small arteries from obese humans	-perivascular adipocytes, or macrophages in PVAT	-loss of vasodilator effect of PVAT; likely due to down regulation of NOS by TNFα
Angiotensin II[72]	-increased expression in the PVAT of SH rats	-perivascular adipocytes	-increased vaso-constriction of aortic rings, blocked by incubation with ATIIR blocker
Visfatin[80]	-increased expression in SD rat PVAT	-perivascular adipocytes	-stimulation of vascular smooth muscle proliferation *in vitro*
Resistin[64]	-increased expression in PVAT from humans with ACS	-macrophages in PVAT?	-stimulates endothelial cell permeability *in vitro*
Complement component 3[81]	-identified in proteomic analysis of PVAT from thoracic aorta of SD rats	-perivascular adipocytes	-stimulates differentiation and migration of adventitial myofibroblasts
Secretory Type II Phospholipase A2	-increased expression in EAT of patients with CAD	-macrophages in PVAT	-promotes formation of inflammatory lipid mediators in EAT

SD=Sprague Dawley rat, SH=Spontaneously Hypertensive rate, EAT=epicardial adipose tissue, CAD=coronary artery disease, PVAT=perivascular adipose tissue, NOS=Nitric oxide synthase, VSMC=Vascular smooth muscle cell, ATIIR=angiotensin II receptor, ACS=acute coronary syndrome

Specific Aims

It is well established that VAT rather than SAT confers an increased risk of cardiovascular disease. This is thought to be due to the propensity for increased VAT to cause insulin resistance. Mechanisms by which VAT causes insulin resistance include increased rates of lipolysis, chronic inflammation, and fatty acid spillover from VAT to peripheral organs such as the liver and skeletal muscle. The latter phenomenon, referred to as “lipotoxicity”, results in the clinically apparent manifestations of the metabolic syndrome which include: hyperglycemia, hypertriglyceridemia, low HDL cholesterol, and increased systolic blood pressure. These risk factors in turn confer the excess cardiovascular risk associated with abdominal obesity.

The propensity for VAT to become inflamed, yet SAT to remain comparatively non-inflamed, has stimulated interest in the unique features of anatomically distinct fat depots in humans and mice. Perivascular adipose tissue (PVAT) is one such depot. PVAT has been proposed as a direct link between obesity and cardiovascular disease. Therefore, we aimed to test the hypothesis that PVAT, like VAT, becomes inflamed in mouse models of obesity or vascular disease. The specific aims of our studies were:

To compare the degree of inflammation in PVAT and VAT in a mouse model of diet induced obesity.

To determine if inflammation in PVAT is associated with atherosclerosis in the apolipoprotein E knockout mouse.

CHAPTER II: Similarity of Mouse Perivascular and Brown Adipose Tissue and their Resistance to Diet Induced Inflammation

Disclaimer:

All experiments were performed by the author except for the following; Figure 2.4 which was done by Greg Hendricks; Figure 2.8 which was done by Sophia Kogan; Figures 2.6 and 2.7 were done by the Morphology Core and the microarray hybridizations by the Genomics Core of the Diabetes and Endocrine Research Center (DK-32520). Jeurg Straubhaar uploaded the microarray data to MACE and performed detailed statistical analyses.

This chapter is in the format published:

Timothy P. Fitzgibbons, Sophia Kogan, Myriam Aouadi, Greg M. Hendricks, Jeurg Straubhaar, and Michael P. Czech. Similarity of mouse perivascular and brown adipose tissues and their resistance to diet-induced inflammation. *Am J Physiol Heart Circ Physiol* 301: H1425-H1437, 2011.

Abstract

Thoracic PVAT is a unique adipose depot that likely influences vascular function and susceptibility to pathogenesis in obesity and metabolic syndrome. Surprisingly, PVAT has been reported to share characteristics of both brown and white adipose, but a detailed direct comparison to inter-scapular BAT has not been performed. Here we show by full genome DNA microarray analysis that global gene expression profiles of PVAT are virtually identical to BAT, with equally high expression of uncoupling protein 1 (*Ucp-1),* cell death-inducing DFFA-like effector A (*Cidea)* and other genes known to be uniquely or very highly expressed in BAT. PVAT and BAT also displayed nearly identical phenotypes upon immunohistochemical analysis, and electron microscopy confirmed that PVAT contained multi-locular lipid droplets and abundant mitochondria. Compared to white adipose tissue (WAT), PVAT and BAT from C57BL6/J mice fed a high fat diet for 13 weeks had markedly lower expression of immune cell-enriched mRNAs, suggesting resistance to obesity induced inflammation. Indeed, staining of BAT and PVAT for macrophage markers (F4/80, CD68) in obese mice showed virtually no macrophage infiltration, and FACS analysis of BAT confirmed the presence of very few CD11b+/CD11c+ macrophages in BAT (1.0%) in comparison to WAT (31%). In summary, murine PVAT from the thoracic aorta is virtually identical to inter-scapular BAT, is resistant to diet induced macrophage infiltration, and thus may play an important role in protecting the vascular bed from inflammatory stress.

Introduction

The burgeoning prevalence of obesity and diabetes throughout the world threatens to accelerate the incidence of associated cardiovascular diseases, including coronary artery disease, hypertension, and congestive heart failure. Although the mechanism by which obesity causes vascular disease is not fully understood, insulin resistance and the metabolic syndrome are thought to play a major role [8, 13, 82, 83]. In human obesity as well as mouse models of obesity, enlarged adipocytes in visceral adipose tissue become insulin resistant and fail to effectively store excess triglyceride through decreased capacity for lipogenesis and increased lipolysis [8, 12, 13, 84, 85]. These changes in adipose function lead to infiltration of immune cells, which are thought to cause chronic low grade inflammation in obese subjects with the metabolic syndrome [13, 86]. Lipid overload in the face of decreased capacity of adipocytes to store triglycerides leads to ectopic lipid deposition in liver and muscle resulting in systemic insulin resistance [13, 34]. Prolonged obesity with these associated disorders is thought to be the major cause of beta cell failure and type 2 diabetes in humans.

It is now well established that expansion of VAT, rather than SAT, confers a high risk for the metabolic syndrome and incident cardiovascular disease [8, 82, 87]. Hypotheses for this observation include: increased expression of angiotensinogen and complement, a greater rate of monocyte infiltration, and increased IL6 secretion in VAT compared to SAT [54]. It has also been postulated that the elevated rates of lipolysis in VAT compared to SAT render the

former less able to sequester triglycerides away from liver and muscle [88]. These and other important differences between VAT and SAT have stimulated interest in the discovery of additional adipose depots which might have similar or increasingly pathologic functions in obesity. One such adipose depot is perivascular adipose tissue (PVAT), which was recently proposed to be a potential link between diabetes and cardiovascular disease [61, 65, 74, 76, 89]. The outermost connective tissue or adventitia surrounding an artery, including PVAT, may be prone to the same inflammation as VAT, and the idea that vascular disease could be impacted and perhaps promoted by factors in the adventitia has long-standing support [55-58].

Initial studies of PVAT from human coronary arteries surprisingly detected expression of some BAT-specific genes (PR domain containing 16 (*PRDM16), UCP-1,* carnitine palmitoyl transferase 1B (*CPT1B)*) to a degree that appeared intermediate to white and brown adipose tissues [89]. These studies suggested PVAT might be an example of the recently described “brite” adipose tissue—white adipose that retains many of its usual characteristics but also displays some expression of BAT genes, including *Ucp-1* [90]. Interestingly, in rodents, PVAT surrounding the abdominal aorta displays characteristics of white adipose tissue, whereas PVAT surrounding the thoracic aorta appears quite different, and is known to express some BAT genes [74, 91]. Although thoracic PVAT showed similarities to BAT in morphology and expressed *Ucp-1*, a direct detailed genomic comparison to true inter-scapular BAT has not yet been made [74, 91].

The extent to which thoracic PVAT in mice is more similar to human coronary PVAT, which displays only partial similarity to BAT, or to true inter-scapular BAT is an important question since mice are frequently used as models of human cardiovascular disease.

We addressed this question by directly comparing genome wide expression of thoracic PVAT to brown and white adipose depots from mice fed a normal or high fat diet for 13 weeks. Remarkably, PVAT and BAT had virtually identical gene expression profiles. Furthermore, in comparison to the infiltration of macrophages into VAT of obese mice and the increased expression of macrophage enriched genes in this tissue, thoracic PVAT and BAT were strikingly resistant to inflammation induced by high fat feeding, as shown by microarray, immunohistochemistry, and FACS analysis. We conclude that PVAT surrounding the murine thoracic aorta is virtually identical to inter-scapular BAT, and like BAT is resistant to inflammation under HFD conditions.

Experimental Procedures

Animal Studies- Male C57BL6/J mice were purchased from the Jackson Laboratory (Bar Harbor, ME). All animals were fed normal chow until 8 weeks of age. Animals were then divided into two groups; one fed normal chow and one fed high fat diet (45 kcal% fat, D12451 Research Diets) for 13 or 20 weeks. Animals were fed *ad libitum* with free access to water and housed in the UMASS Animal Medicine facility with a 12:12 light dark cycle. Animals were weighed

weekly for the duration of the diet study. Intraperitoneal (i.p.) glucose tolerance testing (GTT) was performed as previously described [92]. Area under the curve for the GTT was calculated using the trapezoidal method [92]. At the completion of the high fat diet, mice were fasted for 6 hours and then euthanized with CO2 inhalation and bilateral pneumothorax. SAT (inguinal), VAT (epididymal) and BAT(inter-scapular) were harvested and snap frozen in liquid nitrogen. Blood was drawn via cardiac puncture into heparin coated tubes and the circulatory system was perfused with ice cold PBS. Thoracic PVAT directly adjacent to the lesser curvature of the aortic arch was then harvested and snap frozen in liquid nitrogen. All experiments were performed in accordance with protocols approved by the Animal Care and Use Committee at UMASS Medical School.

Insulin levels- Blood was collected via cardiac puncture at the time of euthanasia into heparin coated microcentrifuge tubes and centrifuged at 3000 x g for 15 minutes. Serum was then decanted and stored at -80 °C. Fasting insulin levels were measured in duplicate with 10 µl of serum using a Rat/Mouse Insulin ELISA (Millipore, St. Charles, MO) according to the manufacturers' instructions.

Quantitative PCR- Adipose tissue was isolated as previously described, snap frozen in liquid nitrogen and stored at -80°C. Tissues were homogenized and total RNA was isolated with RNA Mini Lipid kits (Qiagen, Valencia, CA). 250 ng total RNA was reverse transcribed with the Bio-Rad iScript cDNA Synthesis Kit (Bio-Rad, Hercules, CA). cDNA was diluted 1:5 and 2.5 µl was used in a 12.5 µl

reaction volume; each reaction was performed in duplicate. Real time qPCR was performed with a Bio-Rad C1000 Thermal Cycler and SYBR Green Master Mix (Bio-Rad, Hercules, CA) using the following cycle parameters: 95.0° C for 3 min, 95.0° for 0:10 min, 60.0° C for 0:15 min, 72.0° C for 0:30 min for 40 cycles. Expression was normalized to the reference gene *36b4* and expressed as relative to expression in SAT of normal diet mice using the $2^{-\Delta\Delta ct}$ method [93]. Melt curve analysis and agarose gel electrophoresis was performed to determine the specificity of the PCR reaction products. Primer sequences were: *Ucp-1* for AGGCTTCCAGTACCATTAGGT, *Ucp-1* rev CTGAGTGAGGCAAAGCTGATTT, *Acrp30* for TGTTCCTCTTAATCCTGCCA and *Acrp30* rev CCAACCTGCACAAGTTCCCTT, *36b4* for TCCAGGCTTTGGGCATCA, *36b4 rev* CTTTATCAGCTGCACATCACTCAGA, *Cidea* for ATCACAACTGGCCTGGTTACG, *Cidea* rev TACTACCCGGTGTCCATTTCT, *PPARγ2* for ATGGGTGAAACTCTGGGAG, and *PPARγ2* rev GTGGTCTTCCATCACGGAGA.

Microarray Analysis- RNA was isolated from SAT, VAT, BAT, and PVAT as previously described. RNA concentrations were determined using a Nanodrop 2000 Spectrophotometer (Thermo Fisher, Willmington, DE). The RNA quality was assessed using an Agilent 2100 Bioanalyzer (Agilent Technologies, Santa Clara, CA). Only samples with a RNA Integrity Number >7.5 and normal 18 and 28s fractions on microfluidic electrophoresis were used. RNA from two mice per tissue and diet was pooled for a total of 250 ng total RNA template for cDNA

synthesis and *in vitro* transcription using the Ambion WT Expression kit (Ambion, Carlsbad, CA). Second strand cDNA was then labeled with the Affymetrix WT Terminal Labeling kit and samples were hybridized to Affymetrix Mouse Gene 1.0 ST arrays (Affymetrix, Santa Clara, CA). Gene chip expression array analysis for individual genes was performed as previously described [94], filtering for $p < 0.05$ and a fold change of >2. Three biological replicate hybridizations per tissue and diet were performed, for a total of 24 hybridizations. Robust multi-array average (RMA) was adopted in the UMASS Microarray Computational Environment (MACE) to preprocess raw oligonucleotide microarray data. The algorithm was implemented as a function of the R package Affy [95], which is part of the Bioconductor project [96] using the statistical computing language R (R Foundation for Statistical Computing, Vienna, Austria). All statistical calculations are performed using the R statistical computing environment and results are stored in a relational database. The preprocessed data are stored as base 2 log transformed real signal numbers and are used for fold-change calculations and statistical tests and to determine summary statistics. Mean signal values and standard deviations are computed for each gene across triplicate experiments and stored in the database. The fold change of expression of a gene in two experiments is the ratio of mean signal values from these experiments and is always a number greater than one. If the ratio is less than one, the negative value of the inverse ratio is stored as fold change. All down regulated genes therefore have a negative fold change value, up regulated

genes have a positive fold change. In both cases this value is greater or equal than one.

To determine differential expression of genes in two hybridization experiments MACE internally conducts a Student's t-test with the expression signal values of the two hybridizations for all genes in the set. The t-test value and test p-value are stored in MACE and can be queried through the MACE user interface. The p-values stored and displayed as a result of a query are not adjusted for multiple testing. The data discussed in this publication have been deposited in NCBI's Gene Expression Omnibus [97] and are accessible through GEO Series accession number GSE28440 (http://www.ncbi.nlm.nih.gov/geo/query/acc.cgi?acc=GSE28440).

Histology and Immuno-histochemistry- Adipose tissue samples (n=3 per group) from normal and high fat diet animals were fixed in 4% formalin for immunohistochemistry. Briefly, samples were embedded in paraffin, sectioned, and stained with a rat anti-mouse F4/80 (ABd Serotec, Raleigh, NC)(1:50 dilution) or rat anti-mouse CD68 primary antibody (ABd Serotec, Raleigh, NC)(1:40 dilution). Staining was visualized with a HRP linked rabbit anti-rat secondary anti-body. Staining with the secondary antibody alone was performed as a negative control. Images were taken with a Zeiss Microscope and PixeLINK SE Software.

Transmission electron microscopy of adipose tissue samples- Adipose tissue samples were fixed in 2.5% glutaraldehyde in PBS (pH 7.2). Tissue samples

were dissected into 1 mm blocks and the tissues washed three times and left overnight in fresh buffer. The next morning the samples were post-fixed for 1 hr in 1% osmium tetroxide. The fixed adipose tissue samples were then washed again in the PBS and dehydrated through a graded series of ethanol to 100% and transferred through two changes of propylene oxide and finally into a 50:50 (v/v)mixture of propylene oxide: epoxy resin (SPON 812/Araldite 502) and left overnight to infiltrate. The following morning the adipose tissue samples were processed through two changes of fresh epoxy resin and embedded, allowing the blocks to polymerize 48 hrs at 70°C. Blocks of tissue were then selected, cut out and attached to blank epoxy stubs with a drop of Super Glue. Ultrathin sections were cut on a Reichart-Jung ultramicrotome using a diamond knife. The sections (64 nm thick) were collected and mounted on copper support grids and contrasted with lead citrate and uranyl acetate and examined on a Philips CM 10 transmission electron microscope at 80 Kv accelerating voltage.

FACS Analysis- Mice were euthanized and BAT and VAT was removed and treated with 4 mg/mL and 2 mg/mL collagenase respectively in 4% BSA in PBS at pH=7.4 for 1 hour. Samples were filtered through 200μM and 30 μM spectra mesh sequentially and stained with CD31 (BD Biosciences, Franklin Lakes, NJ; 1:1000 dilution), CD11b (BD Biosciences, Franklin Lakes, NJ; 1:200 dilution) and CD11c (BD Biosciences, Franklin Lakes, NJ; 1:200 dilution) according to the manufacturer's instructions. Samples were run on a BD LSRII flow cytometer (BD

Biosciences, Franklin Lakes, NJ) and analyzed in Flow Jo, gating for CD31 negative cells.

Statistical Analysis- All values are shown as mean ± SEM. For experiments other than the microarray analyses, the Student's *t* test for two tailed distributions with equal variances was used for comparison between 2 groups; for comparisons greater of ≥ 3 groups, two way ANOVA followed by the Bonferroni correction was used. Differences less than $p \leq 0.05$ were considered significant. Data was entered into Microsoft Excel and statistical analyses were performed with Graph Pad Prism 5.

Results

Cidea and Ucp-1 are highly expressed in BAT and PVAT independent of obesity.

HFD mice (n=12) gained more weight than ND mice (n=12) beginning at 3 weeks and remained significantly more obese until the end of the study (30.9 ± 0.75 vs. 42.08 ± 0.78 gms $p<0.001$)(Fig 2.1A). At the end of 13 weeks, HFD mice were more glucose intolerant as shown by an elevated fasting blood glucose concentration (136.4 ± 1.22 vs. 185.8 ± 21.4 mg/dL $p<0.02$), elevated fasting insulin levels (2.1 ± 0.64 vs. 5.4 ± 1.03 ng/mL $p<0.02$), and increased area under the curve for the IPGTT ((min*mg/dL) =29352 ± 753 vs. 38983 ± 1928 $p<0.01$)(Fig 2.1B).

Analysis of mRNA from adipose tissue samples by qPCR showed that *Cidea* and *Ucp-1* were highly expressed in PVAT and BAT compared to SAT. Remarkably, the relative expression between these two depots was similar for both genes (Fig 2.2A,B). Interestingly, *Cidea* expression was reduced >50% by HFD in both PVAT and BAT; this effect was not observed for *Ucp-1* (Fig 2.2A,B). With respect to other markers of adipose differentiation, *PPARγ2* expression was slightly greater in VAT, PVAT, and BAT than SAT and significantly reduced by HFD in these depots (Fig 2.2D). Adiponectin (*Acrp30)* expression was significantly greater in VAT and decreased with HFD (Fig 2.2C); expression of this gene was similar in all other depots. Therefore, PVAT expresses *Cidea* and *Ucp-1* to an equivalent degree as BAT, suggesting that it may be more similar to BAT than “brite” adipose tissue. Furthermore, it is responsive to HFD and not different from other adipose depots with respect to makers of adipose differentiation, such as *PPARγ2* and *Acrp30*.

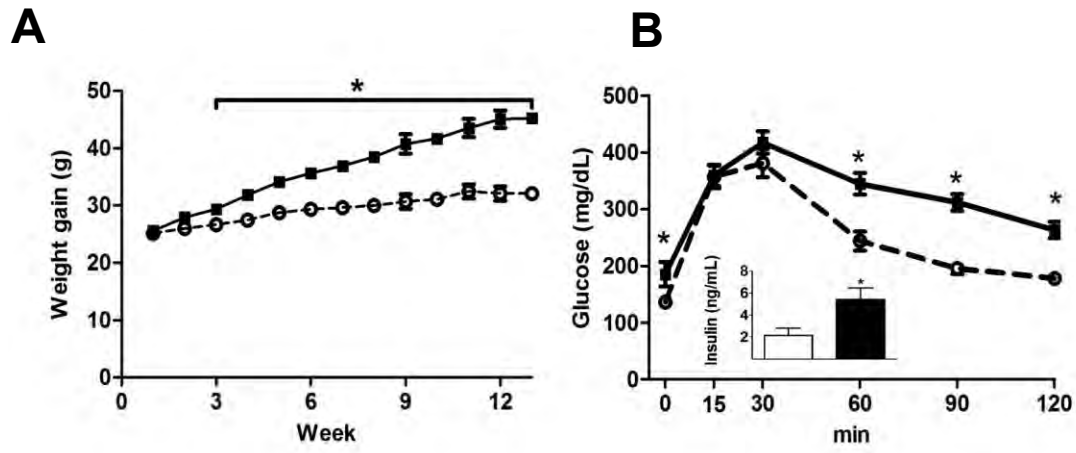

FIGURE 2.1. Thirteen weeks of HFD results in obesity, glucose intolerance and hyperinsulinemia in C57BL6/J Mice. (A) Growth curves of normal diet (n=12, dashed line) and high fat diet mice (n=12, solid line). Weights were significantly different at all time points after 3 weeks. Data points are mean ± SEM. *p<0.05 vs. ND using the Student's t test. (B) Intraperitoneal glucose tolerance test from C57BL6/J mice fed normal (n=12, dashed line) or high fat diet (n=12, solid line) for 13 weeks. Results are mean ± SEM. *p<0.05 vs. ND using the Student's t test. (Inset) Fasting insulin levels in normal (n=12, white) and high fat diet mice (n=12, black). Results are mean ± SEM. *p<0.05 vs. ND using the Student's t test.

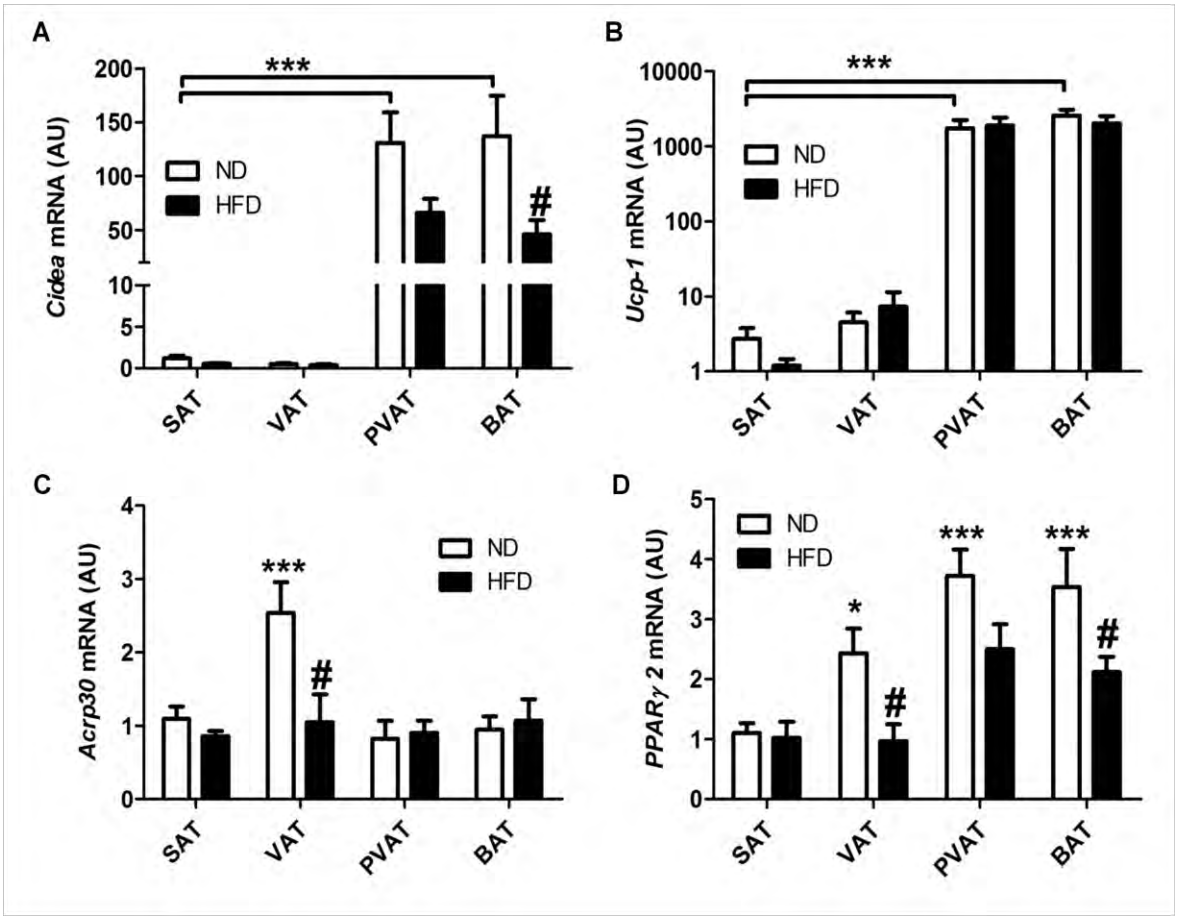

FIGURE 2.2*. Cidea* and *Ucp-1* are highly expressed in BAT and PVAT independently of obesity. (A,B,C,D) *Cidea, Ucp-1, Pparγ2* and *Acrp30* expression in normal and high fat diet mice. qPCR was performed on total RNA isolated from inguinal (SAT), epididymal (VAT), inter-scapular brown (BAT) and perivascular adipose from the aortic arch (PVAT). Expression levels were calculated with the $2^{-\Delta\Delta ct}$ method using *36b4* as the reference gene and normalized to expression in SAT from normal diet conditions. *Ucp-1* expression is shown in log10 scale. (ND n=12 white, HFD n=12, black) Results are mean ± SEM. *** $p<0.001$ vs. SAT ND, # $p<0.05$ ND vs. HFD of the same fat depot using two way ANOVA and the Bonferonni correction.

Mouse Thoracic PVAT is morphologically similar to BAT.

In order to test the hypothesis that thoracic PVAT is virtually identical to inter-scapular BAT, we performed microscopic analysis of these adipose depots. As judged by light microscopy on hematoxylin and eosin stained sections of PVAT and BAT under ND and HFD conditions, PVAT appeared very similar to BAT, with round nuclei, and small, multi-locular lipid droplets (Fig 2.3*G*). The majority of PVAT surrounding the thoracic aorta had the appearance of BAT, with small areas of adipose tissue resembling WAT (Fig 2.3*G*). BAT lipid droplet architecture was obviously distorted by 13 weeks of HFD, with enlargement and coalescence of lipid droplets (Fig 2.3F). Surprisingly, this effect was not apparent in PVAT, although it did occur with a longer duration of HFD.

Transmission electron microscopy confirmed the BAT phenotype of thoracic PVAT, and detected some interesting differences compared to inter-scapular BAT (Fig 2.4). Both PVAT and BAT from mice fed ND were densely packed with mitochondria and had multi-locular lipid droplets which were darkly stained with osmium tetroxide (Fig 2.4*A, C*). Interestingly, lipid droplets in BAT tended to lose their avidity for osmium when obtained from mice after high fat feeding, mostly appearing white (Fig 2.4*B*). This effect was not observed in PVAT (Fig 2.4*D*). High fat feeding resulted in significant mitochondrial swelling and unfolding of cristae in PVAT (Fig 2.4*D*), which was not apparent in BAT at this time point, but visible after a longer duration of HFD (Data not shown). These observations

correlated with changes in gene expression. For example, *Fads1* was significantly down regulated (-1.82) in BAT compared to PVAT in HFD conditions. Likewise, a search for alterations in the expression of mitochondrial genes revealed that expression of the pro-apoptotic gene *Bid* and mitochondrial solute carrier genes *Slc25a35* and *Slc25a37* were up regulated in PVAT compared to BAT in HFD conditions; a third member of this latter gene family, the calcium binding carrier protein Aralar1(*Slc25a12*), was significantly up regulated in BAT compared to PVAT (2.58 FC, p=0.002). Therefore, thoracic PVAT and BAT appear virtually identical upon analysis by both light and electron microscopy, with the exception of subtle differences in lipid droplet and mitochondrial morphology, which correlate with changes in gene expression.

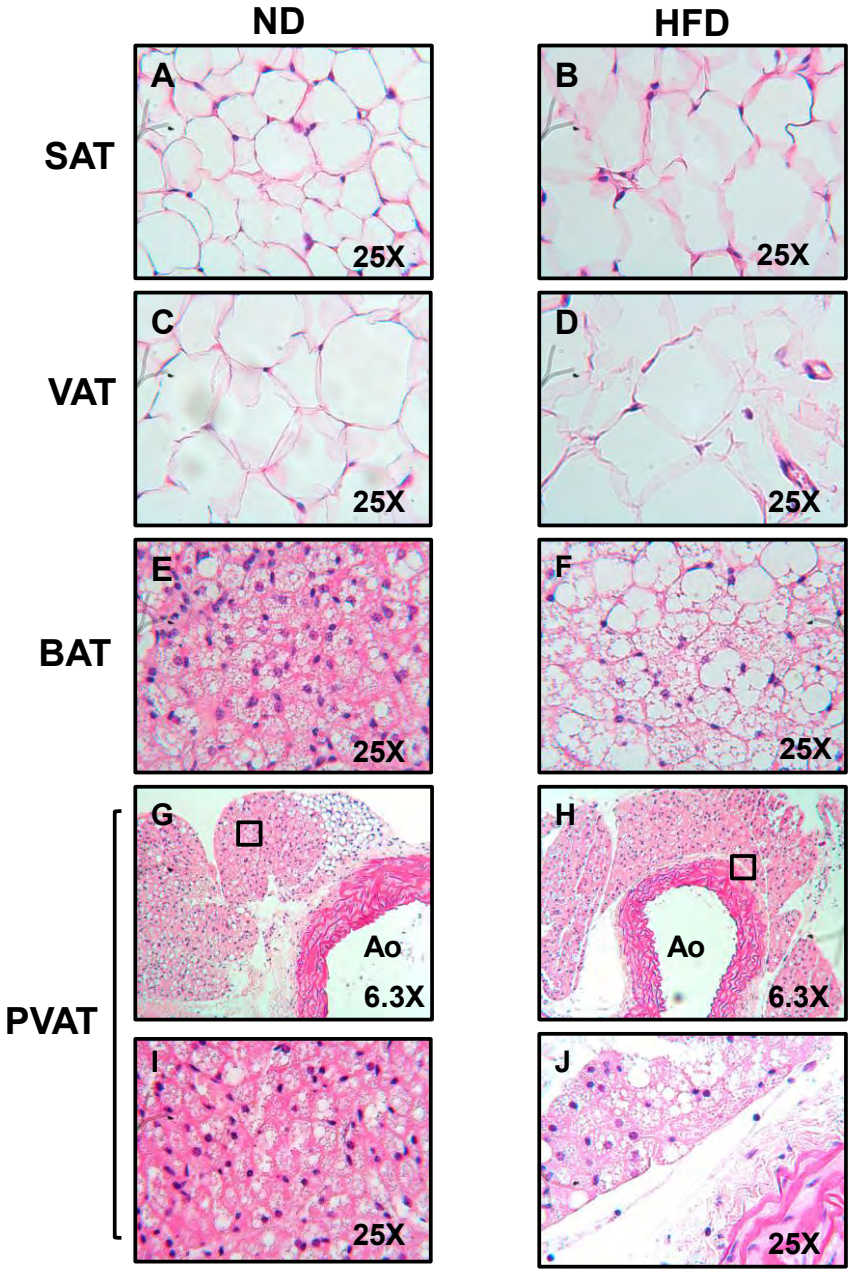

FIGURE 2.3. Perivascular adipose tissue appears morphologically similar to brown adipose tissue. Fat was harvested from subcutaneous, visceral, inter-scapular brown and perivascular adipose tissue from the lesser curvature of the aortic arch from normal and high fat diet fed mice and then fixed in formalin. Tissues were stained with hematoxylin and eosin and visualized at 25x. Images G and H are low magnification images (6.3x) of I and J. (Ao=aortic lumen)

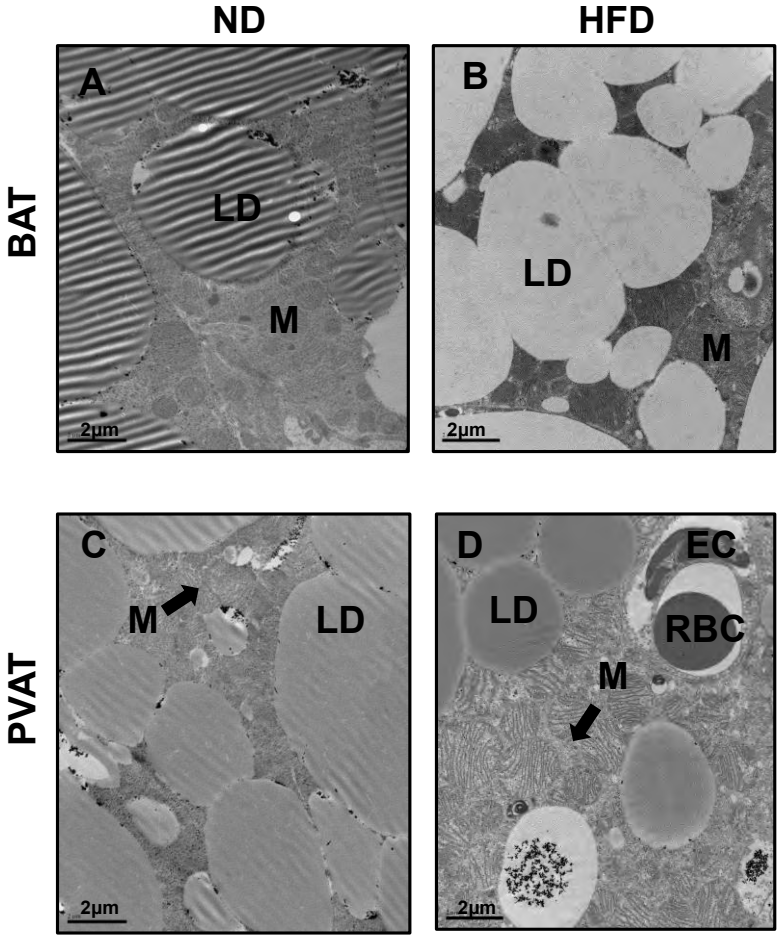

FIGURE 2.4. Transmission electron microscopy reveals many similarities between perivascular and brown adipose tissues. Sections of brown (A,B) and perivascular adipose (C,D) were taken and stained with osmium tetroxide. In normal diet conditions, brown (A) and perivascular adipose (C) appear very similar with multi-locular lipid droplets and abundant mitochondria. Two prominent changes were noted in high fat feeding conditions; lipid droplets in brown adipose tissue, but not perivascular, lose their avidity for osmium tetroxide (B), and mitochondria become swollen with unfolded cristae (D); the latter effect was more prominent in perivascular adipose but also observed in brown adipose after a longer duration of HFD. (Magnification 7900x, scale bar= 2 microns, LD=lipid droplet, M=mitochondria, EC=endothelial cell, RBC=red blood cell)

Microarray analysis confirms PVAT has a characteristic brown adipose gene expression signature.

To validate and expand the above findings, DNA microarrays were used to contrast global differences in gene expression between adipose depots from mice under control and high fat feeding conditions. Total RNA was hybridized to Affymetrix Mouse Gene 1.0 ST chips, each of which contains probes targeting 28,853 genes. Analysis of the full genome set of gene expression differences among the four adipose depots showed high similarity of PVAT to BAT, and a much greater divergence of gene expression when compared to white adipose depots (SAT,VAT)(Figure 2.5, Table 2.1, Supplementary Tables S1-4). When comparing PVAT to BAT in normal diet conditions, only 228 genes demonstrated significantly different expression (Fig 2.5, Supplemental Table S3). With regard to the specific genes which were differentially expressed, in comparison to BAT, PVAT had greater expression of immunoglobulin genes (*IgK, Igh-6*), complement (*Cfh, C7*), and mast cell specific genes (*Mcpt4*)(Supplemental Table S3). In contrast, the vast majority of genes whose expression was greater in BAT than PVAT were related to skeletal muscle differentiation and function (Supplemental Table S3). Interestingly, additional genes expressed to a greater extent in BAT than PVAT were highlighted by the mesodermal developmental genes *Tbx15* (3.8 fold), *Myf6* (3.2 fold), and *Zic1* (2.1 fold)(Supplemental Table S3).

Next, we refined this analysis by comparing gene expression differences in PVAT relative to BAT and SAT from mice fed ND with respect to selected specific gene categories (Table 2.1). Strikingly, there were no significant differences between PVAT and BAT in levels of expression of any genes known to be highly expressed in brown adipocytes (Table 2.1). Nor were there any differences between PVAT and BAT under ND conditions in the expression of the majority of specific genes examined, with the exception of *Fads1* (Table 2.1). In contrast to these virtually identical gene expression profiles between PVAT and BAT, highly significant decreases in expression were displayed by brown adipocyte enriched genes in SAT and VAT compared to PVAT (Table 2.1). As expected, expression of white adipose enriched genes was significantly greater in SAT and VAT compared to PVAT (Table 2.1). In other gene categories, expression of the adipokines *Lep, Retn*, *Rbp4,* and *Adipoq* was higher in SAT and VAT, whereas the receptors for *Adipoq* (*Adipor1/Adipor2*) were more highly expressed in PVAT (Table 2.1). In regards to lipid metabolism genes, those involved in synthesis or storage (*Fads1, Fads3, Cidec*) were expressed to a greater extent in SAT and VAT, whereas those functioning in lipid oxidation (*Gpam, Acss1, Acsl5*) were more highly expressed in PVAT and BAT (Table 2.1). Surprisingly, expression of immune cell enriched genes, such as chemokines *(Ccl5, Ccl8),* T cell receptors (*Cd3g*, *Cd3d),* and macrophage markers (*Cd68, Emr1)* was significantly greater in SAT and VAT compared to PVAT and BAT even under ND conditions (Table 2.1). Given this dramatic difference in

expression of immune cell genes in white compared to brown adipose depots, we compared the effects of high fat feeding on changes in expression of immune cell enriched genes in the four adipose depots.

Shown in Table 2.2 are the fold changes in expression for a series of selected immune cell enriched genes when comparing ND to HFD conditions in PVAT, BAT, SAT and VAT depots. VAT demonstrated the greatest fold increase in expression of immune cell genes after high fat feeding (Table 2.2). Although the other depots exhibited some trends for changes in gene expression between ND and HFD fed mice, none of them met statistical significance (Table 2.2). Taken together, the data in Figure 2.5 and Tables 2.1 and 2.2 reveal a remarkably similar global gene expression profile between PVAT and BAT. These two adipose depots show no significant differences in expression in the majority of genes previously shown to be enriched in brown adipocytes, white adipocytes or immune cells. In addition, the data in Table 2.2 is particularly revealing in that the levels of expression of immune cell genes, as reflected by their probe set signals, is uniformly higher in both SAT and VAT compared to PVAT and BAT in both ND and HFD conditions. These data imply that the PVAT and BAT depots are relatively resistant to inflammation induced by high fat feeding compared to WAT depots.

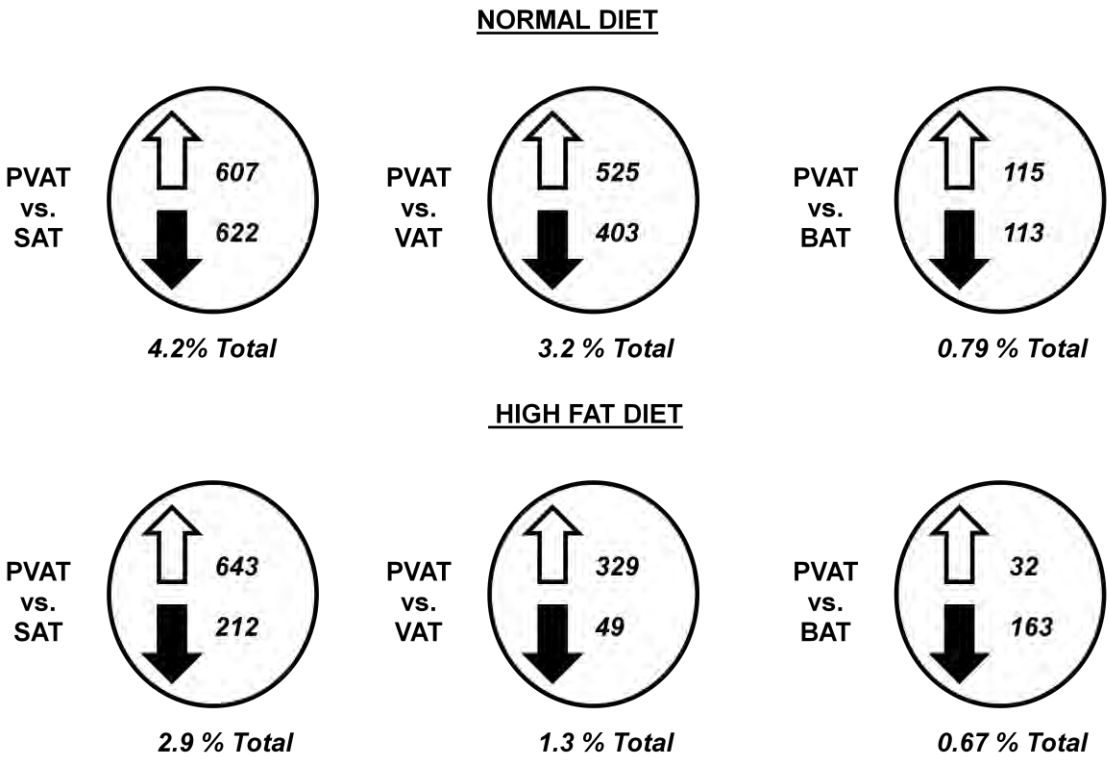

FIGURE 2.5. Microarray analysis reveals that PVAT is more similar to BAT than SAT or VAT. The MACE database was queried in ND and HFD conditions for genes with a >2.0 fold change in expression at P<0.05 level of significance between adipose depots. In normal diet conditions, PVAT was very similar to BAT, with differential expression of only 228 genes (0.79% of genes); in contrast, expression of 1229 genes was differentially regulated when comparing PVAT and SC (4.2% of genes). After high fat feeding, PVAT became more similar to white adipose, as the number of genes differentially regulated between PVAT and SC was reduced to 855 (2.9% of genes).

	PVAT vs. SAT		***PVAT vs. VAT***		***PVAT vs. BAT***	
Symbol	**FC**	**P value**	**FC**	**P value**	**FC**	**P value**
			Most Highly Enriched Genes			
Ucp1	**21.6**	**<0.001**	**31.2**	**<0.001**	1.0	NS
Elovl3	**19.3**	**<0.001**	**29.3**	**<0.001**	1.1	NS
Slc27a2	**17.9**	**<0.001**	**17.2**	**<0.001**	1.4	NS
Cox7a1	**16.1**	**<0.001**	**23.1**	**<0.001**	1.0	NS
Cpt1b	**14.5**	**<0.001**	**24.7**	**<0.001**	1.0	NS
Kng2	**14.0**	**<0.001**	**12.4**	**<0.001**	1.2	NS
Acot11	**12.6**	**<0.001**	**15.8**	**<0.001**	1.0	NS
Cidea	**12.6**	**<0.001**	**31.8**	**<0.001**	1.1	NS
			Brown adipose-enriched genes			
Ucp1	**21.6**	**<0.001**	**31.2**	**<0.001**	1.0	NS
Elovl3	**19.3**	**<0.01**	**29.2**	**<0.001**	1.1	NS
Slc27a2	**17.8**	**<0.001**	**17.1**	**<0.001**	1.4	NS
Cox7a1	**16.1**	**<0.001**	**23.0**	**<0.001**	1.0	NS
Cpt1b	**14.5**	**<0.001**	**24.7**	**<0.001**	1.1	NS
Cidea	**12.6**	**<0.001**	**31.7**	**<0.001**	1.1	NS
Dio2	**8.0**	**<0.001**	**9.9**	**<0.001**	-1.1	NS
Prdm16	**1.8**	**<0.001**	**2.41**	**<0.001**	1.0	NS
			White adipose-enriched genes			
Hoxc8	*-9.7*	*<0.001*	*-17.7*	*<0.001*	2.1	NS
Apol7c	*-8.2*	*<0.01*	-1.6	NS	1.2	NS
Dapl1	*-6.3*	*<0.01*	-2.0	NS	1.8	NS
Nnat	*-6.1*	*<0.01*	*-6.9*	*<0.01*	1.1	NS
Sncg	*-4.2*	*<0.01*	*-5.5*	*<0.001*	1.0	NS
Stap1	*-4.7*	*<0.05*	-1.4	NS	2.9	NS
Grap2	*-3.9*	*<0.01*	-1.4	NS	1.5	NS
Mest	*-3.8*	*<0.01*	*-14.2*	*<0.001*	1.0	NS

			Immune cell-enriched genes			
Il7r	*-5.7*	*<0.01*	-1.3	NS	2.4	NS
Ccl5	*-5.6*	*<0.05*	-1.3	NS	1.6	NS
Cd3g	*-5.0*	*<0.01*	-1.7	NS	2.3	NS
Ccl8	*-4.1*	*<0.01*	1.0	NS	-1.3	NS
Ccr7	*-4.0*	*<0.05*	-1.3	NS	1.4	NS
Cd3d	*-3.1*	*<0.05*	-1.2	NS	-1.1	NS
Cd68	*-2.3*	*<0.05*	*-1.9*	*<0.05*	-1.3	NS
Emr1	*-2.1*	*<0.05*	*-2.3*	*<0.01*	-1.3	NS
			Fatty acid biosynthesis and metabolism			
Fads3	*-2.5*	*<0.01*	*-4.5*	*<0.001*	-1.1	NS
Fads1	1.5	NS	*-1.8*	*<0.01*	*-1.7*	*<0.05*
Cidec	*-1.1*	*<0.05*	*-1.6*	*<0.01*	-1.3	NS
Scd1	-1.0	NS	-1.0	NS	1.0	NS
Fasn	-1.5	NS	-1.5	NS	1.0	NS
Gpam	**2.6**	**<0.001**	**1.4**	**<0.01**	1.0	NS
Acss1	**3.2**	**<0.001**	**4.9**	**<0.001**	1.1	NS
Acsl5	**3.7**	**<0.001**	**4.2**	**<0.001**	1.1	NS
			Adipokine and related effector genes			
Lep	*-2.7*	*<0.05*	*-4.6*	*<0.01*	-1.3	NS
Retn	*-1.8*	*<0.001*	*-2.1*	*<0.001*	-1.8	NS
IL6st	*-1.4*	*<0.001*	*-1.4*	*<0.01*	-1.2	NS
Rbp4	*-1.4*	*<0.05*	*-2.3*	*<0.001*	-1.0	NS
Adipoq	*-1.3*	*<0.05*	*-1.6*	*<0.01*	-1.1	NS
Tnfaip6	*-1.3*	*<0.05*	*-1.2*	*<0.05*	-1.0	NS
Adipor1	**1.3**	**<0.01**	**1.1**	**<0.05**	-1.0	NS
Adipor2	**1.4**	**<0.05**	-1.1	NS	1.0	NS

TABLE 2.1. Depot specific expression of select gene categories in normal diet conditions.

*The eight most highly up-regulated genes in PVAT vs. SAT in normal diet conditions were ranked in descending order. Expression levels of the same genes in PVAT vs. VAT and PVAT vs. BAT in normal diet conditions were then queried, and are entered in the last two columns for comparison. Expression of genes from select categories was also queried in normal diet conditions, and ranked according in descending order according to expression in SAT. Genes with significantly increased expression in PVAT are in bold and genes with significantly decreased expression in PVAT are italicized. NS=non-significant

	SAT				*VAT*				*PVAT*				*BAT*			
Symbol	**ND**	**HFD**	**FC**	**P**	**ND**	**HFD**	**FC**	**P**	**ND**	**HFD**	**FC**	**P**	**ND**	**HFD**	**FC**	**P**
Il7r	2038	1299	-1.5	NS	***268***	***2779***	***10.4***	***<0.001***	178	350	1.9	NS	62	164	2.6	NS
Tlr13	564	531	-1.1	NS	***397***	***2404***	***6.0***	***<0.001***	133	343	2.6	NS	151	243	1.6	NS
Il1rn	444	499	1.1	NS	***367***	***1923***	***5.2***	***<0.001***	220	403	1.8	NS	208	269	1.2	NS
Cd84	665	574	-1.2	NS	***426***	***2079***	***4.9***	***<0.001***	128	281	2.2	NS	92	171	1.9	NS
Mpeg1	1527	1292	-1.2	NS	***713***	***3311***	***4.6***	***<0.001***	240	555	2.3	NS	233	520	2.2	NS
Cd68	2434	2160	-1.1	NS	***2097***	***6895***	***3.3***	***<0.001***	586	1451	2.5	NS	500	914	1.8	NS
Ccl3	303	329	1.1	NS	***207***	***662***	***3.2***	***<0.001***	111	194	1.7	NS	116	182	1.6	NS
Emr1	1247	1177	-1.1	NS	***1276***	***3800***	***3.0***	***<0.001***	283	604	2.1	NS	242	475	2.0	NS
Ccl2	536	556	1.0	NS	***546***	***1174***	***2.1***	***<0.05***	158	225	1.4	NS	138	185	1.3	NS
Ccl9	1457	1691	1.1	NS	***1529***	***3262***	***2.1***	***<0.01***	347	780	2.2	NS	249	467	1.8	NS
Tnfrsf1b	911	735	-1.2	NS	***682***	***1183***	***1.7***	***<0.01***	226	304	1.3	NS	184	256	1.4	NS

TABLE 2.2. Comparative expression of immune cell enriched genes in VAT, SAT, PVAT, and BAT in normal and high fat diet conditions.
Querying the MACE dataset for genes with the greatest fold increase in expression from normal to high fat diet conditions, showed that VAT had the greatest increase in expression of inflammatory genes. The same probe sets showed non-significant increases in SAT, and much smaller signals in PVAT and BAT. Bold face, italicized genes are significantly up regulated. NS=non significant.

***Thoracic PVAT and inter-scapular BAT are relatively resistant to macrophage infiltration under HFD conditions*.**

In order to directly test the extent of macrophage infiltration into BAT and PVAT, we immunostained sections of SAT, VAT, BAT and PVAT from the thoracic aorta for the macrophage marker *F480* (Fig 2.6). Feeding mice a HFD for 13 weeks resulted in significant macrophage infiltration in VAT and SAT, as expected (Fig 2.6*B,D*). In contrast, little or no F4/80 staining was detected in BAT or PVAT from these same mice (Fig 2.6*F,H*). In order to test whether a longer duration of HFD would result in inflammation of BAT or PVAT, we continued HFD for 20 weeks in a second cohort of animals (Fig 2.7). Again, visceral fat showed abundant macrophage infiltration (Fig 2.7*D*), but despite marked enlargement and coalescence of lipid droplets in BAT and PVAT, macrophages were absent (Fig 2.7*F,H*). The same results were obtained after staining BAT and VAT from animals fed a HFD for 20 weeks with a second macrophage marker, CD68 (Data not shown).

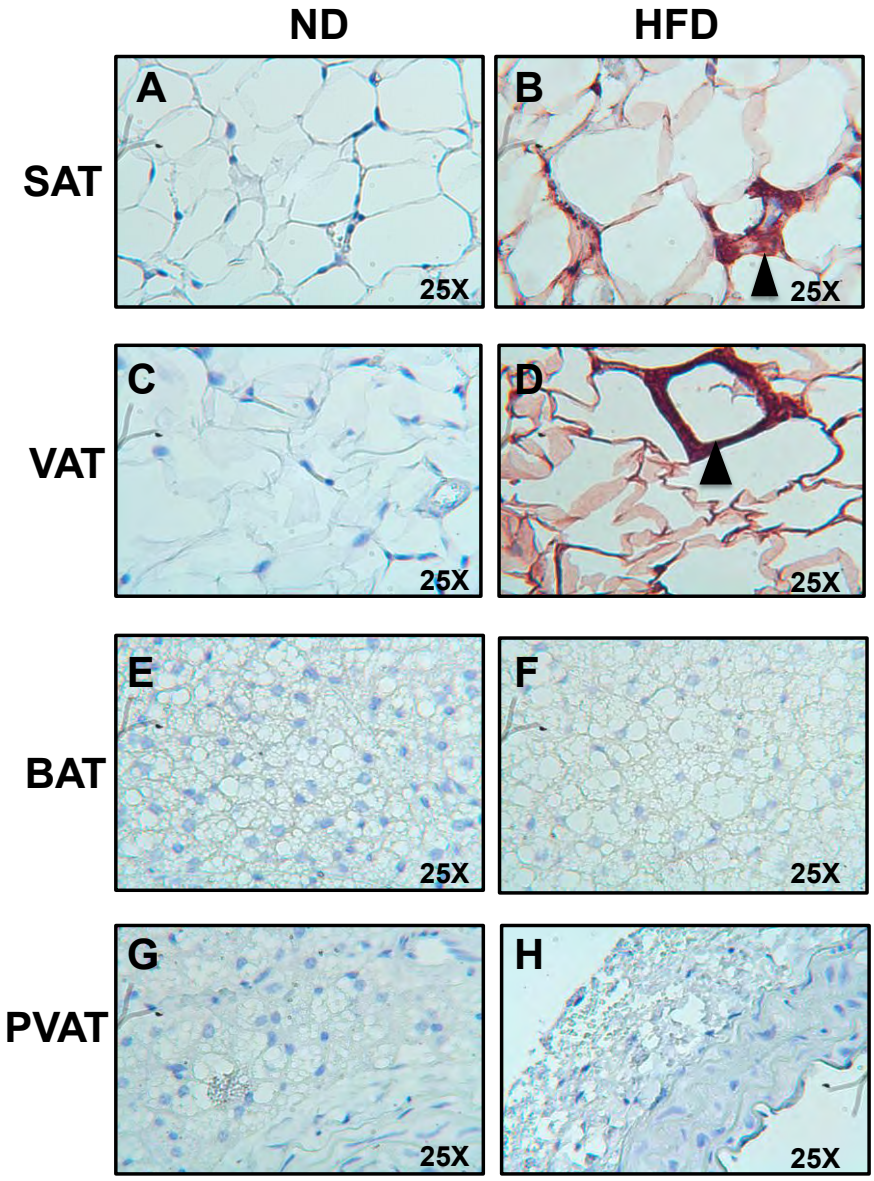

FIGURE 2.6. Perivascular and brown adipose tissue are resistant to inflammation after 13 weeks high fat diet . SAT, VAT, BAT, and PVAT from the aortic arch was harvested from lean and obese mice (n=3 per group). Samples were fixed in 4% formalin, sectioned, and stained with a rat anti-mouse F4/80 primary antibody (ABd Serotec). Staining was visualized with a HRP linked rabbit anti-rat secondary anti-body. Abundant macrophages were seen predominantly in VAT, but also SAT, forming crown like structures (arrowheads). No macrophages were seen in brown or perivascular adipose tissue. (Magnification 25x)

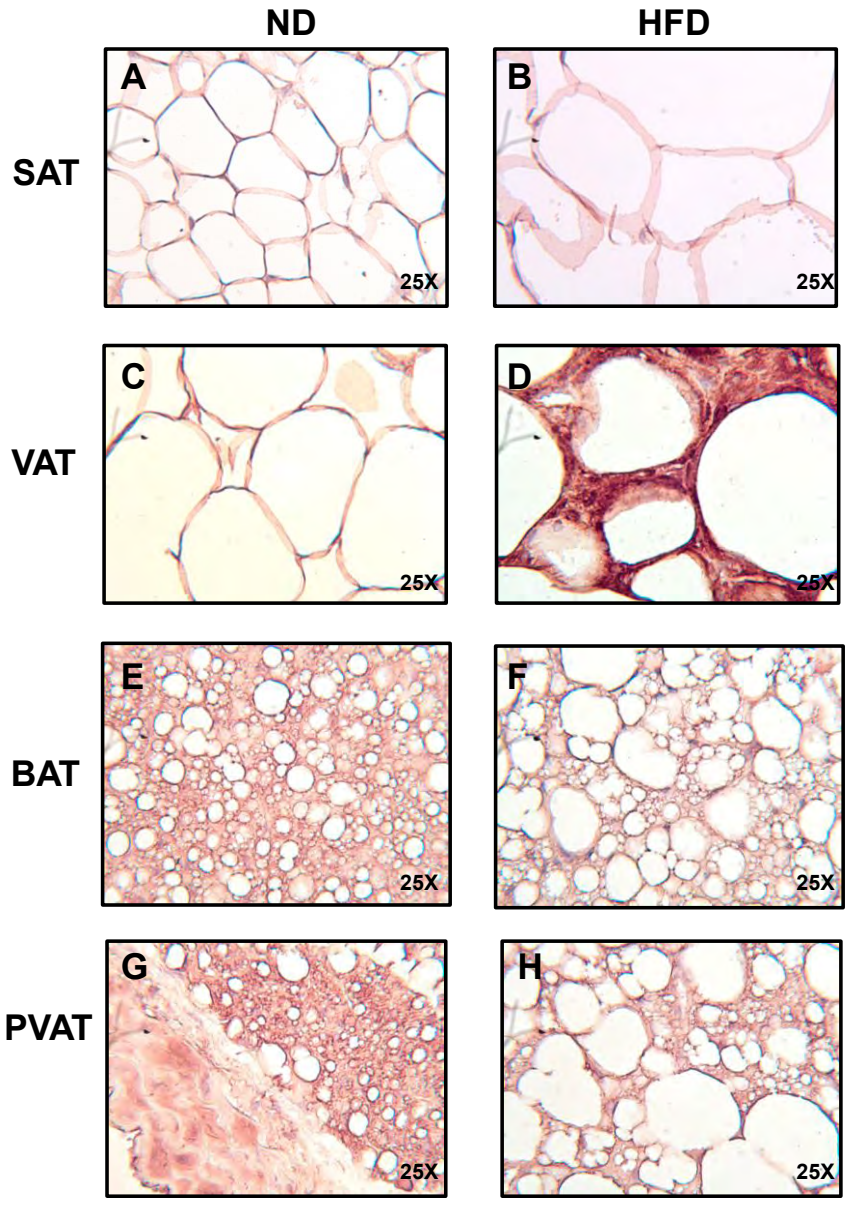

FIGURE 2.7. Perivascular and brown adipose tissue are resistant to inflammation after 20 weeks high fat diet . SAT, VAT, BAT, and PVAT from the aortic arch was harvested from lean and obese mice (n=3 per group). Samples were fixed in 4% formalin, sectioned, and stained with a rat anti-mouse F4/80 primary antibody (ABd Serotec). Staining was visualized with a HRP linked rabbit anti-rat secondary anti-body. Abundant macrophages were seen predominantly in VAT, but also SAT, forming crown like structures (arrowheads).

FACS analysis confirms prolonged HFD in mice results in little macrophage infiltration of BAT compared to VAT.

In order to better characterize the levels of macrophage accumulation in VAT versus BAT, we performed FACS analysis on the stromal vascular fraction (SVF) of collagenase digested adipose tissue from VAT and BAT in ND and HFD conditions. CD68 and F4/80 markers define total macrophage populations in adipose tissue, but do not differentiate between cells at various levels of activation [22, 29, 98]. Therefore, after exclusion of CD31+ endothelial cells from the SVF, we chose to doubly stain cells for CD11b and CD11c, the latter being a marker of classical (M1) macrophage differentiation [98]. Eleven weeks of HFD resulted in a striking and significant enrichment of CD11b+/CD11c+ macrophages in VAT compared to that observed for BAT (31.7% vs. 1.03%)(Fig 2.8*A*). As we failed to observe macrophage recruitment into BAT with 11 weeks of HFD, we extended the duration of the HFD to 20 weeks (Fig 2.8*B*). This prolonged HFD duration resulted in a marked, significant increase in CD11b+/CD11c+ macrophages in VAT, while BAT showed no enrichment of this cell population. Unfortunately, we were unable to perform FACS on PVAT due to the small quantity of this tissue in the aortic arch. However, the results of FACS analysis confirm that VAT is enriched with M1 macrophages after 11 and 20 weeks of HFD, while BAT was resistant to this effect.

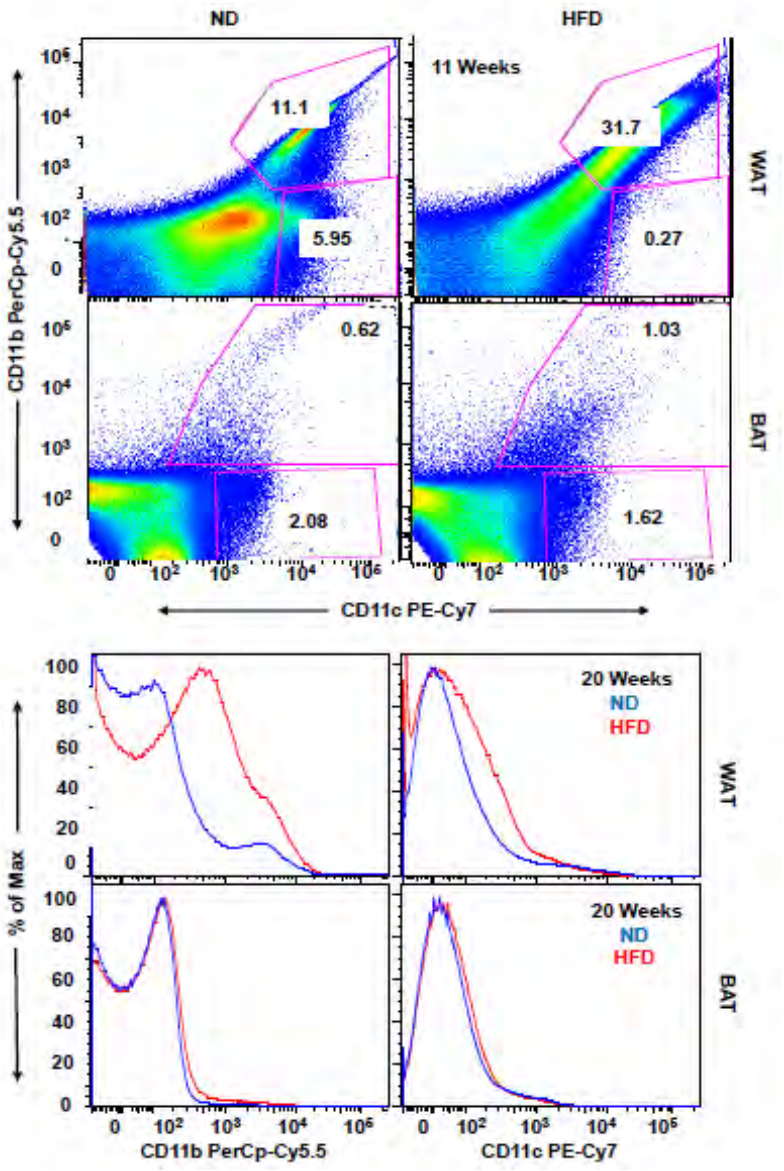

FIGURE 2.8. Brown adipose tissue is resistant to inflammation after 11 and 20 weeks of HFD. (Top) After 11 weeks HFD, the SVF was isolated from VAT and BAT and stained with CD31-PE, CD11b-PerCp Cy5.5, and CD11c-PE Cy7. Samples were analyzed on a LSRII flow cytometer, gating for CD31 negative cells. High fat feeding resulted in a significant increase in the percentage of CD11b and CD11c positive cells in the SVF of visceral but not brown adipose (31.7% vs. 1.03%). (Bottom) Similar results were obtained after 20 weeks of HFD. Results are representative of three independent experiments.

Discussion

A major finding of the present studies is that PVAT from the murine thoracic aorta displays a gene expression pattern that is nearly identical to inter-scapular BAT (Fig 2.5, Table 2.1, Supplementary Tables S3 & S4). The similarity of gene expression between PVAT and BAT includes identical expression levels of the brown adipocyte genes *Cidea*, *Ucp-1, Dio2,* and *Prdm16*. Only 0.79% of genes represented on chip were differentially regulated between PVAT and BAT in normal diet conditions at the stringency level used. Interestingly, immunoglobulin genes were expressed to a greater extent in PVAT; this has also been demonstrated in human coronary PVAT [60]. We hypothesize that this due to the presence of vascular associated lymphoid tissue [99], although we have been unable to visualize such tissue using B cell specific markers (Data not shown).

In contrast to these subtle differences between PVAT and BAT, major differences between PVAT and WAT were observed in the expression of genes previously shown to be highly and selectively expressed in brown or white adipose tissues (Table 2.1). Our data thus clarify and definitively substantiate previous indications that mouse thoracic PVAT is similar to BAT [74, 91, 100]. Importantly, these previous studies demonstrate that PVAT can have characteristics of both BAT and WAT, but this dichotomy largely depends upon the anatomical context; that surrounding the abdominal aorta resembling WAT and that surrounding the thoracic aorta BAT [74, 91]. Our studies directly

comparing thoracic PVAT gene expression (Table 2.1, Supplementary Tables S1-S4, and Fig 2.5) and histological appearance (Fig 2.3) to mouse inter-scapular BAT show unequivocally that these two adipose depots are virtually identical. This appears different from human coronary PVAT which demonstrates an intermediate phenotype between white and brown adipose [89].

After 13 weeks of high fat feeding, VAT displayed the expected dramatic increase in expression of many immune cell enriched genes, while thoracic PVAT and BAT did not. This was somewhat surprising because some previous reports indicated that increased infiltration of macrophages and T cells into both PVAT [54, 74, 76] and BAT [101, 102] could be detected in mouse models. Xu *et al*. reported that genetic and diet induced obesity resulted in chronic inflammation in WAT but not BAT[29]. Thus the extent of BAT inflammation may greatly depend upon the mouse strain and conditions used. Our data are consistent with the results of Xu *et al*. suggesting BAT is comparatively resistant to inflammation in C57BL6/J mice after HFD feeding.

In contrast to our present findings of very low inflammation of PVAT in mice after 13 weeks of HFD, some investigators have proposed that PVAT is an intrinsically pro-inflammatory depot [60, 61, 89]. For example, humans with established coronary artery disease have higher mRNA and protein levels of IL-1β, IL-6, MCP-1, and TNFα in epicardial adipose than in paired SAT samples. More recently, Chatterjee *et al.* published data regarding human coronary PVAT

and murine thoracic PVAT, the same anatomic fat depot we have studied here. In control mice, relative mRNA expression of *Acrp30*, *Pparγ* and *Fabp4* was lower in PVAT than SAT. With two weeks of HFD feeding, expression of these adipocyte specific genes further declined, while expression of the pro-inflammatory genes *Lep* and *Mip1α* increased [89]. The authors concluded that in comparison to SAT, PVAT was poorly differentiated and intrinsically pro-inflammatory, and hence possibly an etiologic factor in the development of vascular disease [89].

Our findings are in contrast to the above [89] in that expression of *Acrp30* and *Pparγ2* was not different in thoracic PVAT compared to other fat depots. A possible explanation for the difference in expression of *Acrp30* and *Pparγ2* between the two studies is that there may be diet or age dependent changes in the expression of these two genes; Chatterjee *et al*. used a shorter duration HFD and younger mice [89]. For example, it may be that younger and older mice than those studied herein (21 weeks) are prone to inflammation of PVAT. Two studies which have reported obesity associated inflammation of abdominal and femoral PVAT, used 40 week and 22 week old mice respectively[74, 76]. Therefore it is likely that many factors including age, strain, diet, and specific anatomic location influence whether or not PVAT becomes inflamed. Finally, although they did not report expression of BAT genes in their mouse model, their failure to observe significant expression of immune cell specific genes C*d68* and *Cd3* by qPCR does concur with our results [89].

Importantly, both we and Chatterjee *et al.* have studied PVAT from the thoracic aortic arch, as this a segment of the aorta prone to atherosclerosis both in humans and mice [89]. Although PVAT was originally hypothesized to signal in a "vasocrine" fashion to influence vascular tone [59], it has subsequently been implicated in adventitial inflammation which might promote atherosclerosis [54, 59-61, 89]; our study was designed to test these latter hypotheses.

The overall evidence from the literature combined with our present work suggests that PVAT can have different characteristics depending upon its anatomical location. Thus BAT-like adipose surrounds the thoracic aorta and WAT surrounds the abdominal aorta [74, 91]. As such, we suggest that PVAT surrounding the abdominal aorta, like its visceral fat counterpart, is prone to the dysregulated adipocyte biology of obesity and subsequent inflammation. This idea has been verified by Takaoka *et al*., who demonstrated that PVAT surrounding the femoral artery is WAT that has beneficial properties in lean conditions which are mediated by the paracrine effects of adiponectin (*Acrp30*)[76]. In obese states, inflammation and macrophage infiltration of PVAT surrounding the femoral artery results in decreased adiponectin secretion and increased *Tnfα* expression, both of which facilitate pathological neointimal hyperplasia in response to vessel injury [76]. In humans, neointimal hyperplasia contributes to the pathophysiology of coronary artery disease. For example, diabetes and obesity are associated with increased rates of in-stent restenosis following percutaneous intervention (PCI) due to neointimal hyperplasia [77]. A

scenario in which white PVAT is beneficial in lean conditions, but becomes dysfunctional in obese conditions, is analogous to the current model of obesity induced insulin resistance [13]. These and other reports support the concept that PVAT with white adipose features conforms to this model [65, 74, 76, 103]. The important contribution of our work is that brown PVAT surrounding the thoracic aorta appears to be resistant to obesity induced inflammation, and hence may offer protection from the associated changes to the arterial adventitia.

The finding that PVAT and BAT display little or macrophage infiltration under HFD conditions, while WAT does, raises the interesting question: what is unique to WAT that causes infiltration of macrophages? A recent paper by Kosteli *et. al* may shed insight into this important question [34]. Using caloric restriction of previously HFD fed mice, the authors showed that rates of adipocyte lipolysis correlate with macrophage infiltration. These studies suggest that the chronic elevation in WAT lipolysis observed in obesity causes increased release of fatty acids, which serve to stimulate macrophage infiltration [34]. This hypothesis offers a potential explanation for why BAT and BAT-like PVAT fail to attract immune cells. The unique function of BAT and PVAT to rapidly metabolize fatty acids via high capacity for beta-oxidation likely results in relatively low rates of local free fatty acid release from the cells in comparison to WAT [104]. A second possibility, is that the fatty acid species released by BAT and PVAT may also afford an anti-inflammatory effect. The ratio of saturated to polyunsaturated fatty acids has been shown to increase in the VAT and abdominal PVAT of high

fructose fed rats [105]. Thus under these conditions WAT may release relatively higher levels of saturated fatty acids, which may be more active in stimulating macrophage chemotaxis [36, 106]. Finally, abdominal or white PVAT may secrete pro-inflammatory adipokines or cytokines. We have found that although white adipose (SAT, VAT) has greater expression of adiponectin, which has anti-inflammatory effects, it also has greater mRNA expression of adipokines which correlate with vascular disease (*Rbp4, Resistin*)(Table 2.1)[107, 108]. Furthermore, abdominal PVAT has been shown to secrete greater amounts of the chemokine MCP-1 than thoracic PVAT; our data also confirm that *Mcp-1(Ccl-2)* mRNA is increased in VAT but not thoracic PVAT after high fat feeding (Table 2.2)[74]. The comparatively greater diameter of white adipocytes in VAT and abdominal PVAT may be one factor responsible for increased *Mcp-1* transcription [109, 110].

In summary, results from this present study demonstrate that PVAT surrounding the thoracic aorta is effectively BAT, as shown by light and electron microscopy, and full genome expression analysis. Thoracic PVAT and inter-scapular BAT are resistant to inflammation induced by 13 and 20 weeks of HFD, as shown by reduced expression of immune cell enriched genes, immunohistochemistry with macrophage markers, and FACS analysis for activated macrophages. This work provides an important mandate to study expression of BAT genes in human PVAT from patients with and without vascular disease. In light of the recent discovery of functional BAT in adult humans, and

given the known beneficial metabolic and herein described anti-inflammatory properties of BAT, promotion of a BAT phenotype in the perivascular niche may have important effects in preventing vascular diseases such as hypertension and atherosclerosis.

Limitations

We acknowledge that there are many limitations to our study. First and foremost, it is merely associative and does not provide any information regarding causality, and even if we did observe macrophage infiltration, the HFD fed mouse does not develop atherosclerosis or vascular disease. We are limited in studying the effect of perivascular fat in that there are no mouse models of “depot” specific fat ablation. Creation of such technology would greatly advance the field. It is interesting that the lipodystrophic A-FIP/F-1 mouse is hypertensive [111]. However, these mice have specific white adipose tissue ablation and the remaining brown adipose is functionally converted to white.

Second, immunohistochemistry of PVAT is not a very sensitive or specific technique to exclude the presence of macrophages. We could not do FACS with PVAT due to the limited amount of tissue (10-100 mg). In the future, we may consider verifying our results with rat PVAT, which would provide enough tissue to do FACS.

Finally, one must question the relevance of the study of brown adipose tissue to human physiology. However, the observation that human epicardial fat

expresses intermediate levels of BAT specific genes (*PRDM16, UCP-1, CPT1B*), is what motivated our interest in the first place [89, 112]. Furthermore, the recent reports of functional brown adipose tissue in adult humans has reinvigorated the field and provided some legitimate rationale for our studies [113, 114].

CHAPTER III: Protection against diet induced obesity and insulin resistance in the apoE knockout mouse is accompanied by an attenuated transcriptional response in visceral fat.

Contributions: All experiments were performed by me. Sarah Nicoloro assisted with the RNA preparation for the microarrays. Phyllis Spatrick from the DERC Genomics Core made the cRNA, hybridized and scanned the chips. Jeurg Straubhaar uploaded the microarray data to MACE and performed detailed statistical analyses. The UMASS Mouse Phenotyping Center performed the body composition analysis and metabolic cages. Darleen Lessard from Quantitative Health Sciences assisted with the ANCOVA. The DERC morphology core made the slides and performed the immunohistochemical staining.

Abstract

Despite severe hyperlipidemia leading to the development of atherosclerosis, apolipoprotein E knockout (EKO) mice are protected from diet induced obesity and insulin resistance. This is counterintuitive to the prevailing hypothesis that increased circulating free fatty acids (FFA) and triglyceride rich lipoproteins (TGRL) cause peripheral insulin resistance, and may be due to defective lipid uptake in target organs of EKO mice. We tested the hypothesis that in this model of atherosclerosis, inflammation of PVAT occurs. EKO mice fed HFD for 24 weeks were leaner and more insulin sensitive than WT littermates. HFD EKO mice had increased post-prandial VO2 and serum β-hydroxybutyrate. We were surprised to find that macrophage specific gene expression, as determined by either microarray analysis or RT-PCR was not increased in either the PVAT or the VAT of HFD fed EKO mice. While the VAT of WT mice had extensive alterations in gene expression in response to HFD, in particular, enrichment of inflammatory gene expression and broad down regulation of PPARγ target and adipogenic genes, EKO VAT did not. Importantly, the EKO VAT instead showed increased expression of genes encoding enzymes in fatty acid oxidation pathways. HFD fed EKO VAT was also characterized by smaller adipocyte size and, in comparison to WT HFD, decreased staining for the macrophage marker F480+. We conclude that, 1) Inflammation in thoracic PVAT does not occur in conjunction with atherosclerosis in EKO mice, 2) EKO mice have increased post–prandial VO2 (ml/hr) and

hepatic lipid oxidation, both of which may contribute to their lean phenotype, and 3) EKO mice remain lean on a HFD despite hyperlipidemia. The decreased adiposity of EKO mice correlates with reduced adipocyte size, reduced adipose tissue inflammation and *increased* expression of genes encoding enzymes responsible for oxidation of fatty acids. Consistent with previous work showing apoE controls adipocyte uptake and deposition of TG, its absence prevents adipocyte hypertrophy and resultant inflammation of VAT. Thus, limiting adipocyte acquisition of fatty acids may be advantageous, provided that compensatory mechanisms to prevent sustained hyperlipidemia and peripheral organ lipotoxicity can be activated.

Introduction

Apolipoprotein E (apoE) is a 34 kD glycoprotein which is a component of all lipoprotein particles except low density lipoprotein (LDL)[115]. It is a ligand for the clearance of chylomicrons and intermediate density lipoprotein particles (IDL) from the circulation via the low density lipoprotein receptor (LDLR), very low density lipoprotein receptor (VLDLR) and low density lipoprotein related protein 1(LRP1)[116]. EKO mice have dramatic elevations of plasma cholesterol (5 fold normal) and reduced high density lipoprotein (HDL) concentrations [44, 45]. These findings mimic those of human patients with Type III hyperlipoproteinemia, which results in increased plasma triglyceride (TG) and cholesterol and premature atherosclerosis.

Apoe is highly expressed in the liver, adipose tissue, macrophages, and other tissues of humans and mice. In adipocytes, apoE expression is increased by PPARγ agonists and decreased by TNF-α [117]. Multiple recent studies have documented protection of the EKO mouse from diet induced obesity (DIO) and insulin resistance [118-121]. Whole body deficiency of apoE also prevents weight gain and insulin resistance in genetic models of obesity such as the *ob/ob* or *Ay/+* mouse [119, 121, 122]. Protection from diet induced obesity can be reversed by adenoviral over expression of apoE in the liver, suggesting an important role for circulating apoE in adipose tissue lipid uptake [119].

On the other hand, endogenous adipocyte apoE expression is required for the uptake and storage of TG. For example, primary adipocytes from EKO mice cultured *in vitro* synthesize less TG than WT when incubated with VLDL [123]. Furthermore, EKO adipocytes transplanted into WT mice fail to increase in size in response to 10 weeks of HFD [123]. There are at least two mechanisms by which the absence of apoE impairs TG uptake in adipocytes [116, 124]. Binding and whole particle uptake of VLDL to EKO adipocytes is impaired due to reduced expression and/or decreased cell surface localization of VLDLR, LDLR, and LRP1[124]. Lipoprotein lipase (LPL) dependent TG synthesis is also decreased in EKO adipocytes. This is thought to be due impaired fatty acid translocation across lipid rafts, as caveolin 1 expression is markedly reduced in EKO adipocytes [124]. These same mechanisms may also account for reduced lipid

uptake in liver and skeletal muscle, protection from lipotoxicity, and preservation of whole body insulin sensitivity despite severe hyperlipidemia [116, 125].

Although EKO mice are protected from the metabolic effects of hyperlipidemia, they develop severe atherosclerosis on a normal chow diet at 8-12 weeks of age [44, 45]. Hyperlipidemia results in the subendothelial retention of apoB containing lipoproteins [35]. Monocytes then enter intimal space and differentiate into macrophages which engulf modified lipoprotein particles and become foam cells [35]. In contrast to adipocytes, uptake of lipid by macrophages is not dependent on apoE. Foam cells take up modified lipoproteins via scavenger receptors, predominantly SRA and CD36 [126]. Rather, apoE in macrophages is important in reverse cholesterol transport and lipidation of ApoA1 and HDL by cholesterol export via ABCA1 and ABCG1[127]. The importance of this function is highlighted by two studies in which bone marrow transplantation of $apoE^{+/+}$ macrophages into EKO mice ameliorates atherosclerosis; this is accompanied by improvements in serum lipoprotein profiles to wild type levels [128, 129]. Therefore, in contrast to adipocytes and other tissues, macrophage specific apoE appears to serve a protective effect in respect to lipid handling [127]. This serves to distinguish the role of the macrophage in atherosclerosis from its role in diet induced obesity, the depletion of which, improves metabolic disease[98].

The specific lipid moieties that stimulate foam cell formation in each case might account for these differences. While it is well established that modified lipoprotein particles are the stimulus for foam cell formation in atherosclerosis, it has only recently been shown that local FFAs may be responsible for foam cell formation in the context of increased lipolysis, such as obesity or fasting [34]. In this regard, adipocytes from EKO mice have been shown to have increased rates of lipolysis *in vitro*, therefore we would expect greater inflammation in the VAT of these mice [117].

Therefore, the aims of this study were to determine 1) is atherosclerosis associated with inflammation in thoracic PVAT, 2) is decreased lipid uptake by VAT associated with increased expression of genes encoding enzymes responsible for *de novo* lipogenesis and 3) is the visceral adipose tissue of EKO mice characterized by increased foam cell accumulation analogous to the atherosclerotic plaque?

Experimental procedures

Animal Studies- An original colony *Apoe*$^{-/-}$ (*Apoe*^{tm1Un}) on the C57BL6/J background was purchased from the Jackson Laboratory (Bar Harbor, ME). Mice were backcrossed to C57BL6/J to obtain WT control littermates. All animals were fed normal chow until 8 weeks of age. Male wild type and EKO mice were then divided into two groups (n=5-6 per group); one fed normal diet (ND) and one fed high fat diet (HFD)(42% Milk fat, 0.2% cholesterol, Harlan

TD88137) for 24 or 38 weeks respectively. Animals were fed *ad libitum* with free access to water and housed in the University of Massachusetts (UMASS) Medical School Animal Facility with a 12:12 hour light-dark cycle. Animals were weighed weekly for the duration of the diet study. Intraperitoneal glucose tolerance testing was performed as previously described [92]. Area under the curve for the GTT was calculated using the trapezoidal method . At the completion of HFD, mice were fasted for 4 hours and then euthanized with CO2 inhalation and bilateral pneumothorax. SAT (inguinal), VAT (epididymal), and BAT (interscapular) were harvested and snap frozen in liquid nitrogen. All experiments were performed in accordance with protocols approved by the Animal Care and Use Committee at UMASS Medical School.

Metabolic Phenotyping- Body composition was determined non-invasively in awake mice using ^{1}H-MRS (Echo Medical System). For metabolic studies, mice were housed under controlled temperature and lighting with free access to food and water. The food/water intake, energy expenditure, respiratory exchange ratio, and physical activity were performed on three consecutive days using metabolic cages (TSE Systems). Post prandial oxygen consumption was calculated by subtracting the pre-fed VO2 (ml/hr)(16:00) from the post-fed (VO2)(6:00) as previously described[130].

Free Fatty Acid and β hydroxybutyrate Levels- Blood was collected via cardiac puncture at the time of euthanasia into heparin coated micro centrifuge tubes and

centrifuged at 3000 x g for 15 minutes. Serum was then decanted and stored at -80 °C. Serum free fatty acids were measured with the NEFA (2) colorimetric kit according the manufacturer's instructions (Wako Diagnostics, Richmond, VA). β hydroxybutyrate was measured with a colorimetric assay (#700190) according to the manufacturer's instructions (Cayman Chemicals, Ann Arbor, MI).

Quantitative PCR- Adipose tissue was isolated as previously described, snap frozen in liquid nitrogen and stored at -80°C. Tissues were homogenized and total RNA was isolated with RNA Mini Lipid kits (Qiagen, Valencia, CA). 250 ng total RNA was reverse transcribed with the Bio-Rad iScript cDNA Synthesis Kit (Bio-Rad, Hercules, CA). cDNA was diluted 1:5 and 2.5 µl was used in a 12.5 µl reaction volume; each reaction was performed in duplicate. Real time qPCR was performed with a Bio-Rad C1000 Thermal Cycler and SYBR Green Master Mix (Bio-Rad, Hercules, CA) using the following cycle parameters: 95.0° C for 3 min, 95.0° for 0:10 min, 60.0° C for 0:15 min, 72.0° C for 0:30 min for 40 cycles. Expression was normalized to the reference gene *36b4* using the $2^{-\Delta\Delta ct}$ method [93]. Melt curve analysis was performed to determine the specificity of the PCR reaction products.

Microarray Analysis- RNA was isolated from epididymal VAT as previously described. RNA concentrations were determined using a Nanodrop 2000 Spectrophotometer (Thermo Fisher, Willmington, DE). The RNA quality was assessed using an Agilent 2100 Bioanalyzer (Agilent Technologies, Santa Clara, CA). Only samples with a RNA Integrity Number >7.5 and normal 18 and 28s

fractions on microfluidic electrophoresis were used. 250 ng total RNA was used as template for cDNA synthesis and *in vitro* transcription using the Ambion WT Expression kit (Ambion, Carlsbad, CA). Second strand cDNA was then labeled with the Affymetrix WT Terminal Labeling kit and samples were hybridized to Affymetrix Mouse Gene 1.0 ST arrays (Affymetrix, Santa Clara, CA). Gene chip expression array analysis for individual genes was performed as previously described [94], filtering for $p < 0.05$ and a fold change of >2. Four biological replicate hybridizations per genotype and diet were performed, for a total of 24 hybridizations. Robust multi-array average (RMA) was adopted in the UMASS Microarray Computational Environment (MACE) to preprocess raw oligonucleotide microarray data. The algorithm was implemented as a function of the R package Affy [95], which is part of the Bioconductor project [96] using the statistical computing language R (R Foundation for Statistical Computing, Vienna, Austria). All statistical calculations are performed using the R statistical computing environment and results are stored in a relational database. The preprocessed data are stored as base 2 log transformed real signal numbers and are used for fold-change calculations and statistical tests and to determine summary statistics. Mean signal values and standard deviations are computed for each gene across triplicate experiments and stored in the database. The fold change of expression of a gene in two experiments is the ratio of mean signal values from these experiments and is always a number greater than one. If the ratio is less than one, the negative value of the inverse ratio is stored as fold

change. All down regulated genes therefore have a negative fold change value, up regulated genes have a positive fold change. In both cases this value is greater or equal than one.

To determine differential expression of genes in two hybridization experiments MACE internally conducts a Student's t-test with the expression signal values of the two hybridizations for all genes in the set. The t-test value and test p-value are stored in MACE and can be queried through the MACE user interface. The p-values stored and displayed as a result of a query are not adjusted for multiple testing.

Histology and Immunohistochemistry- Adipose tissue samples (n=3 per group) from normal and high fat diet animals were fixed in 4% formalin for immunohistochemistry. Briefly, samples were embedded in paraffin, sectioned, and stained with a rat anti-mouse F4/80 (ABd Serotec, Raleigh, NC)(1:40 dilution). Staining was visualized with a HRP linked rabbit anti-rat secondary anti-body. Staining with the secondary antibody alone was performed as a negative control. Images were taken with a Zeiss Microscope and PixeLINK SE Software.

Statistical Analysis- All values are shown as mean ± SEM. For experiments other than the microarray analyses, the Student's *t* test for two tailed distributions with equal variances was used for comparison between 2 groups; for comparisons greater of ≥ 3 groups, two way ANOVA followed by the Bonferroni correction was used. Differences less than $p < 0.05$ were considered significant.

Data was entered into Microsoft Excel and statistical analyses were performed with Graph Pad Prism 5.

Results

Atherosclerosis is not associated with increased expression of F480, CD68, or Mcp-1 in thoracic PVAT

In order to test the hypothesis that atherosclerosis is associated with increased inflammation in PVAT, we dissected PVAT from the lesser curvature of the aortic arch in WT ND, WT HFD, EKO ND and EKO HFD mice (n=6 per group). We also isolated VAT and inter-scapular BAT and SAT as positive and negative controls respectively. qPCR for the macrophage markers *F480*, *Cd68*, and the chemokine *Mcp-1* are shown in Figure 3.1. Expression was normalized to SAT ND for each gene. Expression of *F480* and *Cd68* was significantly increased in the VAT of WT HFD mice compared to SAT ND ($p<0.05$). Although *Mcp-1* expression was also increased in HFD VAT, it did not reach statistical significance. Expression of *F480*, *Cd68*, and *Mcp-1* was not significantly increased in the PVAT of ND or HFD EKO mice compared to ND SAT. Interestingly, expression of these genes was also not increased in the VAT of the HFD EKO mouse. Therefore we concluded that atherosclerosis is not associated with increased expression of *F480*, *Cd68*, or *Mcp-1* in thoracic PVAT.

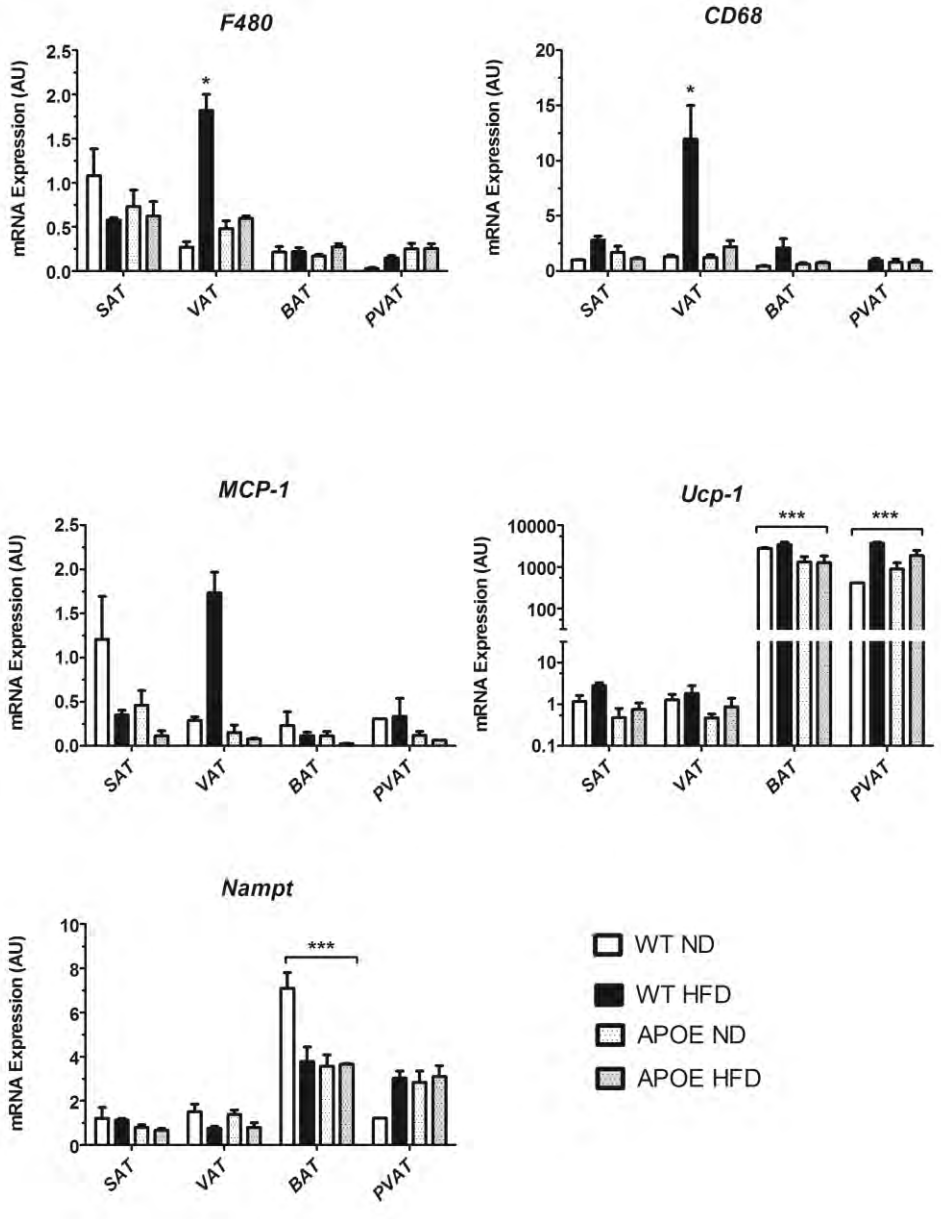

FIGURE 3.1. Expression of macrophage markers *F480* and *Cd68* is increased in the VAT of HFD mice but not the PVAT or VAT of EKO mice. WT and EKO mice were fed ND or HFD for 24 weeks. RNA was harvested from SAT, VAT, BAT and PVAT from the aortic arch. qPCR was performed and expression was normalized to ND SAT using the $2^{-\Delta\Delta ct}$ method with *36B4* as the reference gene. *p<0.05 vs. WT ND SAT, ***p<0.001 vs. WT ND SAT using the Students t test

EKO mice are resistant to DIO after 24 and 38 weeks of HFD

Male WT and EKO mice were started on ND or HFD at 8 weeks of age (n=5-6 per group). After 24 weeks, WT HFD mice were significantly more obese than their ND littermates (48.0 ± 1.6 vs. 33.0 ± 0.8 gms, $p<0.001$)(Figure 3.2A). In contrast, there was no difference between ND and HFD fed EKO mice (34.9 ± 0.5 vs. 34.8 ± 1.1 gms, p=NS). Fasting plasma glucose was significantly lower in HFD EKO than HFD WT controls and FFA were significantly higher (Table 3.1). Intra-peritoneal GTT revealed that HFD WT mice had impaired glucose tolerance compared to their ND controls at all time points ($p<0.05$)(Figure 3.2C). In contrast, there was no significant difference in glucose tolerance between ND and HFD fed EKO mice.

In a second cohort of animals, we decided to extend the duration of HFD to determine if age related impairments in insulin sensitivity might influence fat accumulation in EKO mice. Surprisingly, even after 38 weeks of HFD, there was no difference in weight between ND and HFD fed EKO mice (32.4 ± 0.44 vs. 30.20 ± 0.54, p=NS), nor were there differences in glucose tolerance as seen by IP GTT (Figure 3.2D, F).

Body composition analyses of mice at 24 weeks of HFD revealed a fivefold increase in fat mass of WT mice, whereas HFD EKO mice had a non significant doubling of fat mass (Table 3.1). Diet and genotype had no influence on lean body mass (Table 3.1).

In summary, 24 and 38 weeks of a diet high in saturated fat and cholesterol results in obesity and diabetes in WT but not EKO mice. Increased body mass is due to a five-fold increase in fat mass of HFD fed WT mice. This is consistent with prior studies and extends these data to high fat feeding of chronic duration.

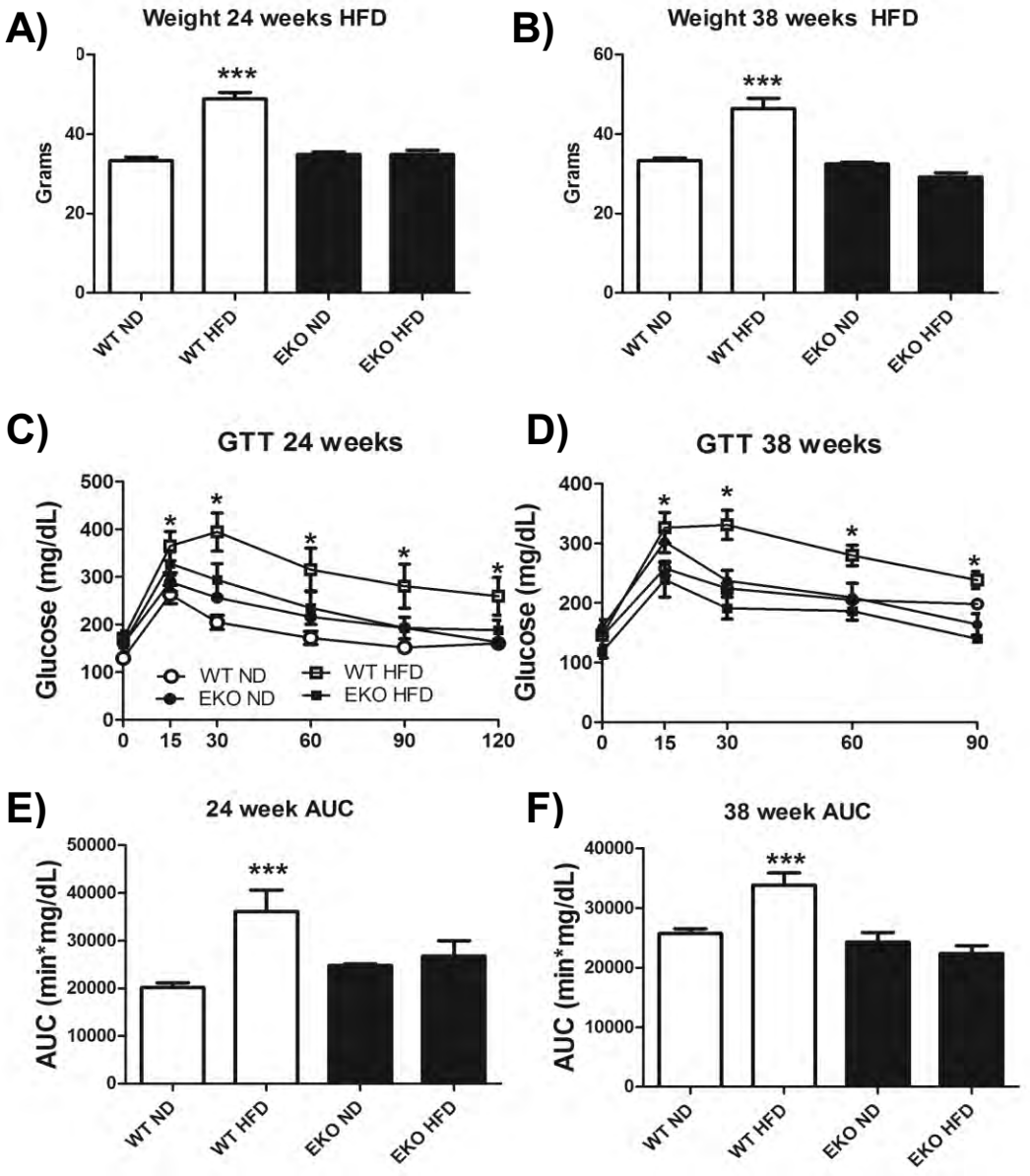

FIGURE 3.2. EKO mice are resistant to diet induced obesity and impaired glucose tolerance after 24 and 38 weeks of HFD. A,B) Weight of WT and EKO mice after 24 and 38 weeks of HFD (n=5-6 per group). C,D) Intraperitoneal GTT in WT and EKO mice after 24 and 38 weeks of HFD. E,F) Area under the curve for the IP GTT at 24 and 38 weeks. *p< 0.05 vs. WT ND, ***p<0.001 vs. WT ND using the Student's t-test

	WT ND (n=5)	WT HFD (n=5)	EKO ND (n=5)	EKO HFD (n=6)
Weight (gms)	31.4 ± 0.7	*41.9 ± 0.3***	32.0 ± 1.0	35.0 ± 2.3
Fat mass (gms)	3.6 ± 1.0	*15.3 ± 0.2***	3.1 ± 0.7	7.0 ± 1.9
Lean mass (gms)	26.9 ± 0.8	25.8 ± 0.3	28.3 ± 0.7	27.3 ± 0.8
24 Hour VO2 Consumption (ml/hr/kg)	3512 ± 126	3073 ± 24	3671 ± 126	*3804 ± 294**
Light phase VO2 Consumption (ml/hr/kg)	3424 ± 116	2883 ± 57	3470 ± 38	*3670 ± 267***
Dark phase VO2 Consumption (ml/hr/kg)	3801± 142	3263 ± 21	4001 ± 150	*4066 ± 333 **
24 Hour VCO2 Production (ml/hr/kg)	3038 ± 138	2379 ± 49	3112 ± 143	*2988 ± 251**
24 Hour Energy Expenditure Rate (kcal/hr/kg)	*17.6* ± 0.65	14.7 ± 0.13	17.9 ± 0.65	18.3 ± 1.43
Raw 24 Hour VO2 Consumption (ml/hr)	112.8 ± 3.2	128.0 ± 1.05	117.2 ± 3.3	125.8 ± 2.8
Respiratory Exchange Ratio (RER)	0.8 ± 0.01	*0.7 ± 0.01*†††	0.8 ± 0.01	*0.7 ± 0.01*†††
Food intake (gms/day)	3.6 ± 0.55	2.3 ± 0.33	4.3 ± 0.47	2.7 ± 0.14
Physical activity (counts/day)	4853 ± 413	4853 ± 456	5886 ± 1219	4717 ± 726
Free fatty acids (mmol/L)	0.5 ± 0.05	0.8 ± 0.16	*2.2 ± 0.35*^^^	*3.1 ± 3.1*^^^
Fasting plasma glucose (mg/dl)	185 ± 13	204 ± 11	146 ± 14	*148 ± 13**
GTT AUC (min*mg/dl)	32367 ± 2724	44748 ± 3384***	26532 ± 2976	32735 ± 2352
β hydroxybutyrate (mM)	0.36 ± 0.08	0.83 ± 0.24	3.0 ± 0.24	*4.9 ± 0.56†*

***p<0.001 vs. WT ND using the Student's t-test,
*p<0.05, **p<0.01 vs. WT HFD using two way ANOVA and the Bonferroni correction
††† p<0.001 vs. ND within genotype using two way ANOVA and the Bonferroni correction
^^^p<0.001 vs. WT ND, HFD using two way ANOVA and the Bonferroni correction.
† p<0.001 vs. EKO ND using two way ANOVA and the Bonferroni correction.

Table 3.1 Metabolic parameters of WT and EKO mice fed ND and HFD for 24 weeks.

Metabolic cage studies reveal no differences in energy expenditure, food intake, or physical activity

We hypothesized that EKO mice might have increased energy expenditure or decreased food intake which would account for failure to increase their fat mass with high fat feeding. Metabolic cage analyses were performed for 3 consecutive days after mice had been fed HFD for 23 weeks. There were no differences in food intake or physical activity between genotypes; HFD mice tended to eat less than their normal chow controls (Table 3.1).

EKO mice have increased post-prandial, but not total, VO2 or EE

EKO HFD fed mice had significantly greater rates of VO2 (ml/hr/kg) over a 24 hour period than WT HFD fed mice (3804 ± 294 vs. 3073 ± 24 ml/hr/kg, $p<0.05$)(Table 3.1)(Figure 3.3A). Increased rates of VO2 in EKO mice were present in both the light and dark phases. However, when non-normalized VO2 (ml/hr) rates were compared, there was no genotype effect, but there was an effect of HFD to increase VO2 (ml/hr)(Figure 3.3B)(Table 3.1). ANCOVA confirmed that there was no statistically significant relationship between genotype and VO2 or EE (Table 3.2). In contrast, HFD increased VO2 (R^2 0.58, $p<0.05$) and EE (R^2 0.76, $p<0.001$) in both genotypes (Table 3.2).

As it has been shown that EKO mice have a prolonged clearance time of dietary TG, we hypothesized that they might have an increased post-prandial VO2. Indeed, the difference between pre-prandial (16:00 hours) and post-

prandial (6:00 hours) VO2 (ml/hr/kg) was significantly greater in EKO HFD than WT mice on both diets ($p<0.05$)(Figure 3.5A). This effect remained significant when non-normalized VO2 (ml/hr) was used (Figure 3.4B).

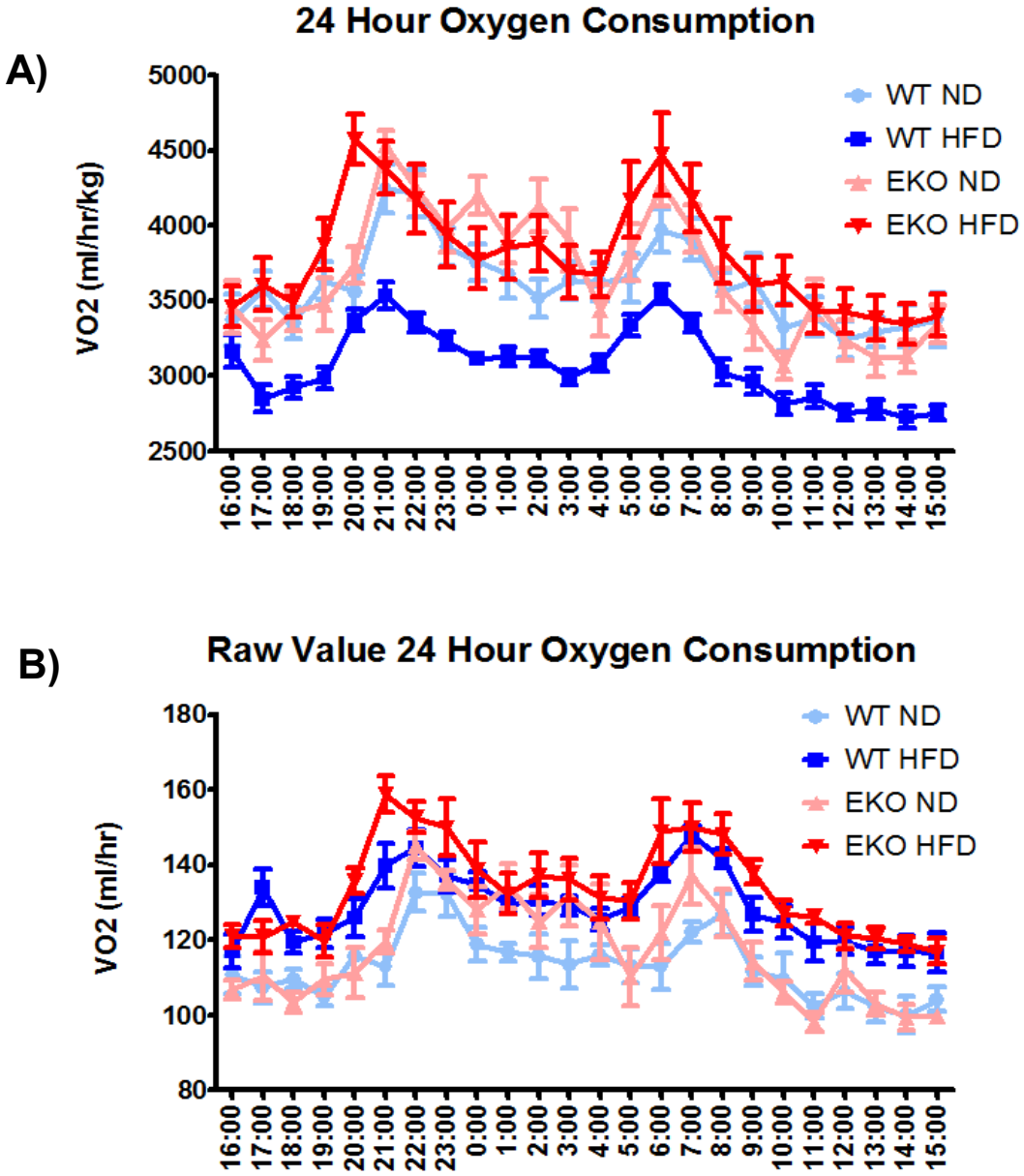

FIGURE 3.3. High fat feeding increases VO2 irrespective of genotype. (A) VO2 (ml/hr/kg) was measured using metabolic cages over three consecutive days after 23 weeks of HFD in WT and EKO mice (n=5-6 per group). EKO HFD mice had significantly greater rates of VO2 over 24 hours than WT HFD mice ($p<0.05$, Table 3.1). (B) When normalization by weight is removed, there is no effect of genotype on total 24 VO2 (ml/hr).

Model for EE	Source	DF	F Value	P value
	Genotype	1	1.93	0.186
	Diet	1	29.08	<0.001*
	Genotype * Diet	1	5.32	0.036*
	Weight	1	0.11	0.746
	Fat Mass	1	0.01	0.942
	Lean Body Mass	1	0.71	0.413
Model for VO2	**Source**	**DF**	**F Value**	**P Value**
	Genotype	1	0.36	0.560
	Diet	1	8.41	0.011*
	Genotype * Diet	1	1.87	0.193
	Weight	1	0.16	0.699
	Fat Mass	1	0.11	0.749
	Lean Body Mass	1	0.33	0.572

*Diet is a significant independent predictor of EE and VO2 using ANCOVA. Diet remains significant in the EE model when the interaction term Genotype * Diet is removed.

Table 3.2 ANCOVA reveals that VO2 (ml/hr) and EE (kcal/ hr) are associated with HFD but not genotype.

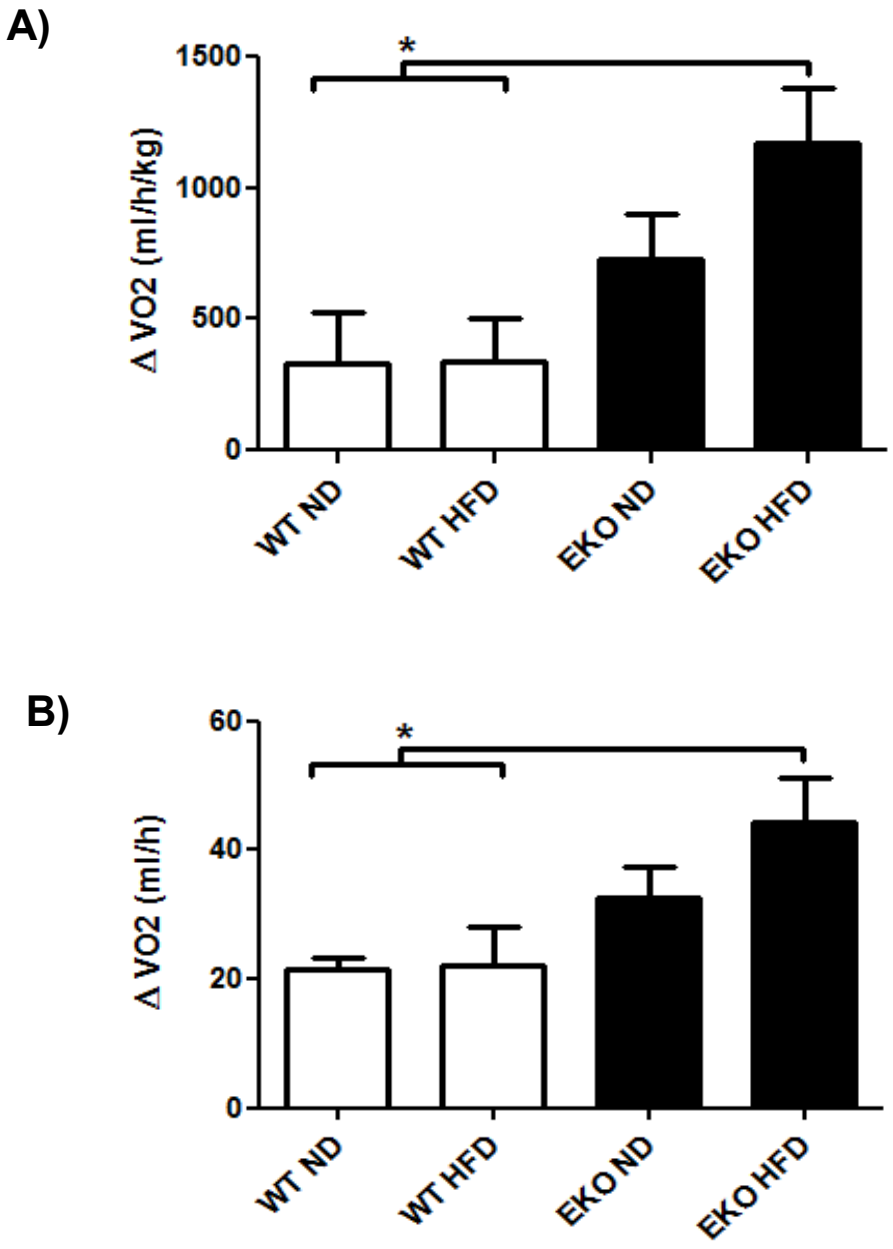

FIGURE 3.4. Post-prandial VO2 is increased in HFD EKO mice compared to wild type ND and HFD mice. (A) The difference in VO2 (ml/hr/kg) before and after the dark (feeding) cycle. The difference VO2 was significantly greater in EKO HFD than WT ND and WT HFD fed mice. (B) The difference in post-prandial VO2 (ml/hr) remained when normalization by weight was removed. *<0.05 vs. WT ND, WT HFD using two way ANOVA and the Bonferonni correction.

EKO mice are protected against hepatic steatosis induced by 24 weeks of HFD

Although it is well known that EKO mice have severe elevations of blood cholesterol and TG, given that they have greater rates of VO2 (ml/hr) in the post-prandial period, we hypothesized that they may be consuming some fraction of this excess fatty acid via hepatic β-oxidation. Light microscopy showed that HFD EKO mice were protected from hepatic steatosis, while HFD fed WT mice had severe hepatosteatosis with hepatocyte ballooning and large lipid droplet formation (Figure 3.5). In addition, serum β-hydroxybutyrate concentrations were 5 fold higher in EKO HFD than wild type HFD mice (4.9 ± 0.56 vs. 0.83 ± 0.24 mM, $p<0.001$)(Table 3.1). This supported our hypothesis that decreased fat storage in adipose tissue results in increased delivery of fatty acids to the liver, which is used as substrate for β-oxidation and ketone formation.

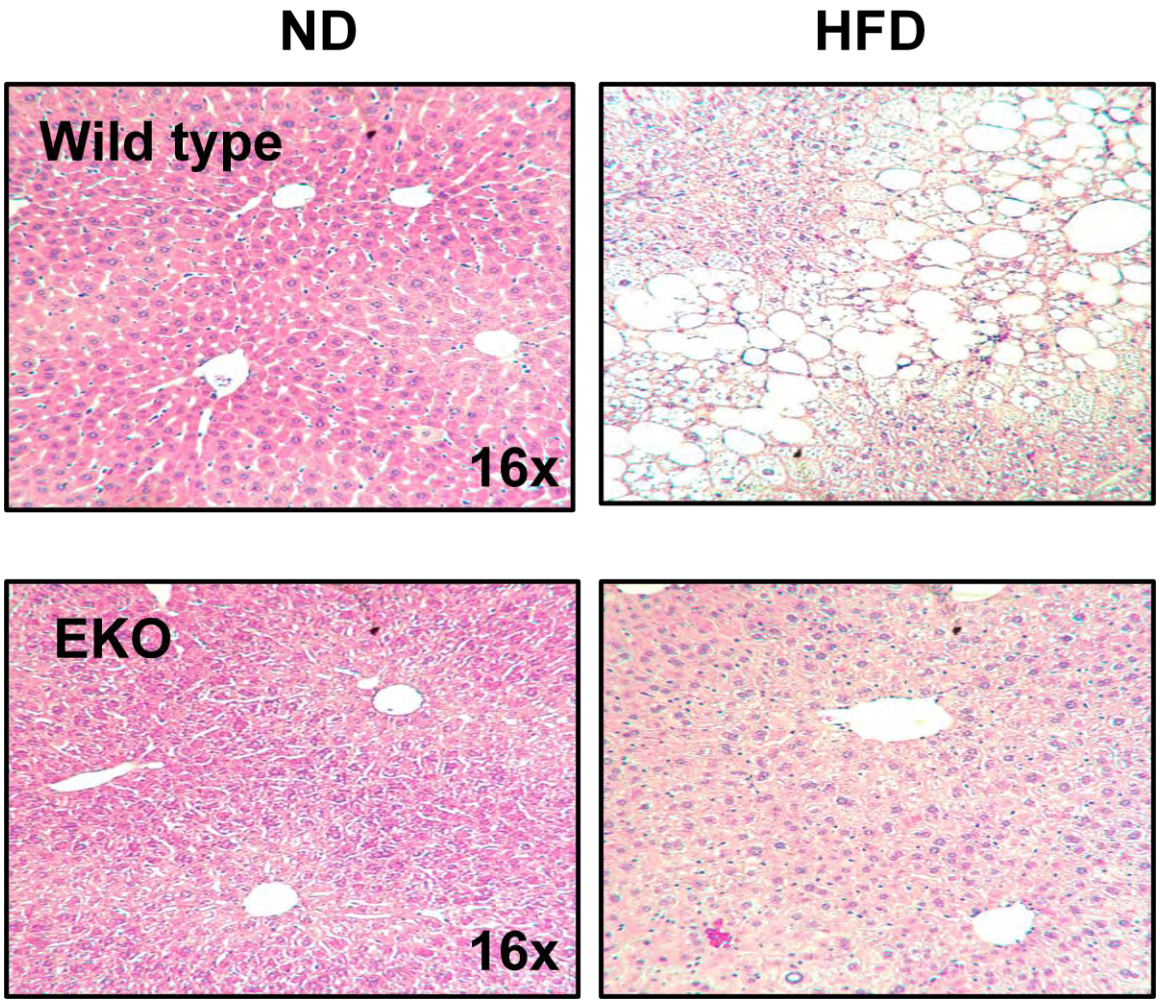

FIGURE 3.5. EKO mice are protected against hepatic steatosis induced by 24 weeks of HFD. Hematoxylin & eosin staining of liver sections from WT (top) and EKO mice (bottom) after 24 weeks of ND (left) or HFD (right). WT HFD mice have severe hepatocyte ballooning and macrosteatosis. In contrast, EKO HFD mice have much less lipid accumulation and hepatocyte ballooning.

Comparative insensitivity of EKO VAT gene expression in response to HFD

Given that EKO mice have an impaired ability to uptake and store dietary fat as TG, we hypothesized that adipocytes might compensate by stimulating *de novo* lipogenesis. Increased glucose uptake by adipose tissue would allow for this and partially explain the improved glucose tolerance of EKO mice. Therefore, we queried expression of key transcription factors (*Srebf1, Nr1h3/Lxrα*) and regulatory enzymes (*Acly, Fasn*) which regulate *de novo* lipogenesis using qPCR. We were surprised to find that obese HFD WT mice had significantly increased expression of *Fasn (3.3 fold), Acly (4.3 fold), Srebf1 (3.0 fold)*, and *Dgat2 (5.9 fold)* while HFD EKO mice had no such increase (Figure 3.6). In comparison to ND controls, HFD fed EKO mice had a decrease in expression of all these genes, two of which were statistically significant (*Lxrα/Nr1h3 0.44 fold, Dgat2 0.33 fold*)(Figure 3.6).

To gain a more comprehensive picture of these changes in gene expression, we performed whole genome expression profiling of VAT from WT and EKO mice fed ND and HFD for 24 weeks using the Affymetrix Mouse Gene 1.0 ST chip. We defined differential expression as a fold change >1.5 at an α of $p<0.05$. When comparing ND WT to HFD WT adipose tissue, expression of 880 genes was significantly different between conditions (3% of represented probes)(Supp. Table 3.1). In contrast to WT VAT, EKO VAT was remarkably insensitive to dietary fat in terms of quantitative changes in gene expression. Expression of

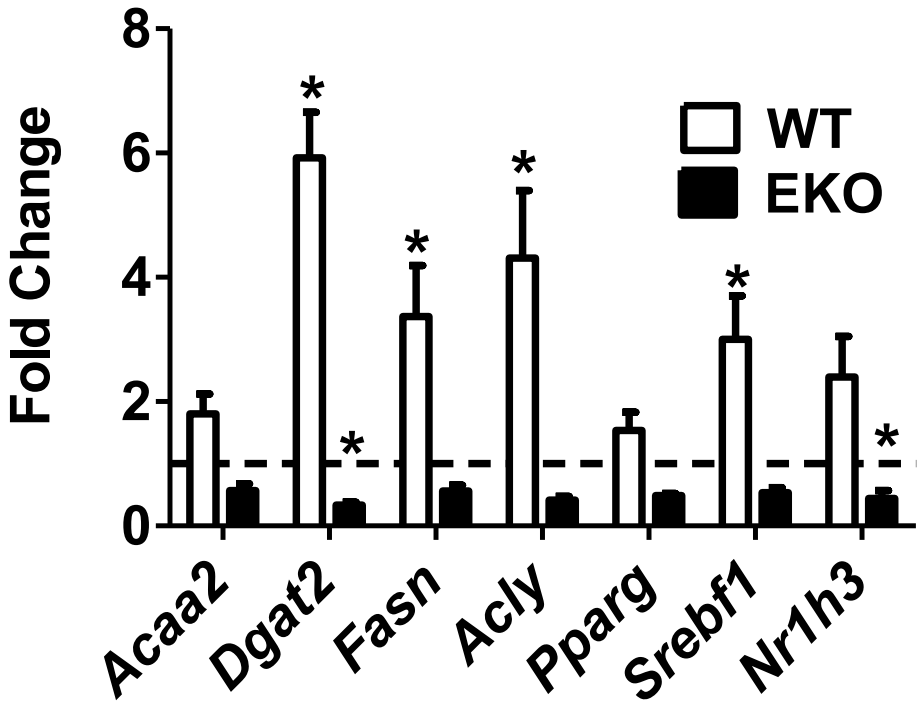

FIGURE 3.6. mRNA expression of genes encoding key transcription factors and metabolic enzymes which regulate fatty acid metabolism are up regulated in WT but not EKO HFD adipose tissue.
qPCR for select genes was performed on RNA isolated from epididymal VAT of normal and HFD fed WT and EKO mice. Fold expression is in comparison to ND controls of the respective genotype. Dashed line is the mean expression in ND controls. *p<0.05 vs. ND control using Student's t-test, N=3 per group. *Acaa2*=Acetyl coA acyltransferase 2 , *Dgat2*=Diacylglycerol O acyltransferase 2, *Fasn*=Fatty acid synthase, *Acly*=ATP citrate lyase, *Pparg*=Peroxisome-proliferator activated receptor gamma, *Srebf1*=Sterol response element binding factor 1, *Nr1h3*=Nuclear receptor sub family 1, group H, member 3

only 53 genes were differentially regulated in EKO adipose tissue when comparing ND versus HFD (0.1% of represented probes)(Supp. Table 3.2). BIOCARTA pathway analysis for this comparison revealed pathways known to be regulated in fatty acid metabolism, including ChREBP2, Leptin, and AT1R pathways (Table 3.3). In contrast, he top ten pathways for the WT analysis were all inflammatory pathways, including T helper, B lymphocyte, and dendritic cell pathways (Table 3.3).

We then specifically queried expression of an *a priori* determined list of genes whose products encode proteins which function in fatty acid metabolism, including PPARγ target genes, pro-adipogenesis genes, β oxidation genes, and cholesterol metabolism genes (Table 3.4). PPARγ target genes such as insulin receptor substrate 1 (*Irs1*), Complement component d (*Cfd*), facilitated glucose transporter member 4 (*Glut4/Slc2a4*), and adiponectin (*Adipoq*) were uniformly and significantly down regulated in response to HFD in WT mice ($p<0.05$)(Table 3.4). In contrast, PPARγ target genes were not down-regulated in EKO adipose tissue. Interestingly, genes belonging to cholesterol metabolism pathways were significantly up-regulated in the HFD fed WT mice, whereas there was no response to HFD in EKO adipose tissue. The only gene set consistently up-regulated in HFD fed EKO mice were those encoding enzymes responsible for fatty acid catabolism and β oxidation (Table 3.4).

Pathway analysis of WT ND vs. HFD VAT					
Index	**Gene Set Category**	**Set Size**	**% up**	**NTK Stat**	**NTK q**
259	*TCRA pathway*	10	0	4.97	<0.001
32	*Extrinsic pathway*	13	15	3.5	<0.001
154	*B Lymphocyte pathway*	9	0	4.8	<0.001
51	*T helper pathway*	12	0	4.3	<0.001
261	*DC pathway*	20	15	4.4	<0.001
237	*T cytotoxic pathway*	12	0	4.0	<0.001
138	*ASB cell pathway*	11	9	3.0	0.012
145	*NO2 IL12 pathway*	16	18	3.4	<0.001
254	*Lair pathway*	15	20	4.0	<0.001
239	*Csk pathway*	19	31	2.8	<0.022
Pathway analysis of EKO ND vs. EKO VAT					
Index G	**Gene Set Category**	**Set Size**	**% up**	**NTK Stat**	**NTK q**
104	*Differentiation pathway in PC12*	40	75	-5.4	0
157	*Granule cell survival pathway*	24	75	-4.0	0
101	*P53 hypoxia pathway*	22	90	-4.2	0
127	*Chrebp2 pathway*	39	82	-5.1	0
40	*Leptin pathway*	11	81	-3.7	0
53	*CTCF pathway*	22	86	-4.1	0
87	*VDR pathway*	11	90	-3.97	0
166	*CARM ER pathway*	34	70	-3.9	0
38	*CD40 pathway map*	33	69	-3.8	0
15	*AT1R pathway*	29	82	-4.8	0

TABLE 3.3 BIOCARTA Pathway Analysis of Differentially Expressed Genes in WT ND vs. HFD and EKO ND vs. HFD

	Symbol	WT FC	P	EKO FC	P
PPARγ Target genes	Irs1	-2.21	0.01	-1.31	0.11
	Cfd	-4.60	0.00	-1.21	0.16
	Slc2a4	-1.52	0.02	-1.09	0.32
	Adipoq	-1.36	0.01	1.02	0.59
	Rxra	-1.18	0.16	-1.26	0.02
	Ppargc1b	-1.31	0.01	1.02	0.89
	Ppargc1a	-1.61	0.03	-1.15	0.42
Adipogenesis	E2f1	1.52	0.01	1.04	0.62
	Fgf2	-1.57	0.05	-1.34	0.05
	Klf15	-1.66	0.03	-1.18	0.22
	Dkk1	-1.09	0.01	1.05	0.54
	Retn	-1.23	0.03	-1.00	0.92
	Sfrp1	1.50	0.08	-1.38	0.02
	Cklf	1.22	0.03	-1.05	0.49
	Agt	-3.63	0.00	-1.38	0.05
	G6pd2	1.59	0.03	1.11	0.13
	Scd1	1.07	0.33	1.08	0.03
	Scd2	3.78	0.02	1.70	0.06
	Plin2	2.17	0.00	1.23	0.04
	Plin4	-1.21	0.02	1.01	0.88
Fatty Acid Oxidation	Plin5	1.16	0.00	1.21	0.04
	Cox8b	1.82	0.12	2.00	0.00
	Acad11	-1.24	0.02	1.32	0.01
	Acadl	1.01	0.95	1.23	0.02
	Acox1	1.20	0.19	1.18	0.01
	Acsl5	1.40	0.02	1.23	0.04
	Acad10	-1.27	0.03	-1.05	0.65
	Acsm5	-2.07	0.00	-1.13	0.52
	Acsm3	-5.41	0.02	1.24	0.60
	Acadsb	-1.73	0.01	-1.20	0.08
Cholesterol metabolism	Lss	3.57	0.01	1.17	0.46
	Insig1	2.69	0.04	1.82	0.19
	Fdps	2.62	0.02	1.07	0.62
	Dhcr7	2.58	0.03	-1.06	0.55
	Nsdhl	2.38	0.00	1.12	0.60
	Hsd17b7	2.11	0.02	-1.20	0.28
	Dhcr24	1.88	0.00	1.00	0.98
	Hmgcs1	1.65	0.02	1.25	0.42
	Tm7sf2	1.59	0.02	1.07	0.40

TABLE 3.4 Differential regulation of metabolic gene sets in response to HFD in WT vs. EKO

Reduced cell size and macrophage F480 staining in EKO HFD VAT

Considering the dramatic increase in expression of inflammatory genes in the WT HFD VAT (Table 3.3)(Supplementary Table 3.1) we decided to confirm the extent of macrophage infiltration with HFD by immunohistochemistry for the macrophage marker F480+ (Figure 3.7). WT HFD VAT had abundant macrophage F480+ staining, with most appearing as large multi-nucleate cells in crown like structures (CLS). In contrast, there very few macrophages or CLS in the EKO HFD VAT. In addition, the diameters of EKO WT and HFD VAT adipocytes were much smaller than WT, which is consistent with previous reports.

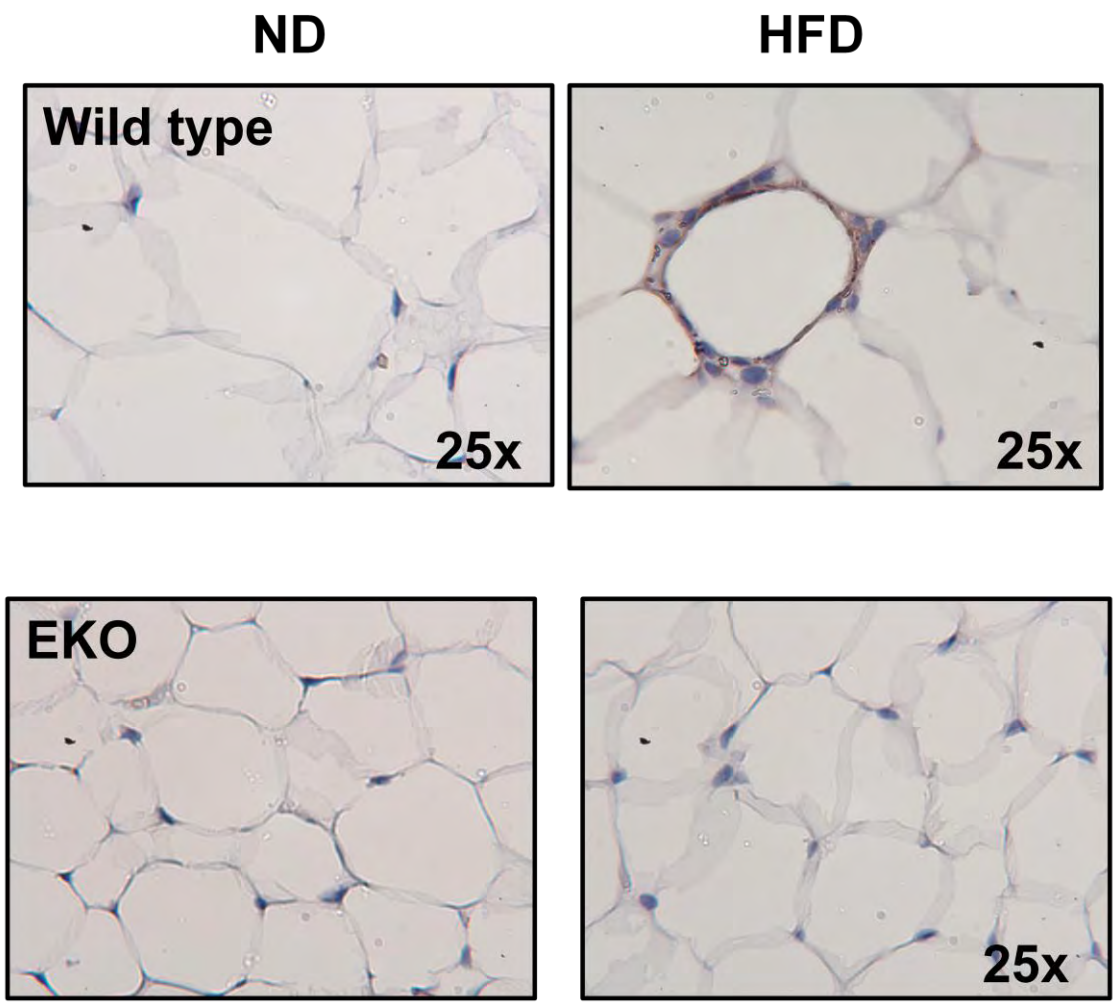

FIGURE 3.7 WT HFD VAT has larger adipocytes and greater F480+ Macrophage staining.
Epididymal VAT from WT and EKO mice fed ND and HFD for 24 weeks was harvested and stained with the macrophage specific marker F480+. WT adipocytes were larger than EKO at baseline and with HFD and contained greater numbers of F480+ cells.

Discussion

It is now well established that the EKO mouse is resistant to DIO and remains glucose tolerant when compared to WT HFD fed controls [118-120, 122, 131, 132]. Our results confirm these prior studies and make three novel contributions: 1) inflammation in PVAT is not associated with atherosclerosis in the EKO mouse, 2) post-prandial, but not total, VO2 (ml/hr) is increased in HFD fed EKO mice, 3) EKO mice remain lean on HFD, and this is associated with decreased adipocyte size, reduced inflammation, and increased expression of fatty acid oxidation genes.

The failure to observe increased macrophage gene expression in thoracic PVAT of EKO mice does not exclude the possibility that PVAT is important in the pathogenesis of atherosclerosis. There are at least two significant limitations to our experiment which prevent us from making this conclusion. One, by 24 weeks of age, atherosclerosis in the EKO mouse is relatively advanced, and may be in a chronic, non-inflammatory stage. In order to determine if inflammation in PVAT is an initiating event, we would have to use younger animals prior to the development of atherosclerosis (approx 6-8 weeks of age)[133]. Second, although we dissected PVAT from an atherosclerosis prone area (the aortic arch), we cannot be sure that there was actual plaque in the adjacent vessel in every mouse. Nonetheless, we are confident that inflammation of PVAT is not an initiating event in the patho-physiology of atherosclerosis. Whether or not it has

significance in other forms of obesity related vascular disease is a topic of future studies (Chapter IV).

Regarding our studies of whole body metabolism, compared to WT controls EKO mice had a significantly reduced fat mass in response to HFD; this was apparent within 8 weeks of starting a HFD, and continued until 24 and 38 weeks (Fig 3.2). WT mice had a 5 fold increase in fat mass after 24 weeks HFD while EKO mice had only a 2 fold increase (Table 3.1). Huang *et al*. have shown that endogenous adipocyte apoE is required for both LPL dependent and VLDR endocytic uptake of triglyceride rich lipoprotein particles, and this would account for reduced fat mass [124]. However, how do we account for the apparent caloric imbalance in EKO mice?

We detected no differences in food intake or physical activity between WT and EKO animals (Table 3.1). Others have shown that intestinal absorption of lipid is normal in the EKO mouse[134]. Therefore, we hypothesized that EKO mice might have increased energy expenditure. Gao *et al*. found that EKO mice on the Ay/+ background had increased VO2 in light and dark phases [119]. In contrast, Hofmann *et al.* found no differences in energy expenditure after 16 weeks of HFD [120]. Indeed, we found that when VO2 was normalized to body weight (ml/hr/per kg body weight) HFD fed EKO mice had greater rates of VO2 (Table 3.1, Figure 3.3A). However, when we analyzed raw or non-normalized VO2 (ml/hr), there was no significant difference between groups (Table 3.1, Figure 3.3B). ANCOVA revealed that diet, but not genotype, was significantly

associated with VO2 (ml/hr) and EE (kcal/hr). The linear model incorporated weight, lean body mass, and fat mass as covariates to account for these independent variables (Table 3.2). Our use of non-normalized measures of energy expenditure and ANCOVA are in conformity with a recent consensus statement by an expert panel of scientists [135]. It is likely that all prior studies which included body weight in the estimation of VO2 (ml/hr/kg) and EE (kcal/hr/kg) erroneously ascribed a greater energy expenditure to EKO mice. Despite these issues, we did find that non-normalized post-prandial VO2 (ml/hr) was significantly greater in HFD EKO mice than HFD WT mice, a factor which, over the life of the animal, may contribute to reduced weight gain (Figure 3.4)[136].

Consistent with prior reports, we found that the livers of HFD fed EKO mice were resistant to hepatosteatosis (Figure 3.5)[118, 119, 132, 134]. As apoE is a ligand for the LDL, VLDL, and remnant receptor (LRP1), the liver cannot take up chylomicron remnants and LDL and therefore may be less prone to lipotoxicity. This highlights the important contribution of dietary fat to hepatic steatosis. However, as VLDL secretion is also dependent upon apoE, and rates of hepatic VLDL secretion are decreased in EKO mice, one might expect hepatic TG to accumulate despite reduced uptake [137, 138]. We observed the exact opposite, that EKO mice were protected from hepatosteatosis with HFD. Increased hepatic β-oxidation of fatty acids may reduce liver TG accumulation in EKO mice

[134]. The increased plasma β-hydroxybutyrate concentrations that we observed in ND and HFD EKO mice are consistent with this idea (Table 3.1).

Perhaps the most dramatic findings of our study stem from the microarray analyses. (Table 3.4 & Supp. Tables 3.1, 3.2) High fat diet feeding in EKO mice resulted in significantly altered expression of only 0.1% of probe sets; in contrast, WT HFD mice had a 30 fold greater number of genes whose expression was altered in response to HFD (3%). We initially hypothesized that EKO adipocytes may compensate for decreased TG uptake by increasing *de novo* fatty acid synthesis. qPCR showed that that genes encoding lipogenic enzymes (*Acly, Fasn, Dgat*) were up-regulated in WT HFD adipocytes but not in EKO adipocytes (Fig 3.6). We then queried the microarray data for an *a priori* determined list of genes involved in fatty acid metabolism. We again failed to detect an increase in expression of the same lipogenic genes in EKO adipocytes. However, we did find some interesting patterns of expression which correlated with our metabolic studies (Table 3.4).

First, important PPARγ target genes such as *Adipoq, Cfd, Irs1 and Glut4/Slc2a4,* were all down regulated in response to HFD in WT VAT; this correlated with the potent inflammatory response in this tissue and impaired whole body glucose metabolism (Table 3.4). Inflammation, specifically TNFα, is thought to reduce PPARγ activity in adipocytes [13]. Second, a panel of genes encoding proteins in the cholesterol biosynthesis pathway (*Hmgcs1, Insig1, Lss,*

Hsd17b7) were up regulated in WT HFD fed VAT (Table 3.4). It has been shown in previous studies that large adipocytes are cholesterol deficient due to their requirement for a large plasma membrane, therefore they activate expression of genes to increase cellular cholesterol [139]. In that regard, it is also notable that the expression of the VLDL (1.4 fold, $p<0.05$) and LDL (1.8 fold, p=NS) receptors was increased (1.4 fold) in the WT HFD mice, likely as an additional mechanism to increase cellular cholesterol (Supp Table 3.1). Cholesterol deficiency causes cellular insulin resistance by reducing signaling through caveolin 2 enriched lipid rafts [139]. Of note, the diameter of WT type adipocytes was much greater than EKO adipocytes at baseline and especially with HFD (Fig 3.7)..

In regards to the increased numbers of macrophages in the WT HFD VAT, the microarray data indicate that multiple mechanisms of macrophage lipid uptake appear to be activated, all of which parallel foam cell formation in the atherosclerotic plaque. For example, enzymatically modified LDL particles are internalized mainly by type 1 (opsonin) and type 2 (complement) mediated phagocytosis [140]. Expression of both *Cd16/Fcgr3*, which binds C reactive protein and IgG coated LDL particles, and *Cd11b*, which binds complement coated LDL particles, is increased in WT HFD VAT (1.48 and 1.71 fold respectively $p<0.05$, Suppl. Table 3.1). Type 1 and type 2 phagocytosis lead to the formation of large, membrane associated lipid droplets [140]. In contrast, expression of the macrophage scavenger receptor *Msr1*, which is responsible for

receptor mediated of predominately oxidized LDL particles, is also increased (1.92 fold, $p<0.05$, Suppl. Table 3.1). Expression of these genes is not altered in EKO VAT with HFD. We do not suggest that modified and oxidized LDL are necessarily the ligands for macrophages in adipose tissue, only that it is likely that there are multiple complex lipid antigens released from dying (or viable) adipocytes in WT HFD VAT which broadly stimulate the innate immune response. The decreased cell size of EKO HFD adipocytes may prevent cellular stress and death thus preventing this inflammatory response.

That we do not see increased macrophages in the VAT of HFD EKO mice is not inconsistent with the results of others who have shown that 1) primary EKO adipocytes have increased rates of lipolysis *ex vivo* and 2) FFA release is a stimulus for macrophage infiltration [34, 117]. On cellular basis, because the lipolytic rate depends on cell surface area ($4\pi r2$), and EKO adipocytes are almost ½ the diameter of WT adipocytes, FFA release per cell is actually likely much smaller in EKO adipocytes. Second, rates of lipid oxidation may be increased in EKO adipocytes, resulting in less release of FFA from hydrolyzed TG. Finally, macrophage infiltration in response to lipolysis has been shown in obese animals subjected to fasting, thus, in negative energy balance, which was not the case for EKO mice [34].

In regard to changes in gene expression in EKO adipose tissue, expression of genes encoding enzymes important for fatty acid oxidation were broadly up-regulated, for example, *Oxpat/Plin5*, *Cox8b*, *Acsl5*, *Acox1*, and *Acadl* (Table 3.4).

Many of the same genes were down regulated in WT HFD VAT. Interestingly, the gene with the highest fold increase in expression in EKO HFD VAT, lactase-like *(Lctl)*, is a recently described member of the fibroblast growth factor family which is specifically expressed only in brown adipose tissue *[141]*(Supp Table 3.2). Whether or not fatty acid oxidation is actually functionally increased in EKO adipocytes, and relates to their decreased cell size, will require further study.

In summary, using a combination of physiologic studies, genomics, and immunohistochemistry, we describe some novel findings regarding the metabolic phenotype of EKO mice which will provide a starting point for future studies. We confirmed the observation that, despite severe hyperlipidemia, EKO mice fed a HFD are more lean and insulin sensitive than their WT littermates. This may be due to failure of adipose, skeletal muscle, and liver to properly metabolize circulating triglyceride rich lipoproteins. Second, using careful statistical analysis of metabolic cage data in accordance with expert guidelines, we show that post-prandial VO2 (ml/hr), but not total VO2 or EE is increased in EKO mice. This may partially account for their lean phenotype. Finally, using the first whole genome comparison of gene expression of WT and EKO adipose tissue, we show that EKO mice have decreased expression of inflammatory genes, and increased expression of genes encoding enzymes responsible for lipid oxidation. These results suggest that limiting adipocyte size or TG uptake may be a viable therapeutic strategy, provided that peripheral mechanisms to prevent atherogenic hyperlipidemia can be activated.

Limitations

We acknowledge the many limitations of this study. We hypothesized that the EKO adipocytes would compensate for reduced lipid uptake by increased *de novo* lipogenesis. Although we did not see increased expression of genes encoding lipogenic enzymes, it is still possible that enzymatic activity is indeed high and that increased rates of de novo lipogenesis do exist. We do plan to specifically measure this in the future using in vivo lipogenesis assays with C^{14} glucose.

The metabolic cage studies should ideally be done at two points in time, one preferably before differences in weight exist (8 weeks of HFD in our case), so that differences in VO2 and EE can be longitudinally associated with the development or prevention of obesity.

Post-prandial VO2 was an estimate based on the metabolic cage data. This experiment should be repeated formally with a test meal and measurement of metabolic rate for 4 hours after the meal [136].

Microarrays were done on whole adipose tissue, which contains multiple cell types, all of which could confound our results. For example, the increased expression of enzymes responsible for cholesterol biosynthesis could be due to increased macrophages/foam cells in the WT HFD VAT.

These limitations aside, we believe that we have made novel contributions to the field of knowledge regarding this fascinating model of lipid metabolism. We conclude that: 1) inflammation in PVAT is not associated with atherosclerosis in

the EKO mouse, 2) post-prandial VO2 (ml/hr) is increased 3) HFD fed EKO mice are protected from hepatic steatosis possibly due to increased hepatic lipid oxidation, 4) EKO mice remain lean on HFD, and 5) this is associated with decreased adipocyte size, reduced inflammation, and increased expression of fatty acid oxidation genes.

CHAPTER 4: Summary and Future Directions

The contributions of obesity and the metabolic syndrome to cardiovascular risk are well described [7, 8, 13]. Visceral adiposity, but not subcutaneous, is the primary trigger for the development of the metabolic syndrome. This contrast between SAT and VAT has motivated interest in the discovery of additional fat depots which might play equally important roles in metabolic disease. Perivascular fat is one such depot, and the work described herein was an attempt to understand if PVAT plays a direct role in vascular disease. Although we did not demonstrate a primary role for PVAT in atherosclerosis, we did make novel observations regarding the characteristics of PVAT in the mouse and how it is influenced by high fat feeding.

In the first chapter of this thesis we established that thoracic PVAT is similar to brown adipose using morphology and whole genome expression analyses. We also demonstrated that thoracic PVAT and BAT are comparatively resistant to HFD induced inflammation. This inflammation is characterized predominantly by F480/Cd11c+ macrophages. We hypothesize that the absence of inflammation in thoracic PVAT and BAT may be due to decreased cell size, decreased chemokine release, or decreased release of FFA.

In the second chapter of this thesis, we asked the question “is atherosclerosis in the mouse associated with inflammation in PVAT?”. We did not find evidence of increased expression of macrophage specific genes in the PVAT of the

thoracic aorta of the EKO mouse by qPCR. We did observe that the EKO mouse was protected from HFD induced obesity and glucose intolerance. EKO mice were less obese and more glucose tolerant than their WT HFD fed littermates. In addition, the VAT of EKO mice was characterized by fewer alterations in gene expression in response to HFD. In particular, very few inflammatory genes appeared to be regulated in the EKO mouse; this was associated with reduced inflammation in VAT as seen by F480+ macrophage staining. These experiments reinforce the importance of dietary fat in genesis of VAT inflammation, and show that apoE is essential for adipose tissue uptake of TG.

The above findings have lead to many new questions and directions for further research. What is the reason for the apparent resistance of BAT to diet induced inflammation? Does PVAT actually have a role in vascular disease? Most importantly, do these questions have relevance to human disease? I will conclude this thesis with a brief description of two experiments we are conducting that will more definitively answer these questions.

Influence of adipocyte specific Mcp-1 knockout on abdominal aortic aneurysm formation in HFD fed mice.

Abdominal aortic aneurysm (AAA) in humans is independently associated with measures of central obesity such as waist circumference and waist to hip ratio [73]. Circulating markers of macrophage function such as resistin and osteopontin have also been associated with the presence of AAA [73, 142].

Inflammation of all three layers of the aorta has been noted on pathological specimens of AAA; however, it is still unclear where exactly local inflammation is incited.

In contrast to thoracic PVAT, PVAT surrounding the abdominal aorta is white adipose tissue, and like VAT, is prone to obesity induced inflammation [74](Figure 4.1). In response to HFD abdominal PVAT has increased expression of *Mcp-1* and *F4/80*(Figure 4.2). In addition, Police *et al*. have shown that Mcp-1 release into conditioned media is greater in abdominal than thoracic PVAT, and this is accompanied by a greater ability of conditioned media from abdominal, but not thoracic PVAT, to stimulate macrophage migration [74].

The significance of these observations is that AAA in obese mice and humans is associated with macrophage infiltration of the local PVAT, whereas the thoracic aorta is spared from aneurysm formation in obesity [61, 74] Hence, it seems that abdominal PVAT is very much like visceral fat. However, a major question remains *is the adipocyte the primary source of Mcp-1 in HFD induced obesity?* Therefore, we will test the hypothesis that adipocyte specific knockout of *Mcp-1* reduces the incidence and size of AAA in HFD fed mice after angiotensin II infusion.

$Mcp1^{LoxP/LoxP}$ mice on the C57BL/6 background haven been generated by Dr. Teizo Yoshimura from the NCI/NIH. Mice will be crossed with an adipocyte specific Cre recombinase driven by the adiponectin promoter($Adipoq^{Cre}$)[143]. $Adipoq^{Cre}Mcp1^{LoxP/LoxP}$ and $Mcp1^{LoxP/LoxP}$ control mice will be started on a HFD at

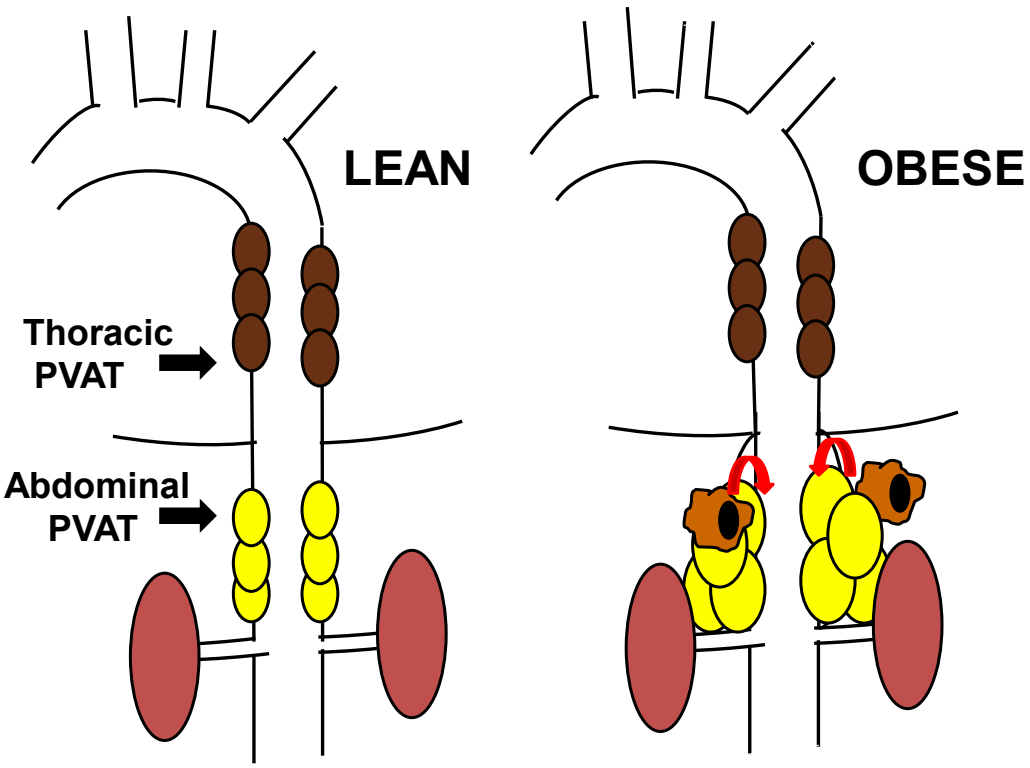

FIGURE 4.1. A working model for the contribution of PVAT to abdominal aortic aneurysm formation in obesity.
In mice, the fat surrounding the thoracic aorta is brown adipose, while that surrounding the abdominal aorta is predominantly white adipose. High fat feeding of rats has been shown to result in increased growth and weight of the abdominal but not the thoracic PVAT. Furthermore, in humans, obesity is independently associated with aneurysms of the abdominal, but not the thoracic aorta. We hypothesize that this is due obesity induced inflammation in the abdominal PVAT, with subsequent weakening of the aortic adventitia and aneurysm formation.

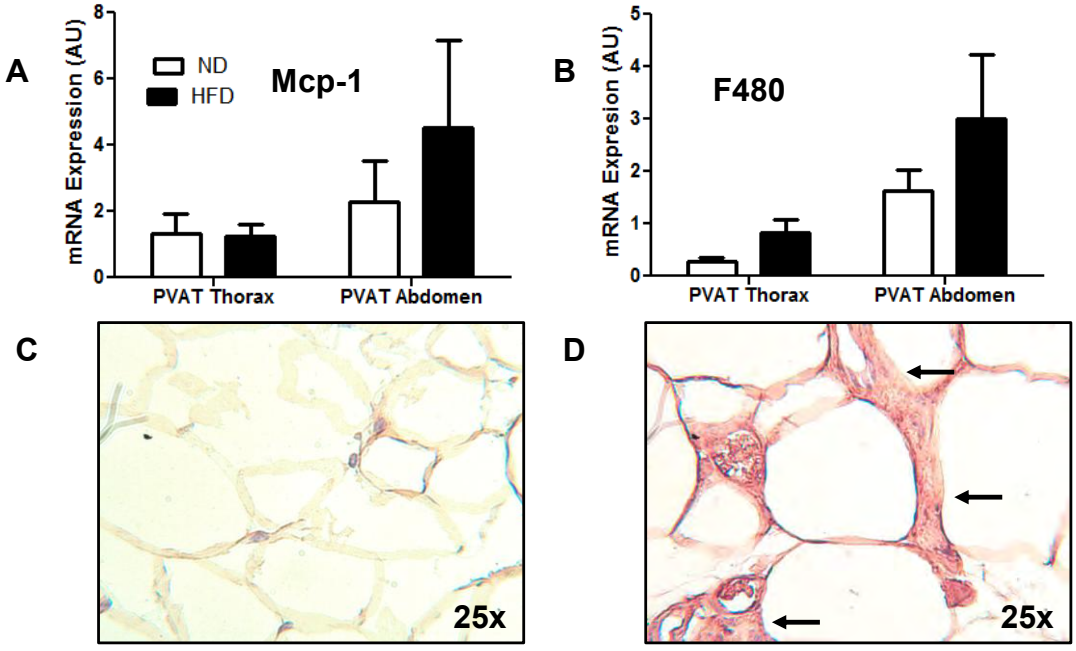

FIGURE 4.2. Increased *Mcp-1* and *F480* mRNA in abdominal PVAT correlates with macrophage infiltration.
RNA was prepared from thoracic and abdominal PVAT and qPCR was performed for Mcp-1 (A) and F480 (B)(n=3 mice per tissue and diet). F480 staining in abdominal PVAT of mice fed ND (C) or HFD (D) for 20 weeks. Abundant macrophages in CLS were apparent in abdominal PVAT of HFD fed mice (arrows). (Tim Fitzgibbons, unpublished data)

8 weeks of age (n=10 mice per group). After 3 months, mice will have blood pressure taken via tail cuff and then we will measure baseline diameter of the suprarenal abdominal aortic with ultrasound. Alzet 2004 minipumps will then be inserted and Angiotensin II will be infused (1000 $ng/kg^{-1}/min^{-1}$) for 28 days to induce AAA formation[74]. Ultrasound will be repeated at the study end to measure abdominal aortic dimension and then mice will be euthanized. The circulation will be perfused with ice cold PBS and SAT, VAT, and abdominal PVAT will be collected and snap frozen in liquid nitrogen. The suprarenal abdominal aorta will photographed in situ using a Nikon dissecting scope, and maximal diameter of the suprarenal aorta will be measured offline.

US measured aortic diameter at baseline and at study end will be compared between the HFD $Mcp1^{LoxP/LoxP}$ and the HFD $Adipoq^{Cre}Mcp1^{LoxP/LoxP}$. *Ex vivo* measurement of the maximal diameter of the suprarenal abdominal aorta will also be compared between groups.

I expect that the diameter of the suprarenal abdominal aorta will be significantly greater in the HFD $Mcp1^{LoxP/LoxP}$ than in the HFD $Adipoq^{Cre}Mcp1^{LoxP/LoxP}$ and the ND $Mcp1^{LoxP/LoxP}$ group. This relation will hold true for both the US and *ex vivo* derived measurements. I expect that incidence of AAA formation, defined as a greater than 50% enlargement of the maximal aortic diameter as measured by US at baseline in comparison to study end [144], will be greater in the HFD $Mcp1^{LoxP/LoxP}$ than in the HFD $Adipoq^{Cre}Mcp1^{LoxP/LoxP}$.

A potential weakness of this study design is that Mcp-1 is not deleted specifically in the abdominal PVAT, but rather in whole body adipose tissue. Nevertheless, documentation of reduced macrophage infiltration by qPCR and immuno-histochemistry, and a reduction in the incidence or size of abdominal aortic aneurysm in the HFD $Adipoq^{Cre}Mcp1^{LoxP/LoxP}$ group would be convincing evidence of an adipose specific effect.

Comparison of inflammatory gene expression from epicardial fat in patients with and without coronary disease.

Multiple studies have demonstrated increase expression of inflammatory genes in epicardial fat from humans with advanced coronary disease [60, 62]. Few of these studies have included control patients without coronary disease. Additionally, there are an increasing number of papers which report increased cardiovascular risk per unit size of epicardial fat thickness/mass. However, much if not all of this risk disappears when measures of visceral adiposity are controlled for (i.e. BMI, waist circumference, or VAT volume by CT/MRI)[69, 70]. Therefore, it remains to be demonstrated whether or not EAT is an independent fat depot with unique features, or merely a marker for increased visceral adiposity.

In this study we will compare gene expression in epicardial fat from patients with and without coronary disease. Our aim is to answer three specific

questions: 1) does the whole genome expression profile of epicardial fat differ from that of visceral fat from age and BMI matched controls?, 2) are BAT specific genes expressed to a greater degree in those without coronary disease, and 3) are inflammatory specific genes expressed to a greater extent in those with coronary disease?

We will enroll 6 controls (patients have valve surgery who do not have CAD) and 6 cases (patients having bypass surgery for CAD)(Figure 4.3). Fasting blood will be drawn on the day of surgery. Samples of EAT proximal to the right coronary artery will be taken, and SAT from the sternotomy incision site. Samples will be snap frozen in liquid nitrogen for subsequent RNA analysis. RNA will be prepared and hybridized to Affymetrix Human Gene 1.0 ST arrays. Data will be uploaded into the UMASS MACE (Microarray Computational Environment).

To determine if EAT has a different whole genome expression profile than VAT, we will compare expression in controls to age and gender matched expression data from VAT which we have from a cohort of gastric bypass patients previously described[25]. We will then compare expression of BAT and immune cell specific genes in cases and controls. We will correlate expression data in cases with the severity of CAD as assessed by scoring angiograms with the Gensini scoring system.

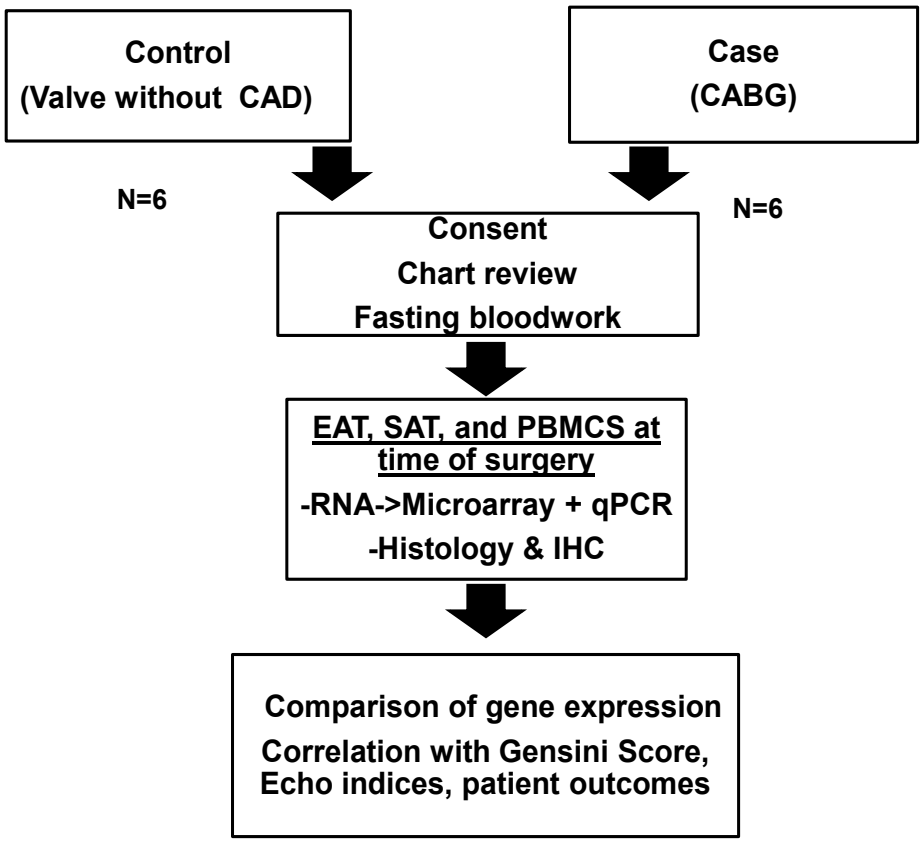

FIGURE 4.3. Experimental design of the REACD (Role of Epicardial Adipose in Coronary Disease) Study.
Cases with and controls without CAD will be enrolled in the study. Fasting blood will be drawn on the day of surgery for isolation of plasma and peripheral blood monocytes. Samples of EAT and SAT will be taken at the time of surgery.

I expect that EAT may have a similar expression profile as VAT, with the exception of patterning and other developmental genes. I also expect that BAT specific genes may be expressed to a low degree and correlate inversely with age, as has been previously shown for *Ucp-1* and *Prdm16 [112]*. Finally, I expect that EAT from patients with CAD will have significantly greater enrichment of inflammatory gene expression. The ultimate aim of these studies is to develop siRNA therapeutics which can be used topically at the time of cardiac surgery to prevent graft restenosis, post-operative atrial fibrillation, or progressive adverse cardiac remodeling.

Conclusion

Obesity is independently associated with an increased risk cardiovascular disease, much of which is mediated by the metabolic syndrome and underlying insulin resistance. Visceral adiposity in particular has been shown to be associated with this risk. We propose that there may be additional, direct mechanisms, by which obesity may impact cardiovascular disease, via perivascular and epicardial fat. In the mouse, we have shown that PVAT around the thoracic aorta is BAT. Whether or not brown perivascular fat exists in humans has yet to be determined, but is a very intriguing hypothesis. Brown fat in the perivascular niche could directly warm the blood, serve to take up and consume triglyceride rich lipoproteins, and protect the underlying artery from inflammation. We believe that the work described herein and our future aims provide an impetus to pursue these important questions.

References

1. Wang, Y., et al., *Will all Americans become overweight or obese? estimating the progression and cost of the US obesity epidemic.* Obesity (Silver Spring), 2008. **16**(10): p. 2323-30.
2. Tontonoz P, S.B., *Fat and beyond: the diverse biology of PPARγ.* Annu Rev Biochem 2008. **77**: p. 289-312.
3. Nissen, S.E. and K. Wolski, *Rosiglitazone revisited: an updated meta-analysis of risk for myocardial infarction and cardiovascular mortality.* Arch Intern Med, 2010. **170**(14): p. 1191-1201.
4. Cypess, A.M. and C.R. Kahn, *Brown fat as a therapy for obesity and diabetes.* Curr Opin Endocrinol Diabetes Obes, 2010. **17**(2): p. 143-9.
5. Kiefer, F.W., et al., *Retinaldehyde dehydrogenase 1 regulates a thermogenic program in white adipose tissue.* Nat Med, 2012.
6. Sjostrom, L., et al., *Bariatric surgery and long-term cardiovascular events.* JAMA, 2012. **307**(1): p. 56-65.
7. Van Gaal, L.F., I.L. Mertens, and C.E. De Block, *Mechanisms linking obesity with cardiovascular disease.* Nature, 2006. **444**(7121): p. 875-80.
8. DeFronzo, R.A., *Insulin resistance, lipotoxicity, type 2 diabetes and atherosclerosis: the missing links. The Claude Bernard Lecture 2009.* Diabetologia, 2010. **53**(7): p. 1270-87.
9. Grundy, S.M., et al., *Diagnosis and management of the metabolic syndrome: an American Heart Association/National Heart, Lung, and Blood Institute Scientific Statement.* Circulation, 2005. **112**(17): p. 2735-52.
10. Litwin, S.E., *Cardiac remodeling in obesity: time for a new paradigm.* JACC Cardiovasc Imaging, 2010. **3**(3): p. 275-7.
11. Iacobellis, G. and H.J. Willens, *Echocardiographic epicardial fat: a review of research and clinical applications.* J Am Soc Echocardiogr, 2009. **22**(12): p. 1311-9; quiz 1417-8.
12. Unger, R.H., *Minireview: weapons of lean body mass destruction: the role of ectopic lipids in the metabolic syndrome.* Endocrinology, 2003. **144**(12): p. 5159-65.
13. Guilherme A, V.J., Puri V, Czech MP. , *Adipocyte dysfunctions linking obesity to insulin resistance and Type 2 Diabetes.* . Nat Rev Cell Biol 2008. **9**: p. 367-377.
14. Karpe, F., J.R. Dickmann, and K.N. Frayn, *Fatty acids, obesity, and insulin resistance: time for a reevaluation.* Diabetes, 2011. **60**(10): p. 2441-9.
15. McQuaid, S.E., et al., *Downregulation of adipose tissue fatty acid trafficking in obesity: a driver for ectopic fat deposition?* Diabetes, 2011. **60**(1): p. 47-55.
16. Belfort, R., et al., *Dose-response effect of elevated plasma free fatty acid on insulin signaling.* Diabetes, 2005. **54**(6): p. 1640-8.

17. Kim, J.K., et al., *Tissue-specific overexpression of lipoprotein lipase causes tissue-specific insulin resistance.* Proc Natl Acad Sci U S A, 2001. **98**(13): p. 7522-7.
18. Mayerson, A.B., et al., *The effects of rosiglitazone on insulin sensitivity, lipolysis, and hepatic and skeletal muscle triglyceride content in patients with type 2 diabetes.* Diabetes, 2002. **51**(3): p. 797-802.
19. Brown, M.S. and J.L. Goldstein, *Selective versus total insulin resistance: a pathogenic paradox.* Cell Metab, 2008. **7**(2): p. 95-6.
20. Biddinger, S.B., et al., *Hepatic insulin resistance is sufficient to produce dyslipidemia and susceptibility to atherosclerosis.* Cell Metab, 2008. **7**(2): p. 125-34.
21. Hotamisligil, G.S., et al., *Increased adipose tissue expression of tumor necrosis factor-alpha in human obesity and insulin resistance.* J Clin Invest, 1995. **95**(5): p. 2409-15.
22. Weisberg, S.P., et al., *Obesity is associated with macrophage accumulation in adipose tissue.* J Clin Invest, 2003. **112**(12): p. 1796-808.
23. Cinti, S., et al., *Adipocyte death defines macrophage localization and function in adipose tissue of obese mice and humans.* J Lipid Res, 2005. **46**(11): p. 2347-55.
24. Curat, C.A., et al., *From blood monocytes to adipose tissue-resident macrophages: induction of diapedesis by human mature adipocytes.* Diabetes, 2004. **53**(5): p. 1285-92.
25. Hardy, O.T., et al., *Body mass index-independent inflammation in omental adipose tissue associated with insulin resistance in morbid obesity.* Surg Obes Relat Dis, 2011. **7**(1): p. 60-7.
26. Harman-Boehm, I., et al., *Macrophage infiltration into omental versus subcutaneous fat across different populations: effect of regional adiposity and the comorbidities of obesity.* J Clin Endocrinol Metab, 2007. **92**(6): p. 2240-7.
27. Cancello, R., et al., *Increased infiltration of macrophages in omental adipose tissue is associated with marked hepatic lesions in morbid human obesity.* Diabetes, 2006. **55**(6): p. 1554-61.
28. Cancello, R., et al., *Reduction of macrophage infiltration and chemoattractant gene expression changes in white adipose tissue of morbidly obese subjects after surgery-induced weight loss.* Diabetes, 2005. **54**(8): p. 2277-86.
29. Xu, H., et al., *Chronic inflammation in fat plays a crucial role in the development of obesity-related insulin resistance.* J Clin Invest, 2003. **112**(12): p. 1821-30.
30. Strissel, K.J., et al., *Adipocyte death, adipose tissue remodeling, and obesity complications.* Diabetes, 2007. **56**(12): p. 2910-8.
31. Strissel, K.J., et al., *T-Cell Recruitment and Th1 Polarization in Adipose Tissue During Diet-Induced Obesity in C57BL/6 Mice.* Obesity, 2010.

32. Lumeng, C.N., J.L. Bodzin, and A.R. Saltiel, *Obesity induces a phenotypic switch in adipose tissue macrophage polarization.* J Clin Invest, 2007. **117**(1): p. 175-84.
33. McNally, A.K. and J.M. Anderson, *Macrophage fusion and multinucleated giant cells of inflammation.* Adv Exp Med Biol, 2011. **713**: p. 97-111.
34. Kosteli, A., et al., *Weight loss and lipolysis promote a dynamic immune response in murine adipose tissue.* J Clin Invest, 2010. **120**(10): p. 3466-79.
35. Moore, K.J. and I. Tabas, *Macrophages in the pathogenesis of atherosclerosis.* Cell, 2011. **145**(3): p. 341-55.
36. Suganami, T., et al., *Role of the Toll-like receptor 4/NF-kappaB pathway in saturated fatty acid-induced inflammatory changes in the interaction between adipocytes and macrophages.* Arterioscler Thromb Vasc Biol, 2007. **27**(1): p. 84-91.
37. Sun, K., C.M. Kusminski, and P.E. Scherer, *Adipose tissue remodeling and obesity.* J Clin Invest, 2011. **121**(6): p. 2094-101.
38. Inouye, K.E., et al., *Absence of CC chemokine ligand 2 does not limit obesity-associated infiltration of macrophages into adipose tissue.* Diabetes, 2007. **56**(9): p. 2242-50.
39. Kanda, H., et al., *MCP-1 contributes to macrophage infiltration into adipose tissue, insulin resistance, and hepatic steatosis in obesity.* J Clin Invest, 2006. **116**(6): p. 1494-505.
40. Weisberg, S.P., et al., *CCR2 modulates inflammatory and metabolic effects of high-fat feeding.* J Clin Invest, 2006. **116**(1): p. 115-24.
41. Kirk, E.A., et al., *Monocyte chemoattractant protein deficiency fails to restrain macrophage infiltration into adipose tissue [corrected].* Diabetes, 2008. **57**(5): p. 1254-61.
42. Fain, J.N., et al., *Comparison of the release of adipokines by adipose tissue, adipose tissue matrix, and adipocytes from visceral and subcutaneous abdominal adipose tissues of obese humans.* Endocrinology, 2004. **145**(5): p. 2273-82.
43. Ohman, M.K., et al., *Monocyte chemoattractant protein-1 deficiency protects against visceral fat-induced atherosclerosis.* Arterioscler Thromb Vasc Biol, 2010. **30**(6): p. 1151-8.
44. Plump, A.S., et al., *Severe hypercholesterolemia and atherosclerosis in apolipoprotein E-deficient mice created by homologous recombination in ES cells.* Cell, 1992. **71**(2): p. 343-53.
45. Piedrahita, J.A., et al., *Generation of mice carrying a mutant apolipoprotein E gene inactivated by gene targeting in embryonic stem cells.* Proc Natl Acad Sci U S A, 1992. **89**(10): p. 4471-5.
46. Breslow, J.L., *Transgenic mouse models of lipoprotein metabolism and atherosclerosis.* Proc Natl Acad Sci U S A, 1993. **90**(18): p. 8314-8.
47. Hansson, G.K. and A. Hermansson, *The immune system in atherosclerosis.* Nat Immunol, 2011. **12**(3): p. 204-12.

48. Keaney, J.F., Jr., *Immune modulation of atherosclerosis.* Circulation, 2011. **124**(22): p. e559-60.
49. Seimon, T.A., et al., *Atherogenic lipids and lipoproteins trigger CD36-TLR2-dependent apoptosis in macrophages undergoing endoplasmic reticulum stress.* Cell Metab, 2010. **12**(5): p. 467-82.
50. Miller, Y.I., et al., *Minimally modified LDL binds to CD14, induces macrophage spreading via TLR4/MD-2, and inhibits phagocytosis of apoptotic cells.* J Biol Chem, 2003. **278**(3): p. 1561-8.
51. Duewell, P., et al., *NLRP3 inflammasomes are required for atherogenesis and activated by cholesterol crystals.* Nature, 2010. **464**(7293): p. 1357-61.
52. Maiellaro, K. and W.R. Taylor, *The role of the adventitia in vascular inflammation.* Cardiovasc Res, 2007. **75**(4): p. 640-8.
53. Sacks, H.S. and J.N. Fain, *Human epicardial adipose tissue: a review.* Am Heart J, 2007. **153**(6): p. 907-17.
54. Vela D, B.M., Madjid M, Burke A, Naghavi M, Willerson JT, Casscells SW, Litovsky S, *The role of periadventitial fat in atherosclerosis: an adipose subset with potential diagnostic and therapeutic implications.* Arch Pathol Lab Med 2007. **131**: p. 481-487.
55. Li, G., et al., *Estrogen attenuates integrin-beta(3)-dependent adventitial fibroblast migration after inhibition of osteopontin production in vascular smooth muscle cells.* Circulation, 2000. **101**(25): p. 2949-55.
56. Okamoto, E., et al., *Perivascular inflammation after balloon angioplasty of porcine coronary arteries.* Circulation, 2001. **104**(18): p. 2228-35.
57. Sartore, S., et al., *Contribution of adventitial fibroblasts to neointima formation and vascular remodeling: from innocent bystander to active participant.* Circ Res, 2001. **89**(12): p. 1111-21.
58. Shi, Y., et al., *Adventitial myofibroblasts contribute to neointimal formation in injured porcine coronary arteries.* Circulation, 1996. **94**(7): p. 1655-64.
59. Yudkin, J.S., E. Eringa, and C.D. Stehouwer, *"Vasocrine" signalling from perivascular fat: a mechanism linking insulin resistance to vascular disease.* Lancet, 2005. **365**(9473): p. 1817-20.
60. Mazurek T, Z.L., Zalweski A, Mannion JD, Diehl JT, Arafat H, Sarov-Blat L, O'Brien S, Keiper EA, Johnson AG, Martin J, Goldstein HJ, Shi Y, *Human Epicardial Adipose Tissue Is a Source of Inflammatory Mediators.* Circulation, 2003. **108**: p. 2460-2466.
61. Henrichot E, J.-A.C., Pernin A, Pache JC, Velebit V, Dayer JM, Meda P, Chizzolini C, Meier CA, *Production of Chemokines by perivascular adipose tissue: a role in the pathogenesis of atherosclerosis? .* Arterioscler Thromb Vasc Biol., 2005. **25**: p. 2594-2599.
62. Karastergiou, K., et al., *Epicardial adipokines in obesity and coronary artery disease induce atherogenic changes in monocytes and endothelial cells.* Arterioscler Thromb Vasc Biol, 2010. **30**(7): p. 1340-6.

63. Sacks, H.S., et al., *Inflammatory Genes in Epicardial Fat Contiguous With Coronary Atherosclerosis in the Metabolic Syndrome and Type 2 Diabetes.* Diabetes Care, 2011. **34**(3): p. 730-733.
64. Langheim, S., et al., *Increased expression and secretion of resistin in epicardial adipose tissue of patients with acute coronary syndrome.* Am J Physiol Heart Circ Physiol, 2010. **298**(3): p. H746-53.
65. Greenstein, A.S., et al., *Local inflammation and hypoxia abolish the protective anticontractile properties of perivascular fat in obese patients.* Circulation, 2009. **119**(12): p. 1661-70.
66. Cheng, K.H., et al., *Adipocytokines and proinflammatory mediators from abdominal and epicardial adipose tissue in patients with coronary artery disease.* Int J Obes (Lond), 2008. **32**(2): p. 268-74.
67. Eiras, S., et al., *Extension of coronary artery disease is associated with increased IL-6 and decreased adiponectin gene expression in epicardial adipose tissue.* Cytokine, 2008. **43**(2): p. 174-80.
68. Iacobellis, G., et al., *Adiponectin expression in human epicardial adipose tissue in vivo is lower in patients with coronary artery disease.* Cytokine, 2005. **29**(6): p. 251-5.
69. Iacobellis, G., et al., *Epicardial adipose tissue is related to carotid intima-media thickness and visceral adiposity in HIV-infected patients with highly active antiretroviral therapy-associated metabolic syndrome.* Curr HIV Res, 2007. **5**(2): p. 275-9.
70. Rosito, G.A., et al., *Pericardial fat, visceral abdominal fat, cardiovascular disease risk factors, and vascular calcification in a community-based sample: the Framingham Heart Study.* Circulation, 2008. **117**(5): p. 605-13.
71. Soltis, E.E. and L.A. Cassis, *Influence of perivascular adipose tissue on rat aortic smooth muscle responsiveness.* Clin Exp Hypertens A, 1991. **13**(2): p. 277-96.
72. Lee, Y.C., et al., *Role of perivascular adipose tissue-derived methyl palmitate in vascular tone regulation and pathogenesis of hypertension.* Circulation, 2011. **124**(10): p. 1160-71.
73. Golledge, J., et al., *Obesity, adipokines, and abdominal aortic aneurysm: Health in Men study.* Circulation, 2007. **116**(20): p. 2275-9.
74. Police SB, T.S., Charnigo R, Daugherty A, Cassis LA. , *Obesity Promotes Inflammation in Periaortic Adipose Tissue and Angiotensin II-Induced Abdominal Aortic Aneurysm Formation.* Arterioscler Thromb Vasc Biol 2009. **29**: p. 1458-1464.
75. Ohman, M.K., et al., *Perivascular visceral adipose tissue induces atherosclerosis in apolipoprotein E deficient mice.* Atherosclerosis, 2011. **219**(1): p. 33-9.
76. Takaoka M, N.D., Kihara S, Shimomura I, Kimura Y, Tabata Y, Saito Y, Nagai R, Sata M, *Perivadventitial adipose tissue plays a critical role in vascular remodeling* Circulation Research, 2009. **105**(9): p. 906-911.

77. Nikolsky, E., et al., *Impact of obesity on revascularization and restenosis rates after bare-metal and drug-eluting stent implantation (from the TAXUS-IV trial).* Am J Cardiol, 2005. **95**(6): p. 709-15.
78. Takaoka, M., et al., *Endovascular injury induces rapid phenotypic changes in perivascular adipose tissue.* Arterioscler Thromb Vasc Biol, 2010. **30**(8): p. 1576-82.
79. Lembo, G., et al., *Leptin induces direct vasodilation through distinct endothelial mechanisms.* Diabetes, 2000. **49**(2): p. 293-7.
80. Wang, P., et al., *Perivascular adipose tissue-derived visfatin is a vascular smooth muscle cell growth factor: role of nicotinamide mononucleotide.* Cardiovasc Res, 2009. **81**(2): p. 370-80.
81. Ruan, C.C., et al., *Perivascular adipose tissue-derived complement 3 is required for adventitial fibroblast functions and adventitial remodeling in deoxycorticosterone acetate-salt hypertensive rats.* Arterioscler Thromb Vasc Biol, 2010. **30**(12): p. 2568-74.
82. Shivalkar, B., et al., *Flow mediated dilatation and cardiac function in type 1 diabetes mellitus.* Am J Cardiol, 2006. **97**(1): p. 77-82.
83. Mathieu, P., et al., *Visceral obesity: the link among inflammation, hypertension, and cardiovascular disease.* Hypertension, 2009. **53**(4): p. 577-84.
84. Czech, M.P., D.K. Richardson, and C.J. Smith, *Biochemical basis of fat cell insulin resistance in obese rodents and man.* Metabolism, 1977. **26**(9): p. 1057-78.
85. Lewis, G.F., et al., *Disordered fat storage and mobilization in the pathogenesis of insulin resistance and type 2 diabetes.* Endocr Rev, 2002. **23**(2): p. 201-29.
86. Donath, M.Y. and S.E. Shoelson, *Type 2 diabetes as an inflammatory disease.* Nat Rev Immunol, 2011. **11**(2): p. 98-107.
87. Fox, C.S., et al., *Abdominal visceral and subcutaneous adipose tissue compartments: association with metabolic risk factors in the Framingham Heart Study.* Circulation, 2007. **116**(1): p. 39-48.
88. Jensen, M.D., *Role of body fat distribution and the metabolic complications of obesity.* J Clin Endocrinol Metab, 2008. **93**(11 Suppl 1): p. S57-63.
89. Chatterjee, T.K., et al., *Proinflammatory phenotype of perivascular adipocytes: influence of high-fat feeding.* Circ Res, 2009. **104**(4): p. 541-9.
90. Petrovic, N., et al., *Chronic peroxisome proliferator-activated receptor gamma (PPARgamma) activation of epididymally derived white adipocyte cultures reveals a population of thermogenically competent, UCP1-containing adipocytes molecularly distinct from classic brown adipocytes.* J Biol Chem, 2010. **285**(10): p. 7153-64.
91. Galvez-Prieto, B., et al., *Comparative expression analysis of the renin-angiotensin system components between white and brown perivascular adipose tissue.* J Endocrinol, 2008. **197**(1): p. 55-64.

92. Powelka, A.M., et al., *Suppression of oxidative metabolism and mitochondrial biogenesis by the transcriptional corepressor RIP140 in mouse adipocytes.* J Clin Invest, 2006. **116**(1): p. 125-36.
93. Livak, K.J. and T.D. Schmittgen, *Analysis of relative gene expression data using real-time quantitative PCR and the 2(-Delta Delta C(T)) Method.* Methods, 2001. **25**(4): p. 402-8.
94. Tang, X., et al., *An RNA interference-based screen identifies MAP4K4/NIK as a negative regulator of PPARgamma, adipogenesis, and insulin-responsive hexose transport.* Proc Natl Acad Sci U S A, 2006. **103**(7): p. 2087-92.
95. Bolstad, B.M., et al., *A comparison of normalization methods for high density oligonucleotide array data based on variance and bias.* Bioinformatics, 2003. **19**(2): p. 185-93.
96. Gentleman, R.C., et al., *Bioconductor: open software development for computational biology and bioinformatics.* Genome Biol, 2004. **5**(10): p. R80.
97. Edgar, R., M. Domrachev, and A.E. Lash, *Gene Expression Omnibus: NCBI gene expression and hybridization array data repository.* Nucleic Acids Res, 2002. **30**(1): p. 207-10.
98. Wu, H., et al., *CD11c expression in adipose tissue and blood and its role in diet-induced obesity.* Arterioscler Thromb Vasc Biol, 2010. **30**(2): p. 186-92.
99. Bobryshev, Y.V. and R.S. Lord, *Vascular-associated lymphoid tissue (VALT) involvement in aortic aneurysm.* Atherosclerosis, 2001. **154**(1): p. 15-21.
100. Cannon, B. and J. Nedergaard, *Brown adipose tissue: function and physiological significance.* Physiol Rev, 2004. **84**(1): p. 277-359.
101. Hageman, R.S., et al., *High-fat diet leads to tissue-specific changes reflecting risk factors for diseases in DBA/2J mice.* Physiol Genomics, 2010. **42**(1): p. 55-66.
102. Herrero, L., et al., *Inflammation and adipose tissue macrophages in lipodystrophic mice.* Proc Natl Acad Sci U S A, 2010. **107**(1): p. 240-5.
103. Withers, S.B., et al., *Macrophage Activation Is Responsible for Loss of Anticontractile Function in Inflamed Perivascular Fat.* Arterioscler Thromb Vasc Biol, 2011.
104. Zhou, Z., et al., *Cidea-deficient mice have lean phenotype and are resistant to obesity.* Nat Genet, 2003. **35**(1): p. 49-56.
105. Rebolledo, A., et al., *Early alterations in vascular contractility associated to changes in fatty acid composition and oxidative stress markers in perivascular adipose tissue.* Cardiovasc Diabetol, 2010. **9**(1): p. 65.
106. Lee, J.Y., et al., *Saturated fatty acids, but not unsaturated fatty acids, induce the expression of cyclooxygenase-2 mediated through Toll-like receptor 4.* J Biol Chem, 2001. **276**(20): p. 16683-9.

107. Choi, H.Y., et al., *Association of adiponectin, resistin, and vascular inflammation: analysis with 18F-fluorodeoxyglucose positron emission tomography.* Arterioscler Thromb Vasc Biol, 2011. **31**(4): p. 944-9.
108. Ingelsson, E. and L. Lind, *Circulating retinol-binding protein 4 and subclinical cardiovascular disease in the elderly.* Diabetes Care, 2009. **32**(4): p. 733-5.
109. Ketonen, J., T. Pilvi, and E. Mervaala, *Caloric restriction reverses high-fat diet-induced endothelial dysfunction and vascular superoxide production in C57Bl/6 mice.* Heart Vessels, 2010. **25**(3): p. 254-62.
110. Gustafson, B., et al., *Inflamed adipose tissue: a culprit underlying the metabolic syndrome and atherosclerosis.* Arterioscler Thromb Vasc Biol, 2007. **27**(11): p. 2276-83.
111. Lamounier-Zepter, V., et al., *Adrenocortical changes and arterial hypertension in lipoatrophic A-ZIP/F-1 mice.* Mol Cell Endocrinol, 2008. **280**(1-2): p. 39-46.
112. Sacks HS, F.J., Holman B, Cheema P, Chary A, Parks F, Karas J, Optican R, Bahouth SW, Garrett E, Wolf RY, Carter RA, Robbins T, Wolford D, Samaha J. , *Uncoupling Protein-1 and related messenger ribonucleic acids in human epicardial and other adipose tissues: epicardial fat functioning as brown fat.* J Clin Endocrinol Metab 2009. **94**: p. 3611-3615.
113. Cypess, A.M., et al., *Identification and importance of brown adipose tissue in adult humans.* N Engl J Med, 2009. **360**(15): p. 1509-17.
114. van Marken Lichtenbelt, W.D., et al., *Cold-activated brown adipose tissue in healthy men.* N Engl J Med, 2009. **360**(15): p. 1500-8.
115. Zhang, S.H., et al., *Spontaneous hypercholesterolemia and arterial lesions in mice lacking apolipoprotein E.* Science, 1992. **258**(5081): p. 468-71.
116. Hofmann, S.M., et al., *Adipocyte LDL receptor-related protein-1 expression modulates postprandial lipid transport and glucose homeostasis in mice.* J Clin Invest, 2007. **117**(11): p. 3271-82.
117. Huang, Z.H., C.A. Reardon, and T. Mazzone, *Endogenous ApoE expression modulates adipocyte triglyceride content and turnover.* Diabetes, 2006. **55**(12): p. 3394-402.
118. Karavia, E.A., et al., *Deficiency in apolipoprotein E has a protective effect on diet-induced nonalcoholic fatty liver disease in mice.* FEBS J, 2011. **278**(17): p. 3119-29.
119. Gao, J., et al., *Involvement of apolipoprotein E in excess fat accumulation and insulin resistance.* Diabetes, 2007. **56**(1): p. 24-33.
120. Hofmann, S.M., et al., *Defective lipid delivery modulates glucose tolerance and metabolic response to diet in apolipoprotein E-deficient mice.* Diabetes, 2008. **57**(1): p. 5-12.
121. Kawashima, Y., et al., *Apolipoprotein E deficiency abrogates insulin resistance in a mouse model of type 2 diabetes mellitus.* Diabetologia, 2009. **52**(7): p. 1434-41.

122. Chiba, T., et al., *VLDL induces adipocyte differentiation in ApoE-dependent manner.* Arterioscler Thromb Vasc Biol, 2003. **23**(8): p. 1423-9.
123. Huang, Z.H., D. Gu, and T. Mazzone, *Role of adipocyte-derived apoE in modulating adipocyte size, lipid metabolism, and gene expression in vivo.* Am J Physiol Endocrinol Metab, 2009. **296**(5): p. E1110-9.
124. Huang, Z.H., R.D. Minshall, and T. Mazzone, *Mechanism for endogenously expressed ApoE modulation of adipocyte very low density lipoprotein metabolism: role in endocytic and lipase-mediated metabolic pathways.* J Biol Chem, 2009. **284**(46): p. 31512-22.
125. Pedrini, M.T., et al., *Human triglyceride-rich lipoproteins impair glucose metabolism and insulin signalling in L6 skeletal muscle cells independently of non-esterified fatty acid levels.* Diabetologia, 2005. **48**(4): p. 756-66.
126. Rader, D.J. and E. Pure, *Lipoproteins, macrophage function, and atherosclerosis: beyond the foam cell?* Cell Metab, 2005. **1**(4): p. 223-30.
127. Kockx, M., W. Jessup, and L. Kritharides, *Regulation of endogenous apolipoprotein E secretion by macrophages.* Arterioscler Thromb Vasc Biol, 2008. **28**(6): p. 1060-7.
128. Boisvert, W.A., J. Spangenberg, and L.K. Curtiss, *Treatment of severe hypercholesterolemia in apolipoprotein E-deficient mice by bone marrow transplantation.* J Clin Invest, 1995. **96**(2): p. 1118-24.
129. Linton, M.F., J.B. Atkinson, and S. Fazio, *Prevention of atherosclerosis in apolipoprotein E-deficient mice by bone marrow transplantation.* Science, 1995. **267**(5200): p. 1034-7.
130. Hoover-Plow, J. and B. Nelson, *Oxygen consumption in mice (I strain) after feeding.* J Nutr, 1985. **115**(3): p. 303-10.
131. Bartelt, A., et al., *Altered endocannabinoid signalling after a high-fat diet in Apoe(-/-) mice: relevance to adipose tissue inflammation, hepatic steatosis and insulin resistance.* Diabetologia, 2011. **54**(11): p. 2900-10.
132. Karagiannides, I., et al., *Apolipoprotein E predisposes to obesity and related metabolic dysfunctions in mice.* FEBS J, 2008. **275**(19): p. 4796-809.
133. Meir, K.S. and E. Leitersdorf, *Atherosclerosis in the apolipoprotein-E-deficient mouse: a decade of progress.* Arterioscler Thromb Vasc Biol, 2004. **24**(6): p. 1006-14.
134. Schreyer, S.A., et al., *LDL receptor but not apolipoprotein E deficiency increases diet-induced obesity and diabetes in mice.* Am J Physiol Endocrinol Metab, 2002. **282**(1): p. E207-14.
135. Tschop, M.H., et al., *A guide to analysis of mouse energy metabolism.* Nat Methods, 2012. **9**(1): p. 57-63.
136. Bost, F., et al., *The extracellular signal-regulated kinase isoform ERK1 is specifically required for in vitro and in vivo adipogenesis.* Diabetes, 2005. **54**(2): p. 402-11.

137. Kuipers, F., et al., *Impaired secretion of very low density lipoprotein-triglycerides by apolipoprotein E- deficient mouse hepatocytes.* J Clin Invest, 1997. **100**(11): p. 2915-22.
138. Maugeais, C., et al., *Hepatic apolipoprotein E expression promotes very low density lipoprotein-apolipoprotein B production in vivo in mice.* J Lipid Res, 2000. **41**(10): p. 1673-9.
139. Le Lay, S., et al., *Cholesterol, a cell size-dependent signal that regulates glucose metabolism and gene expression in adipocytes.* J Biol Chem, 2001. **276**(20): p. 16904-10.
140. Schmitz, G. and M. Grandl, *Endolysosomal phospholipidosis and cytosolic lipid droplet storage and release in macrophages.* Biochim Biophys Acta, 2009. **1791**(6): p. 524-39.
141. Fon Tacer, K., et al., *Research resource: Comprehensive expression atlas of the fibroblast growth factor system in adult mouse.* Mol Endocrinol, 2010. **24**(10): p. 2050-64.
142. Golledge, J., et al., *Association between osteopontin and human abdominal aortic aneurysm.* Arterioscler Thromb Vasc Biol, 2007. **27**(3): p. 655-60.
143. Wang, Z.V., et al., *Identification and characterization of a promoter cassette conferring adipocyte-specific gene expression.* Endocrinology, 2010. **151**(6): p. 2933-9.
144. Thomas, M., et al., *Deletion of p47phox attenuates angiotensin II-induced abdominal aortic aneurysm formation in apolipoprotein E-deficient mice.* Circulation, 2006. **114**(5): p. 404-13.